1-1-1999

The aerodynamic response of airborne discs

Timothy Lewis Mitchell
University of Nevada, Las Vegas

INFORMATION TO USERS

This manuscript has been reproduced from the microfilm master. UMI films the text directly from the original or copy submitted. Thus, some thesis and dissertation copies are in typewriter face, while others may be from any type of computer printer.

The quality of this reproduction is dependent upon the quality of the copy submitted. Broken or indistinct print, colored or poor quality illustrations and photographs, print bleedthrough, substandard margins, and improper alignment can adversely affect reproduction.

In the unlikely event that the author did not send UMI a complete manuscript and there are missing pages, these will be noted. Also, if unauthorized copyright material had to be removed, a note will indicate the deletion.

Oversize materials (e.g., maps, drawings, charts) are reproduced by sectioning the original, beginning at the upper left-hand corner and continuing from left to right in equal sections with small overlaps. Each original is also photographed in one exposure and is included in reduced form at the back of the book.

Photographs included in the original manuscript have been reproduced xerographically in this copy. Higher quality 6" x 9" black and white photographic prints are available for any photographs or illustrations appearing in this copy for an additional charge. Contact UMI directly to order.

UMI®

Bell & Howell Information and Learning
300 North Zeeb Road, Ann Arbor, MI 48106-1346 USA
800-521-0600

THE AERODYNAMIC RESPONSE OF AIRBORNE DISCS

by

Timothy Lewis Mitchell

Associate of Applied Science
Clark College
1988

Bachelor of Science
University of Nevada, Las Vegas
1994

A thesis submitted in partial fulfillment
of the requirements for the degree of

Master of Science Degree
Department of Mechanical Engineering
Howard R. Hughes College of Engineering

Graduate College
University of Nevada, Las Vegas
August 1999

Thesis Approval

The Graduate College
University of Nevada, Las Vegas

June 17, 19 99

The Thesis prepared by

Timothy L. Mitchell

Entitled

The Aerodynamic Response of Airborne Discs

is approved in partial fulfillment of the requirements for the degree of

Master of Science in Mechanical Engineering

Darrell W. Pepper
Examination Committee Chair

Dean of the Graduate College

William H. Culbreth
Examination Committee Member

William P. Graebel
Examination Committee Member

Michelle Schutz
Graduate College Faculty Representative

ABSTRACT

The Aerodynamic Response of Airborne Discs

By

Timothy Lewis Mitchell

Dr. Darrell Pepper, Examination Committee Chair
Professor of Mechanical Engineering
University of Nevada, Las Vegas

A study has been conducted to characterize the flow over a free-flying disc. In this study, three types of discs are analyzed in a series of stationary experiments, and a single disc is analyzed in a spinning experiment. Two dimensionless parameters dominate the experiments, the Reynolds number and the tip speed ratio. The first experiment measured the lift and drag at varying angles of attack on a stationary disc. The second stationary experiment was a unique measurement of the center of lift of a disc as a function of velocity. The third stationary experiment was a tuft test to describe the boundary layer, done at different velocities and angles of attack. The spinning disc experiment utilized smoke to visualize the flow around the disc and ascertain the effects of spin on vorticity and boundary layer separation. Results showed that the center of lift was behind the geometric center at low velocity and moved rapidly forward with increasing velocity. Tuft and smoke tests showed that the boundary layer was attached across the entire surface with strong vorticies shed from the sides and from the rear of the disc. The flow was primarily affected by the disc's leading edge with secondary effects from the domed contour.

ACKNOWLEDGEMENTS

I would like to express profound thanks to my advisor and mentor Dr. Darrell W. Pepper, chairman of the Mechanical Engineering Department, for his endless patience and excellent guidance. Time and again his wisdom, experience, and encouragement steered me away from the pitfalls of higher education.

My special thanks is due to Dr. Peter Lissaman of the University of Southern California, for his far reaching insight into the aerodynamics of free flying objects and his unselfish commitment of ideas and time. The successful completion of this work would not have been possible without his input.

I also wish to thank Dr. Graebel, Dr. Culbreth, and Dr. Schultz for agreeing to serve on my thesis committee.

I must also thank the undergraduate classmen that assisted me in the wind tunnel calibration and testing, John Dornack, Suzanna Munoz, and Fabiola Martinez.

Last but not least, I thank my wife, Margaret, for her assistance, support and patience.

TABLE OF CONTENTS

LIST OF TABLES

LIST OF FIGURES

NOMENCLATURE

m	mass
ψ	angle of attack
g	gravity
ε	initial drag to weight ratio
ρ	density
υ	velocity
A_F	frontal area
C_D	Coefficient of drag
C_L	coefficient of lift

CHAPTER 1

INTRODUCTION

1.1 General Information

Determining the characteristics of flow over circular airfoils is of intellectual interest to many aerodynamicists and is an area in which little research has been published. Furthermore, data related to the aerodynamics of spinning objects is particularly scarce. This work clarifies the affects of spin on airborne discs, and examines their aerodynamic characteristics.

Any airborne disc, whether spinning or not, can be considered a circular airfoil. A common circular airfoil belonging to the general class of spinning projectiles is the free flying disc, widely known as a Frisbee™ (Frisbee is a trademarked name belonging to the Wham-o Corporation). Other circular airfoils in the general class of spinning projectiles are the discus used in pentathlon and decathlon games, and the skeet used in sport shooting.

Though airborne spinning objects can already be found in a multitude of applications, (from the curve ball employed by a baseball pitcher, to the disc shaped radar dome of an AWACS aircraft) their real potential is yet to be seen. For example, the U. S. Air Force and NASA in a collaborative effort to place small payloads in orbit are funding research in a new launch technology using spin stabilized payloads launched by ground based

lasers [23]. The Lightcraft Technology Demonstrator, a 1 meter in diameter vehicle weighing 2 kg, is being researched at the Rensselaer Polytechnic Institute and Lawrence Livermore National Laboratory in cooperation with the BMD laser propulsion program. Currently, a small-scale demonstrator, weighing 52 grams, spins at 6000 rpm and reaches an altitude of 30 meters. A drawing of the Light Technology Demonstrator is shown in Figure 1.1.

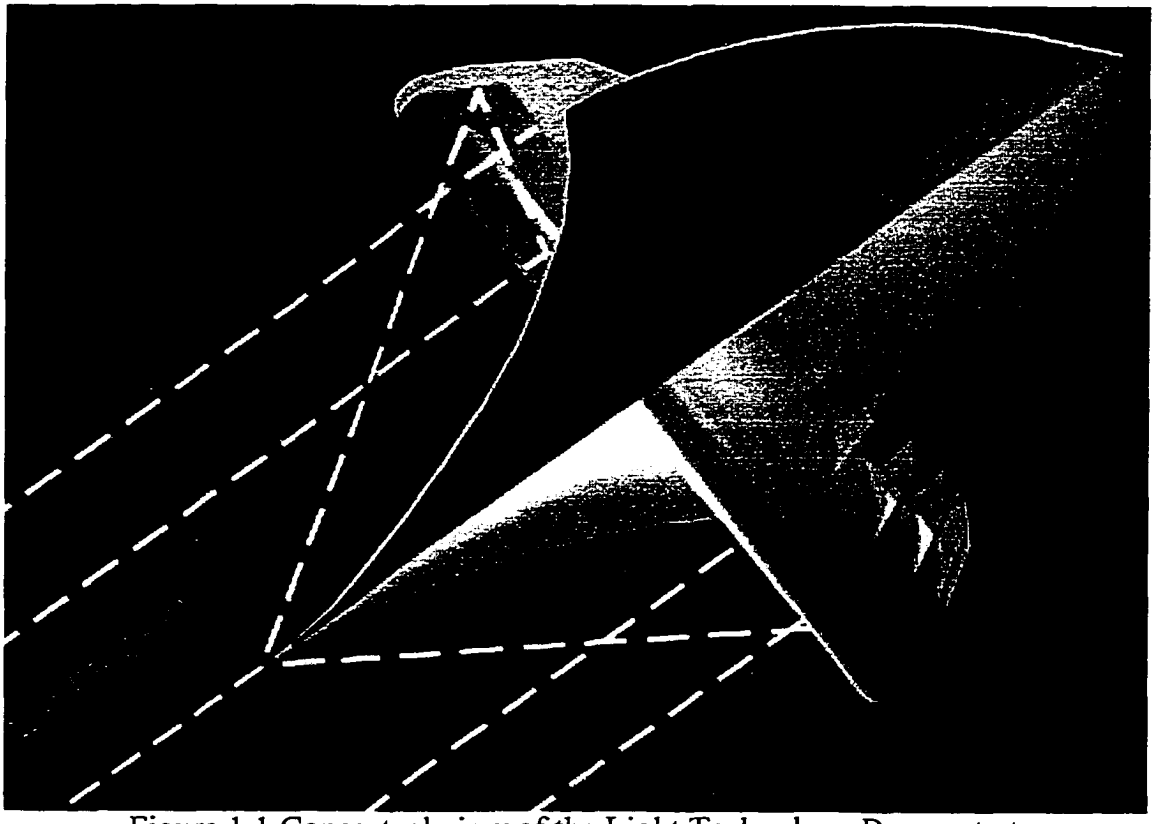

Figure 1.1 Conceptual view of the Light Technology Demonstrator

In addition, the disc shape of circular airfoils is ideal for unmanned underwater research platforms. Their symmetry allows for fast vector changes and 360-degree sensor sweeps. Alternative energy researchers may employ computer-controlled windmills that use these airfoils to take advantage of their unique lift characteristics and improve efficiency.

The U. S. Air Force has already employed a circular airfoil in the development of an unmanned aerial vehicle (UAV). In September, 1998, the UAV Darkstar, which has a disc shaped forward fuselage, successfully completed Phase 1 of its testing and development. However, on April 22, 1996 while testing at Edwards Air Force Base, Darkstar crashed [24]. A photo of this aircraft is shown in Figure 1.2.

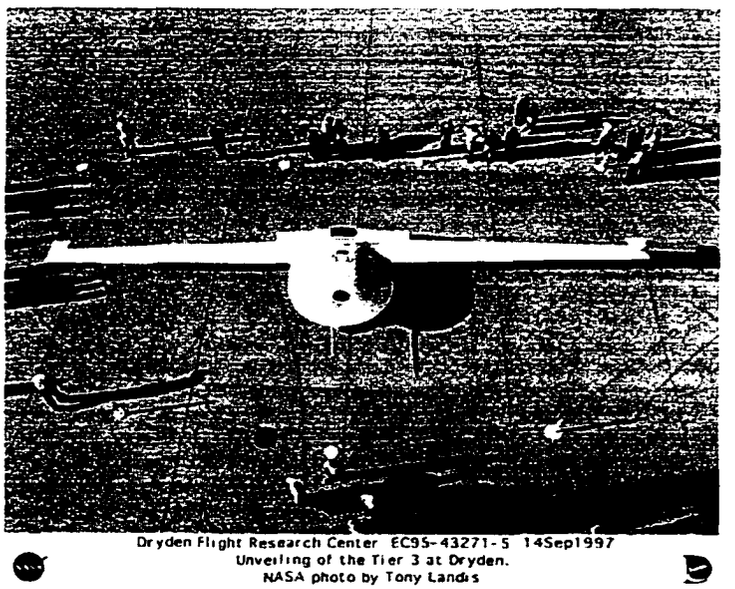

Figure 1.2 The unmanned aerial vehicle Darkstar

The cause of the accident was determined to be an inability of onboard guidance software to compensate for unexpected aerodynamics associated with the forward fuselage. To correct the problem, Boeing completely redesigned the Autonomous Flight Control System. Though this explanation is too vague to be certain, the accident may have been related to the aerodynamic characteristics of disc shaped airfoils.

As mentioned earlier, little is known about the aerodynamic response of spin stabilized discs, and the volume of literature on this subject is surprisingly small. Many times, in the course of this survey, information of research involving rotating objects was received. However, upon further investigation the results of those experiments, with one

exception, were found to be unpublished or proprietary. In an effort to conduct a complete literature survey, the unusual step of referencing web pages was taken. The World Wide Web® is a dynamic and unstructured environment; no tracking, coordinating, or regulating body exists in regards to the tracking of web page content. Of the 26 references in the Bibliography, only 10 are published papers, 6 are web pages, 2 are from non-professional periodicals, 7 are unpublished papers; 3 of the 6 web pages referenced have unknown authors.

Throughout this document measurements are given in metric units or in non-dimensional values. Where actual measurements were converted to metric the raw values will be in parenthesis.

Basic to the aerodynamic consideration of any object are the principles of drag and lift, development of the boundary layer, and the resulting distribution of pressure along the surface. To answers these same questions for the airborne spin-stabilized disc, four experiments were devised. Three of the experiments utilize non-spinning discs, while the remaining experiment utilizes a spinning disc. Cheap to buy and ideally suited to the non-spinning experiments are plastic hand thrown discs, such as the Frisbee. Three different types of discs were tested in the non-spinning experiments to determine the effect of surface contour on the aerodynamic response. Figure 1.3 shows a schematic drawing of these airfoils. To conduct the spinning disc experiment a special aluminum disc of a generalized shape was constructed and tested. A schematic drawing of the aluminum disc is shown in figure 1.4. Measurements were obtained using a force dynamometer, a Pitot tube, a hot-film anemometer, tufts, smoke visualization, video and still photography.

Disc A, Side View
Whammo Imperial Windjammer disc, 233 mm O.D., 105 grams

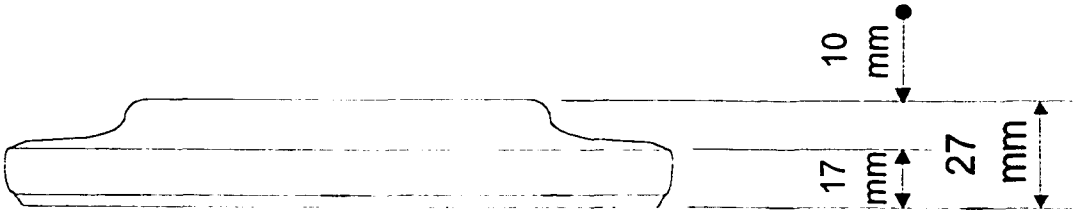

Disc B, Side View
Humphrey Flyer disc, 235 mm O.D., 92 grams

Disc C, Side View
Innova Golf Disc, 213 mm O.D., 176 grams

Figure 1.3 Schematic profile of non-spinning airfoils

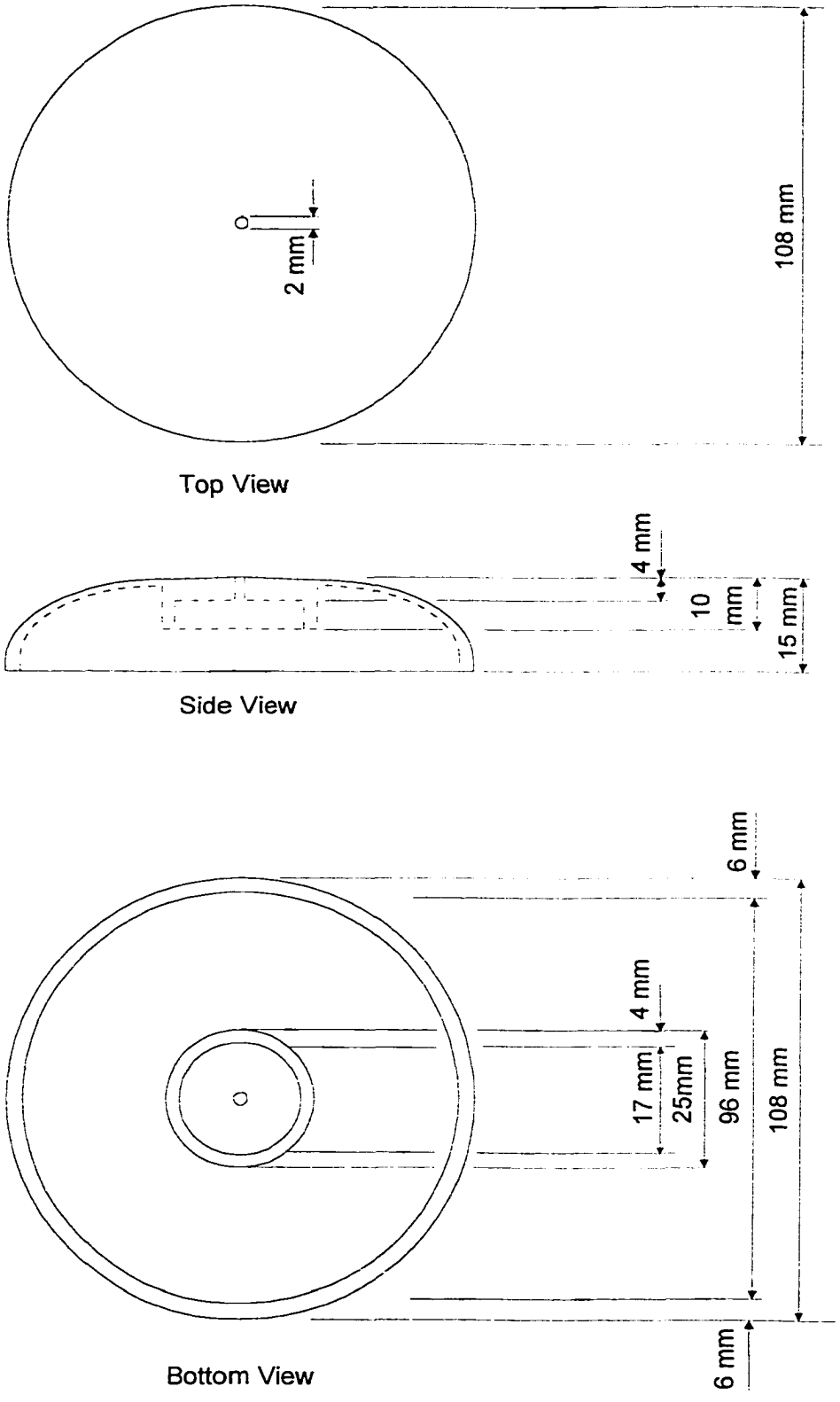

Figure 1.4 Schematic diagram of aluminum spinning disc

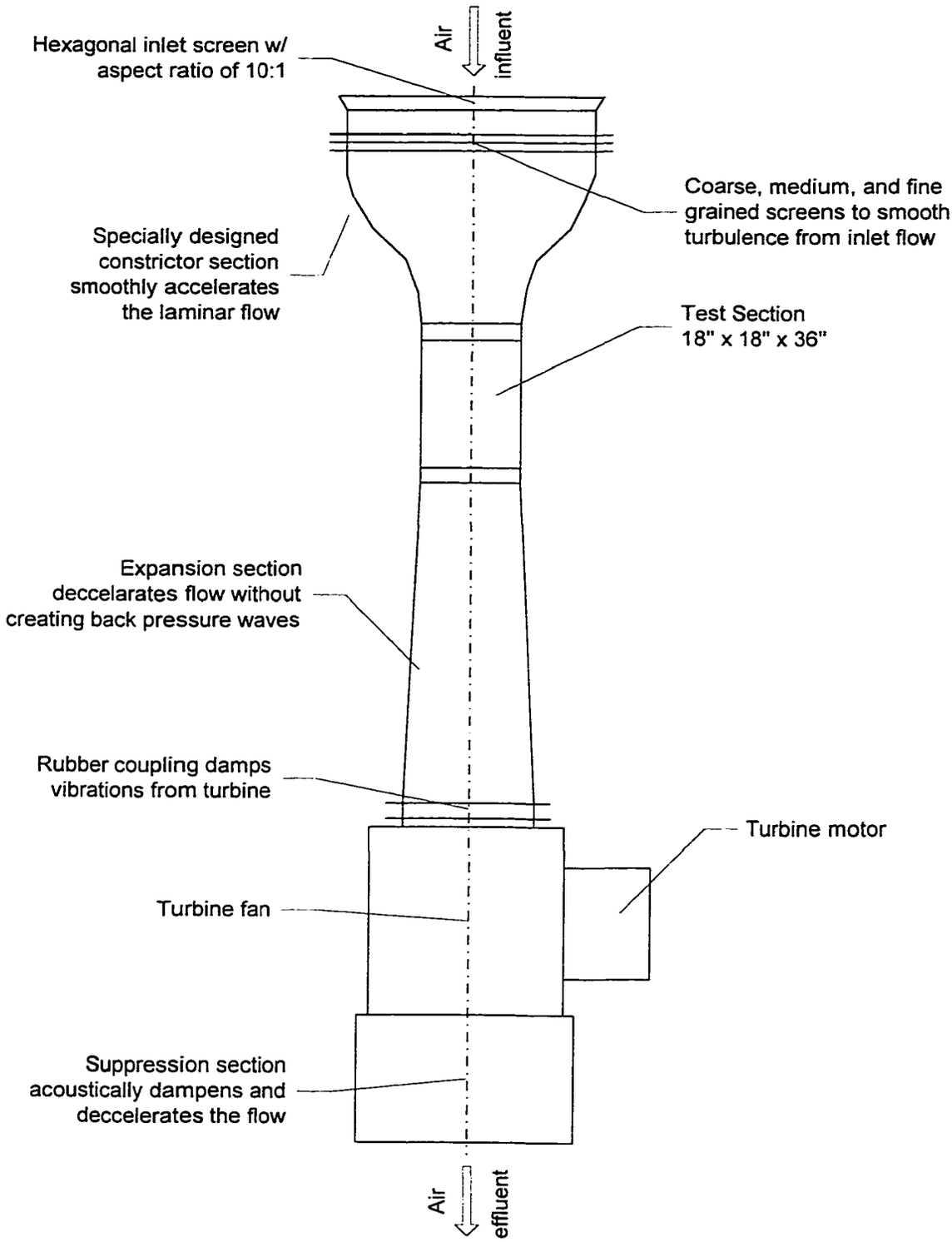

Figure 1.5 Top view of wind tunnel with description

All of the experiments were conducted using the wind tunnel facility at the Thomas T. Beam Engineering complex (Figure 1.5).

The three non-spinning disc experiments were as follows:

1. Lift and drag measurements:
    - To determine the lift and drag coefficients and the lift to drag ratios.
    - To determine how velocity and angle of attack affect the lift and drag.
    - To determine how the disc contour and the leading edge affect the parameters of lift and drag.
2. Center of lift measurements:
    - To determine the aerodynamic center of lift at various Reynolds' numbers.
    - To determine how velocity and angle of attack affect the magnitude and location of the center of lift.
    - To determine how the disc contour and leading edge affect the magnitude and location of the center of lift.
3. Tuft test:
    - To characterize the boundary layer of non-spinning disc.
    - To use in characterizing the affects of spin on the flow around the disc.

The single spinning disc experiment was as follows:

1. Smoke visualization test:
    - To determine the effects of spin on the boundary layer and wake of a free flying disc.

- To compare and contrast the results of the non-spinning tuft test with the results of this test.

In order to duplicate the physical conditions in the experimental confines of a wind tunnel, two non-dimensional parameters are used: the Reynolds number and the tip speed ratio. The Reynolds number is basic to fluid dynamics and is a dimensionless ratio of dynamic forces to viscous forces. This ratio illustrates how the size and speed of an object and viscosity of a fluid effect the flow around the object. The tip speed ratio is defined as the angular velocity over the linear velocity; this ratio shows how the spin can influence the boundary layer and wake aerodynamics. The typical hand thrown spinning disc is 0.255 m (10 inches) in diameter, flies at 9.15 m/s (30 ft/s) and spins at 300 rpm. The Reynolds number for such a hand thrown spinning disc is 1.56×10^5 , while its tip speed ratio is 0.4378.

1.2 MOTIVATION

Motivation for performing this study was provided by the obvious gap in the existing body of knowledge. The performance of the experiments should contribute to that body of knowledge by lending insight into the aerodynamic response of a spin-stabilized disc. Particularly interesting is how spin affects the boundary layer and wake aerodynamics of a disc, and how the leading edge contour influences boundary layer development. Grooves in the surface of a disc, known as lines of Headrick, may provide turbulence to the boundary layer. The flow visualization tests will determine whether there is separation in the boundary layer and whether spin affects separation.

1.3 PROBLEM DESCRIPTION

Aerodynamic behavior in the boundary layer and wake of circular airfoils has been studied experimentally using various measurement techniques. In these experiments, the measurement of lift and drag was accomplished using a force dynamometer. The dynamometer was recalibrated between each set of experiments using graduated masses in the range of 0.05kg to 2kg. Velocity was calibrated using pitot tubes with micromanometers and hot-film anemometry. Boundary layer separation and wake effects were measured using thread tufts and smoke visualization, and boundary layer and wake effects were recorded using photographs. The variation in lift and drag was correlated to boundary layer and wake behavior at various velocities and angles of attack. The leading edge and surface contour of four different disc designs were evaluated to determine its aerodynamic effects on the lift, drag, and center of lift.

CHAPTER 2

LITERATURE SURVEY

2.1 HISTORY

The first recorded act which utilizes an airborne spinning disc occurs in 708 B. C., when the Greeks decided to expand their Olympic games, which previously had consisted of just one event, the sprint. That year they added the pentathlon, a group of five events, one of which was the discus throw. The discus throw remained an event until the end of the Greek Olympic games in 349 A. D. but its impact did not go unnoticed.

> "There are reports of Roman soldiers using their shields as [airborne discs]. Stories tell how, at the Battle of Zarma in 202 B. C., the Roman army confronted Hannibal and the might of Carthage with the Romans obtaining victory helped by the use of razor sharp shields hurled at the opposition." – Ian Scotland [24]

The modern history of the airborne disc begins in 1887 when William Russell Frisbie bought the Olds Baking Company next to the Yale University campus in New Haven, Connecticut and renamed it the Frisbie Pie Company. The company produced pies and cookies which were sold in metal tins. The students attending Yale would throw their

empty pie and cookie tins at each other for entertainment. Tossing Frisbie tins was a healthy way to relax and let off steam. Within a few years it had become a sport around the university campus.

C. E. Davies and William H. Foster may not have seen nor ever heard of Frisbie tin tossing, though they were only 147 miles away at the Glenrock Kennels in Andover, Massachusetts. In 1920, Davies and Foster were developing a way to practice bird hunting in the off season by shooting air launched clay targets. It was the beginning of a new airborne disc sport called Skeet Shooting and within 6 years it would spread nation wide.

For the next twenty years skeet shooting and pie tin tossing grew in popularity, and during the Second World War soldiers spread the sport of pie tin tossing across the country [11]. One such soldier was Walter Frederick Morrison.

In 1948, Morrison, while working at a bottle gas company, became fascinated with the idea of flying saucers from outer space, and began to develop a flying saucer toy which could be thrown like a metal pie tin. His original disc was called Morrison's flyin' saucer; it was made of metal and had 6 vanes mounted on top. Curiously, the vanes were mounted so that they would only work for a left-handed thrower. Morrison intended the vanes to improve lift by utilizing the Bernoulli principle, which they did not [5]. Morrison involved his boss and founder of the bottle gas company, Warren Franscioni. In late 1948, using a lathe, they developed a disc made of a relatively new type of material, plastic [11]. The material they chose was butyl stearate, a hard cellulose material now used in toothbrush handles but then commonly known as Tenite. The Tenite disc, while confirming the aerodynamics of the design, was temperature sensitive

and, in cold weather, would shatter upon impact. They worked to improve the design for the next three years and in 1951 formed the Partners In Plastic Company (Pipco) in San Luis Obispo, California. The company produced its "flyin' saucer" for about 25 cents each and sold them for $1.00 through outlet stores and at Disneyland [11].

Rich Knerr and A. K. Melin, founders of the Wham-o Corporation, saw Pipco's flyin' saucer being tossed at a southern California beach in 1955 and were intrigued by the toy. They approached Morrison and made an offer to buy the rights, and on January 13, 1957, Wham-o began production of its legendary Pluto Platter [5].

While promoting the Pluto Platter on Yale University campus Rich Knerr heard the term 'Frisbie'. With no idea of the historical origins of the term, Knerr trademarked the name as 'Frisbee' and renamed the company's Pluto Platter [5]. Throughout the 1960's the Frisbee™ became an increasingly popular toy and profits for the Wham-o Corporation continued to grow. The Mattel Corporation bought the Wham-o Corporation in 1994 and continues to manufacture and sell Frisbees™ worldwide [11].

2.2 ANATOMY OF A DISC

Figure 2.1, describes the major features found on most airborne discs [15]. Some discs have no cupola such as discs 'A' and 'C'. Others have an extremely different lip, edge, and cheek such as disc 'C'. Despite the differences between the many types of airborne discs, the anatomical nomenclature remains virtually the same. The above nomenclature will be used throughout this document to describe all airborne discs.

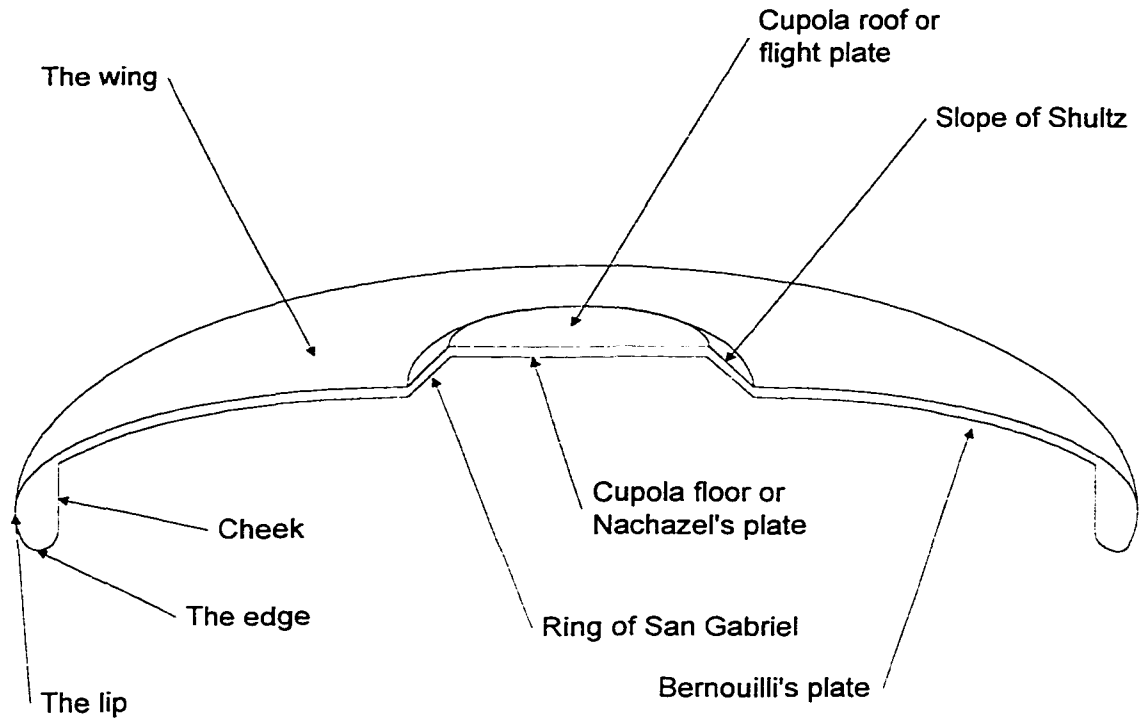

Figure 2.1 The anatomy of an airborne disc

2.3 EXPERIMENTAL WORK

Studies of air-borne rotating discs were conducted by Stilley [17]. These tests involved non-spinning wind tunnel experiments on three basic configurations, and a spinning wind tunnel test on one configuration. These tests used a side mount force dynamometer capable of measuring the pitching moment as well as the lift and drag. The three basic configurations were a clay pidgin skeet molded of plastic, an aluminum right circular cylinder, and an aluminum Frisbee™ type disc. All the wind tunnel data correlated well with the preliminary estimates with the exception of the pitching moment on the Frisbee™ disc. This pitching moment was much smaller than anticipated. Stilley hypothesized that if the center of pressure on this disc was far forward of the geometric

center, the dynamometer would read a much reduced pitching moment. While the side mounted dynamometer provided measurement sensitivity advantages, it also introduced flow interference, which could have caused the measured moments and the measured drag to be high. In addition to these wind tunnel tests, Stilley coordinated the filming of a series of 48 air launched free flight tests to record flight precession and trajectory. A theoretical trajectory model was derived and confirmed by experiment. He found that the spin effect itself is small and domed disc contours generate key aerodynamic characteristics, which are most prominent in the 3:1 to 2:1 diameter-to-thickness ratio (while most commercially available discs, Frisbees™, have an 8:1 diameter-to-thickness ratio). He also found that a spinning disc would precess about its velocity vector if there was an aerodynamic moment resulting from its angle of attack. A domed or cupped disc has a neutral aerodynamic moment at an angle of attack in which the lift equals the weight of the disc. The orientation of the disc, and not the initial flight path direction, was the dominant influence in determining the terminal flight behavior. Stilley thought that the flying disc could be modeled as a thin Magnus rotor. Pursuing this hypothesis, he created a program to simulate the trajectory of spinning discs. The program agreed reasonably well with the experimental data in high velocity, high spin rate simulations but fell short at lower speeds or lower spin rates. He concluded that the equilibrium glide condition for a 9-inch diameter, 8-ounce Frisbee™ would be a velocity of 34 feet per second and a spin rate of 1,399 rpm with an angle of attack of 12.5 degrees.

R. Chapman, P. Johnston, and D. Keenan of the Ryerson Polytechnic Institute conducted several experiments on discs in 1972 [1]. Using an 18" x 18" open circuit

wind tunnel, Chapman et al [1] measured the lift and drag on three different discs, a conventional Frisbee™ with ridges along the top surface, a smooth disc, and a slotted disc. In addition, they tuft tested the conventional disc and lamp black oil tested the smooth disc. To determine the average linear and angular velocity of a disc when thrown by hand, they photographed several free flights and found the average velocity to be 27.8 m/s and average angular velocity to be 322 rpm. They found that the lines of Headrick on a conventional disc increases the angle at which stall occurs but decreases the L/D ratio. Angular velocity tests showed a consistent decrease in drag at any forward velocity. However, their angular velocity tests also showed an inconsistent effect on lift that was probably due to experimental error. During the lamp black oil tests, this group observed a transition in the boundary layer from laminar to turbulent flow at the second row of oil dots (approximately 1 inch from the leading edge). The flow remained attached over the entire surface from 0° to 12° angle of attack. At 12°, the flow begins to detach from the trailing edge and the separation moves forward with increasing angle of attack until it is fully separated at 32° angle of attack. The thread tests were not conclusive. In all cases the smooth disc far outperformed the others at a L/D ratio 3 times higher at an 8-degree angle of attack. The slotted disc performed poorly and behaved contrary to expectations based on the theory of airfoils. Chapman et al [1] conclude that the best flight parameters for a Master Tournament model disc is a 4° angle of attack, with a forward velocity of 30 ft/s, and an angular velocity of 360 rpm. This group's test apparatus clearly influenced the flow within their test section. They compensated for the influence by subtracting the parasitic lift and drag of the apparatus from their experimental results.

During the late 1980's, Nakamura and Fukamachi [12] studied the effect of spin using smoke visualization in a large-scale subsonic wind tunnel. The subsonic wind tunnel measured 2m X 4m X 6m and was tested to a turbulence intensity of 0.12%. Their studies were conducted at a constant velocity of 1 m/s while the tip speed ratio was incrementally increased from 0 to 2.26. They found that rotation greatly increases the strength of a disc's vortex pair and shifts the pair slightly in the direction of rotation. This increased vortex strength causes a corresponding increase in the downwash and downstream turbulence behind the disc. Nakamura and Fukamachi found no evidence of any Magnus force on the disc. They conclude that the longitudinal vortices created by a disc are responsible for generating all of the vertical change in momentum within the flow and hence are responsible for the majority of the lift.

R. Imber and E. Rogers [4] while investigating the effect of forced circulation on circular planform wings performed a series of tests on a non-spinning disc. Like Nakamura and Fukamachi, they also conducted their test at a constant velocity of 20-psf dynamic pressure. Their tests were done at various angles of attack ranging from -5° to 30°. They also discovered the large vortices generated at the lateral edges of a disc. They postulated that stall phenomena begins at the lateral edges and moves inward toward the center. They concluded from their experiments that the boundary condition at the trailing edge of a disc had the most powerful influence on the circulation and therefore the lift of a disc.

Recently, Bill Crowther [26] measured the lift, drag, pitching moment, and rolling moment of discs. He varied the discs' camber, rotation, and angle of attack at several

different wind tunnel velocities. He found that rotation does not affect the coefficient of lift or the coefficient of drag on an airborne disc. However, increasing disc camber does increase lift. Rotation does effect the rolling moment of a disc, and affects the pitching moment of a disc. Increasing the disc forward velocity has a dampening effect on the pitching moment. Crowther's experiment [26] also indicated a tendency for pitching moment to oscillate about a fixed angle of attack given that the forward and angular velocities remain constant. This fixed angle of attack is dependent on the spin rate and is between 3° and 6°, as increasing forward velocity damps the pitching moment the fixed angle of attack narrows to 5°. Crowther's apparatus is quite complex and may have some force coupling occurring within it.

2.4 THEORETICAL WORK

In Neville De Mestre's 'The Mathematics of Projectiles in Sport', there is a simple analytical treatment on the aerodynamics of free-flying discs [2]. De Mestre suggests a Frisbee be treated much like an airfoil. He offers two equations to be solved numerically one for lift and the other for the drag. These equations are Newton's third law, F = ma, applied using the coefficient of lift and the coefficient of drag equations.

For lift:

$$m\frac{d^2x}{dt^2} = -\tfrac{1}{2}\rho A_r v^2 (C_D \cos\psi + C_L \sin\psi)$$

For drag:

$$m\frac{d^2y}{dt^2} = -mg + \tfrac{1}{2}\rho A_r v^2 (C_L \cos\psi + C_D \sin\psi)$$

where x and y represent horizontal and vertical position, respectively, Ψ is the disc's angle of attack, m is the disc's mass, g is gravity, C_L and C_D are the coefficients of lift and drag, A_F is the projected frontal area of the disc, ρ is density, and υ is velocity.

De Mestre introduces the initial-drag-to-weight ratio, ε, and believes this value could determine important flight characteristics about a free-flying disc [3].

$$\varepsilon = \frac{\rho A_F \upsilon_0^2 C_D}{2mg}$$

He discusses precession and states "precession may be thought of as a circular yaw about the center of gravity". He also applies Bernoulli's equation to a disc and concludes a disc's lift is a caused by a difference in air speeds across its top and bottom surfaces.

Dr. P. B. S. Lissaman contributed two papers. In the first, "Stability and Dynamics of a Spinning Oblate Spheroid"[8], Lissaman performed a conventional theoretical analysis of an airborne spinning disc. He showed that discs with more mass require less spin and that spin rate can never stabilize the disc. He describes four modes of disc flight.

Mode 1) The roll-off mode. This mode shows the disc's tendency to roll or precess about its velocity vector. This is known as precession in conventional ballistics.

Mode 2) The plunge mode. This mode shows the disc's tendency to topple end over end in flight. This mode is stabilized by the spin and the drag of the disc and is known as the phugoid mode in conventional aerodynamics.

Mode 3) The Heave-roll mode. This mode shows the disc's tendency to wobble in flight. This mode is stabilized by spin. It is known as the undulation mode in ballistics or as the Dutch-roll mode in aerodynamics.

Mode 4) The nutation mode. This mode is made up of heave, pitch and bank components, and is also stabilized by spin.

The second paper Lissaman offers is "Where Lift Comes From"[9], an extremely interesting paper on the aerodynamics of airfoils, much of which is directly applicable to airborne spinning discs. Lissaman gives a new perspective on the trailing and bound vortices. He shows that the bound vortex system causes lift by a change in momentum ahead of and behind the airfoil. He also shows that the bound and trailing vortices are mutually linked such that one cannot exist without the other. He explains that the trailing vortices are responsible for the drag by inducing a low pressure in the wake of an airfoil. Finally, Lissaman discusses the roll-up problem. Turbulence in the wake of an airfoil causes vortices to induce forces upon one another. The wing tip vortices tend to roll up like a scroll in the wake trailing the airfoil. The aerodynamics of wake vortices is not well understood. However, these effects are clearly evident in the wake of an airborne spinning disc.

Chen Maozhang and Zhu Guojun of Beijing University performed a numerical study on the three dimensional boundary layers of rotating bodies [10]. One such body was the spinning flat plate. They show that centrifugal force increases asymptotically from zero, at the center of the flat plate, to a maximum value at an infinite distance from the plate's center. The Coriolis forces increase initially then decrease to zero the further a streamline is from the center.

The Israeli Ministry of Defense asked Paul Katz to perform an analysis on the free flight of a rotating disc [6]. Katz published the results of his study in the Israel Journal of Technology, February, 1968. Katz linearized the six non-linear equations of motion and

then performed a numerical solution for a supersonic, fast rotating disc. Katz showed that the Magnus Moment diverged the motion of a disc and that precession stabilized that divergence. The Magnus effect was non-conservative and slowed down the rotation of the disc.

T. C. Soong performed a study on the dynamics of discus throws to determine the optimum throw angle of a discus for maximum distance [16]. Soong found that spin does affect the translatory motion or trajectory of a discus. He showed quantitatively that spin and initial angle of attack are prime factors in determining the maximum distance of a discus throw. He also showed numerically that initial angular velocity can affect the flight distance.

CHAPTER 3

EXPERIMENTAL SET-UP AND PROCEDURE

3.1 FACILITY AND EQUIPMENT

To characterize the flow over rotating and non-rotating disks, the University of Nevada, Las Vegas' 18" x 18" open circuit wind tunnel located in the Thomas T. Beam engineering complex at the Howard R. Hughes College of Engineering was used for the experimental studies.

The following is the list of equipment used to perform the calibration, lift and drag tests, center of lift tests, tuft tests, and smoke tests.

For Calibration:

- Force dynamometer with signal processor.
- Hot film anemometer with signal processor.
- Pitot tube.
- Micro-manometer.
- 3 meters of 6 mm diameter surgical rubber tubing.
- Calibration masses ranging from 50 grams to 2 kilograms.
- Calibration mount for the force dynamometer.

For Lift and Drag Tests:

- Force dynamometer with signal processor.
- Variable angle of attack mounting apparatus.

- 3 discs of variable type.
- 35 mm camera.

For Center of Lift Tests:

- Mounting pivot.
- 3 discs with mounting racks attached to underside.
- Pivot pin.
- Spool of 40 gauge steel wire.
- Counter masses.
- Mass shield.
- 35 mm camera.

For Tuft Tests:

- Spool of thread for tufts.
- Super Glue.
- 3 discs of variable type.
- Mounting apparatus with variable angle of attack.
- 35 mm camera.

For Smoke Tests:

- Smoke generator.
- Smoke rake.
- Aluminum disc with bearing mounted in underside.
- Threaded rod rotation rod.
- Variable speed drill.
- Mounting apparatus.

- Video camera.
- Videocassette recorder with TV monitor.
- Exterior lighting
- Non-reflective background material.
- 35 mm camera.

Before beginning the calibration or experiments the entire wind tunnel was moved, aligned, leveled, and balanced. The movement and alignment of the tunnel was necessary to ensure that debris did not block the entrance or exit of the tunnel and that back-pressures in the test section were minimized.

To include the pivot and mounting racks fastened to the underside of each disc, a mounting apparatus was designed and built in the machine shop at the Howard R. Hughes College of Engineering. Detailed drawings of the apparatus fabrication and set-up appear in later sections of the chapter. Before any measurements could be taken, the calibration and repeatability of the apparatus had to be determined.

3.2 CALIBRATION

The wind tunnel is rated for test section velocities of 0 to 150 feet per second with a maximum velocity of 200 feet per second. In actuality, the tunnel's maximum velocity is 153 feet per second and its minimum velocity is 6.4 feet per second. The turbulence intensity varied with velocity but was measured at 0.012 % at 30 feet per second.

To calibrate the test section velocities, a calibrated hot wire anemometer was used over the entire range of wind tunnel velocities, and a curve was generated relating velocity with the turbine power supply readings (see Figure 3.1). The hot wire was

calibrated just prior to wind tunnel test section velocity calibration. The test section velocities were again calibrated using a Pitot tube and micro-manometer to compare and contrast the differences between the hot wire anemometer and Pitot tube readings. Table 3.1 shows the results of the hot-wire anemometer test and Table 3.2 shows the results of the Pitot tube tests.

Wind tunnel Reading In hertz	Anemometer Reading In 1/1000 volt	Calculated Velocity In meters/sec
OFF	1948	0
10	3792	8.18
15	4075	13.41
20	4290	17.63
25	4462	21.75
30	4621	25.87
35	4749	30.00
40	4858	34.11
45	4996	38.24
50	5070	42.36
54.1	5113	45.74

March 23, 1994

Table 3.1 Hot-wire anemometer calibration of wind tunnel, Test 1

Wind tunnel Reading In hertz	Manometer Reading In 1/1000 inch
OFF	238
10	239
15	242
20	246
25	249
30	254
35	260
40	268
45	277
50	288
54.1	298

Table 3.2a Pitot tube calibration of test section, Test 1.

Wind tunnel Velocity In hertz	Manometer Measurement In 1/1000 Inch	Calculated Velocity In Meters/Sec	Calculated Velocity In Feet/Sec	Calculated Velocity In Miles/Hour
OFF	28.8	0.00	0.00	0.00
5.0	44.1	2.62	8.60	5.86
10.0	101.5	5.71	18.73	12.76
15.0	210.0	9.01	29.56	20.14
20.0	365.3	12.28	40.29	27.45
25.0	569.2	15.57	51.08	34.80
30.0	380.4	18.96	62.20	42.38
35.0	1144.0	22.36	73.36	49.98

July 18, 1995 Friday 11:50 am

Table 3.2b Pitot tube calibration of wind tunnel results, Test 2.

Test 3 utilized a different manometer than the first two Pitot tube tests and is more accurate than the first two. The difference in the results is substantial. Following the first test a potential blockage was found in the tubing which connected the Pitot tube to the micro-manometer.

Wind tunnel Velocity In hertz	Manometer Measurement In 1/1000 Inch	Calculated Velocity In Meters/Sec	Calculated Velocity In Feet/Sec
OFF	80	0.00	0.00
5.0	105	3.04	9.98
20.0	750	15.75	51.67
30.0	1695	24.46	80.25
35.0	2315	28.77	94.39
40.0	3075	33.30	109.25
45.0	3905	37.64	123.49
50.0	4895	42.23	138.55
51.0	5115	43.18	141.66
52.0	5320	44.05	144.52
53.0	5555	45.03	147.73
54.3	5870	46.31	151.92

July 21, 1997 Monday 10:00 am Sp. Gravity: 0.826

Table 3.2c Pitot tube calibration of wind tunnel results, Test 3.

As a consequence, the first tests were discarded. Another reason for the discrepancy between the Pitot tube and the anemometer is that the Pitot tubes are 6 inches long. Since the center of the test section is 9 inches from the nearest point on any wall, the pitot tube was unable to extend to the center of the section, a problem which the hot-wire did not have. All this disagreement in velocity prompted an entire recalibration using the hot-wire. The second hot-wire calibration agreed with the first. After checking the hot-wire calibration a third time, the hot-wire anemometer's results appeared reliable.

Once the test section velocities were determined, a NACA 0012 airfoil was tested. This test was necessary to validate the wind tunnel as a measurement system by comparing the results with known values for the airfoil. The results of this test were within 10% of those values known for the NACA 0012 airfoil. One possible explanation for this 10% difference is the gap between the wall of the test section and airfoil itself. This gap measured 1 cm on each side of the airfoil and most likely caused turbulence and increased drag. The tabulated results of this test and some calculated values appear in Table 3.3.

Test NACA 0012 lift/drag calibration
Airfoil chord length: 0.1525 m (6.00 inches)
Airfoil width: 0.0175 m (11/16 inches)
Pressure (atmospheric): 93908 Pa (704.54 mm Hg)
Temperature (atmospheric): 296.8 Kelvin (23.8 degrees Celsius)
Test section velocity for all tests: 17.625 m/s (20.0 Hz)

Test	Lead Edge Height in meters (inches)	Trail Edge Height in meters (inches)	Raw drag in newtons	Raw lift in newtons
1	0.257 10-1/8	0.236 9-9/32	-0.45 +/-0.05	8.0 +/-0.1
2	0.254 10	0.240 9-14/32	-0.35 +/-0.1	6.1 +/-0.1
3	0.251 9-7/8	0.244 9-19/32	-0.3 +/-0.1	4.0 +/-0.1
4	0.248 9-3/4	0.248 9-3/4	-0.3 +/-0.05	2.4 +/-0.05
5	0.244 9-5/8	0.252 9-29/32	-0.45 +/-0.05	1.1 +/-0.2
6	0.240 9-7/16	0.256 10-1/16	-0.55 +/-0.05	-4.7 +/-0.2

Table 3.3a Experimental data from the NACA 0012 airfoil test.

Test	AOA in degrees	Frontal Area (m^2)	Drag Coefficient	Lift Coefficient	Lift/Drag Ratio
1	7.92	0.01085	0.1238	0.5815	4.70
2	5.23	0.00850	0.0893	0.4178	4.68
3	2.63	0.00775	0.0603	0.2369	3.93
4	0	0.00776	0.0602	0.0991	1.65
5	-3.01	0.00775	0.1733	-0.0129	-0.07
6	-6.02	0.00919	0.2097	-0.5126	-2.44

Table 3.3b Calculated results of NACA 0012 airfoil test.

To calibrate the force dynamometer, the dynamometer was isolated upon a calibration mount and loaded with 50, 100, 500, 1000 and 2000-gram weights in both the lift and drag directions. Potentiometers on the back of the signal processor were adjusted to measure the lift and drag loads in Newtons. The potentiometers were then locked into place.

To ensure the overall validity of the wind tunnel test, the hot-wire anemometer was used to determine the turbulence intensity of the test section at a velocity of 17.63 m/s (20 hertz), above the primary test velocities for these disc experiments. The turbulence intensity climbed rapidly after 30.84 m/s (35 hertz).

As part of the calibration, the parasitic lift and drag of the force dynamometer's post and mount was measured without attached experiment. These values were used to

determine the accuracy of the raw lift and drag values measured during experiment. A table outlining the results of the parasitic lift and drag experiment can be found in the Appendix (Table A.1).

3.3 LIFT AND DRAG SET-UP

The first experiment was to determine the lift and drag present upon a non-rotating, free-flying disc. Three different discs were compared in this experiment. Each disc had a unique contour and camber, which yielded noticeable differences in lift, drag and lift/drag ratio. To prepare the test section for this experiment, an aluminum mounting block was machined and fastened securely to the mounting post of the force dynamometer. A 70mm long, 6mm diameter threaded steel rod extended from the top of this block. The top of the rod was drilled and tapped to fit a 2mm-diameter screw. A corresponding 2mm hole was drilled in the top of each disc. A thin steel washer was placed upon the top of the rod and the test disc was placed on top of the washer. The disc was attached to the test stand by the 2mm set screw. The mounting block was designed to allow changes in the angle of attack by pivoting upon a fastening screw. Minimum and maximum angles of attack were –5 degrees and 12 degrees respectively. Figure 3.2 shows a schematic diagram of the lift and drag mount assembly (this diagram is not to scale). A schematic diagram of the assembly setup within the wind tunnel test section is shown in Figure 3.3.

PROCEDURE:

Once the setup was complete, the experiment was ready to begin. The following is the procedure used to attain the data.

1. Set the Angle Of Attack (AOA) on the disc by measuring the distance from the bottom of the test section to the leading and trailing edge of the disc and tightening the mounting block set screw at the desired AOA.
2. Zero the force dynamometer by adjusting the lift and drag thumb wheels and monitoring the signal processor.
3. Turn on the wind tunnel and let it idle for 10 minutes to warm up. NOTE: Failure to allow adequate time for warm up can result in a large hysteresis.
4. Set the starting velocity (8.0 Hz) and allow 1 minute for the velocity in the test section to settle.
5. Record the lift and drag measured on the signal processor.
6. Increment the velocity (4.0 Hz) and allow 1 minute for the velocity in the test section to settle.
7. Repeat steps 5 and 6 until complete.
8. Turn the wind tunnel off and re-zero the force dynamometer to eliminate any hysteresis.
9. Adjust the AOA.
10. Repeat steps 4 through 9 until the experiment is complete.

Once the above steps were completed for one disc another disc would be set in its place and the complete set of steps would be repeated again.

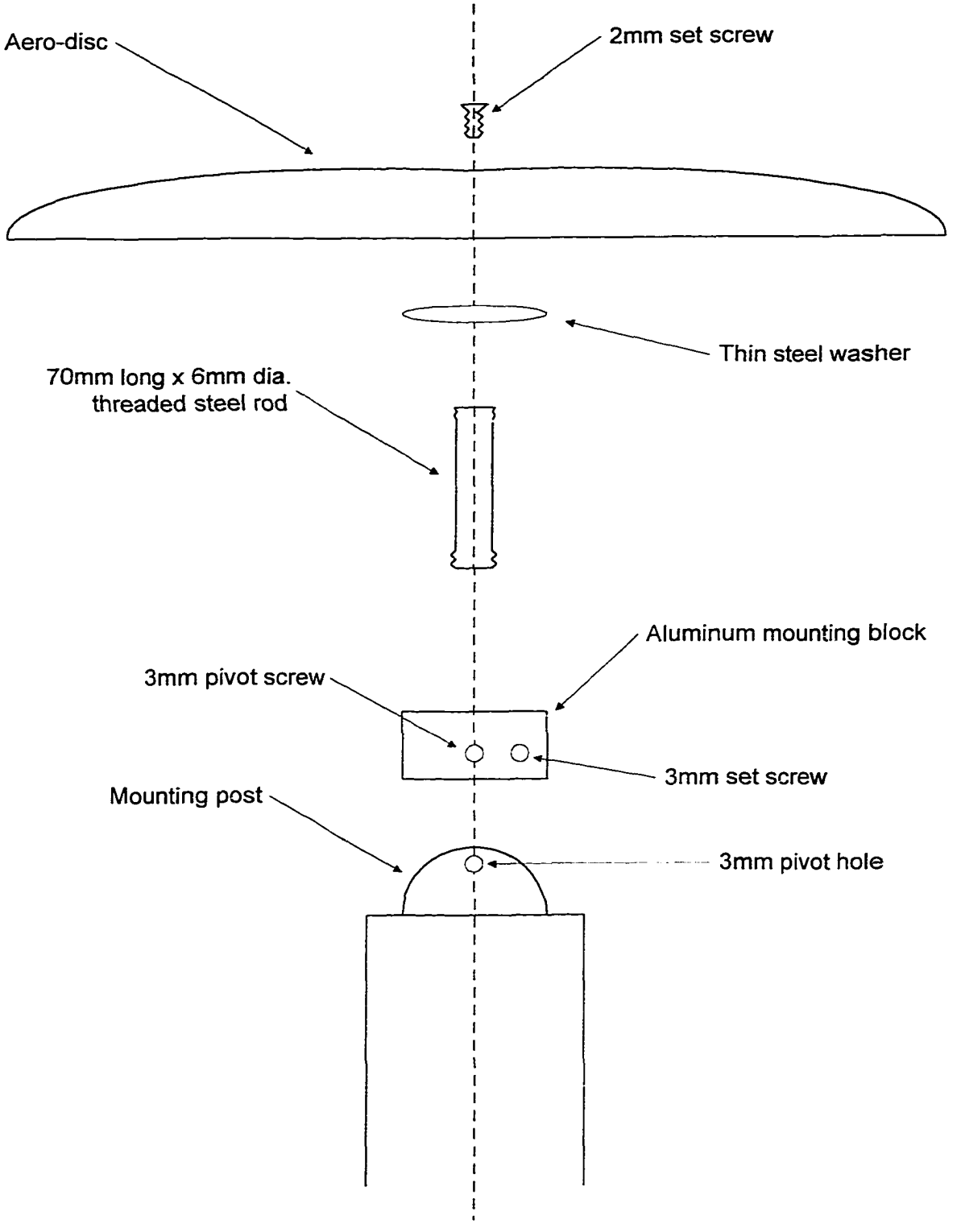

Figure 3.2 Lift and drag mounting assembly.

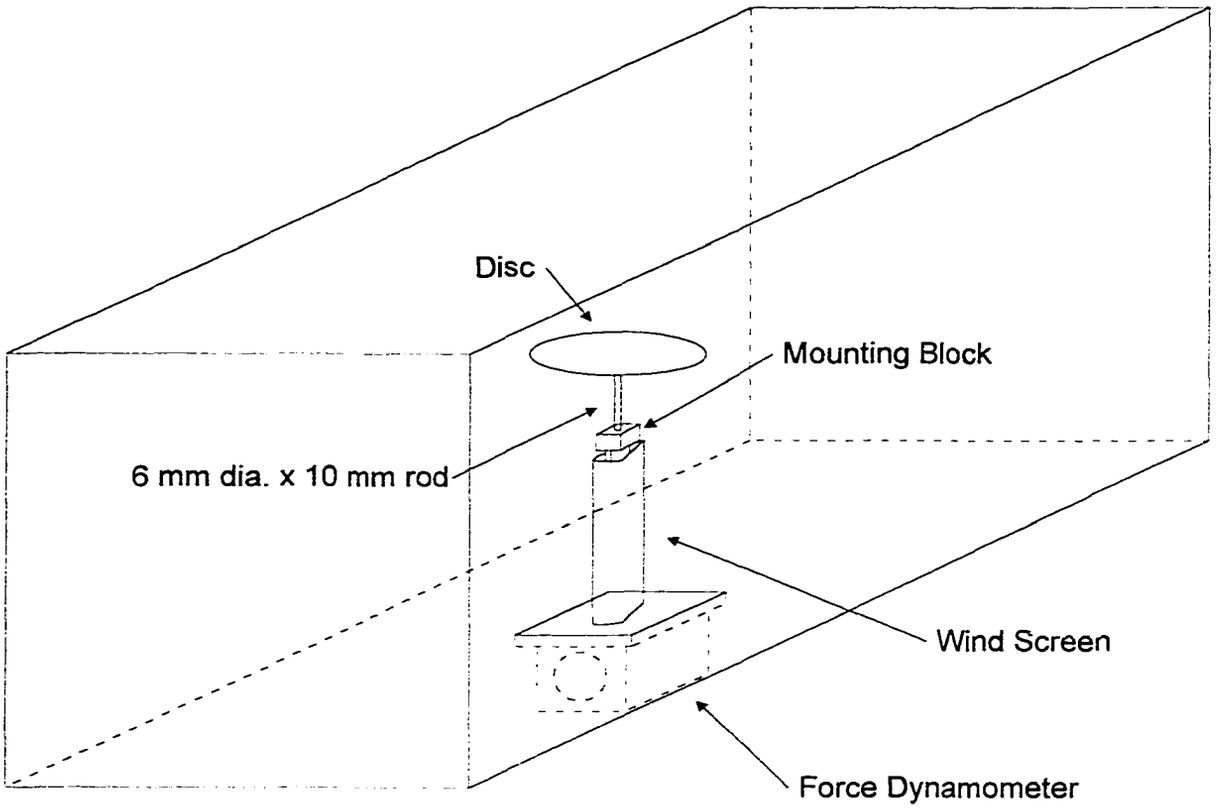

Figure 3.3 Lift and drag setup in test section.

3.4 CENTER OF LIFT SET-UP

The next set of experiments was made to determine the center of lift location of a non-rotating, free-flying disc. Discs of the same contour, camber, and shape as those used in the previous lift and drag experiments were examined. The logic behind this experiment was to balance a disc on a pivot point and to examine under the controlled flow of a wind tunnel whether the disc tends to flip forward or flip backward. A forward flipping tendency would indicate a center of lift location behind the pivot point. Conversely, a backward tendency indicates the center of lift is ahead of the pivot point. By moving the pivot point and re-testing the exact location of the center of lift can be determined.

To allow the disc to pivot about a point two parallel rails were mounted in the concave underside of the discs. Each of the rails were drilled with 2mm holes every 6.5mm. A 2mm pivot pin attaches the disc, through the holes in the rails, to a rigid mount with the test section. It is evident that the pivot point may not, and indeed usually will not, be located under the center of mass of the disc. To hold the disc at a level attitude (0° AOA) a counter mass was hung either from the front or from the rear of the disc. Under test conditions, minute variations in the disc's AOA occurred. To assist in recording these variations a thin rigid wire was mounted horizontally 2mm under the rear of the disc. By examining the change in distance between the wire and the trailing edge, the forward or backward flipping tendency can be recorded. Figure 3.4 is a diagram showing the experiment assembly. A free body diagram outlines the balancing of the disc and is shown in Figure 3.5. Figure 3.6 shows the complete experimental setup.

Procedure:

1. Set the disc in the test section and balance it with the proper counter mass.
2. Turn on the wind tunnel and let it idle for 10 minutes to warm-up. NOTE: Failure to allow adequate time for warm up can result in a large hysteresis.
3. Observe the response of the disc to the wind tunnel at idle. Occasionally, the low velocity that results from the wind tunnel turbine idling upsets the disc's balance.
4. Increment the wind tunnel velocity. Use very small increments. (0.7 m/s).
5. Record the response of the disc.

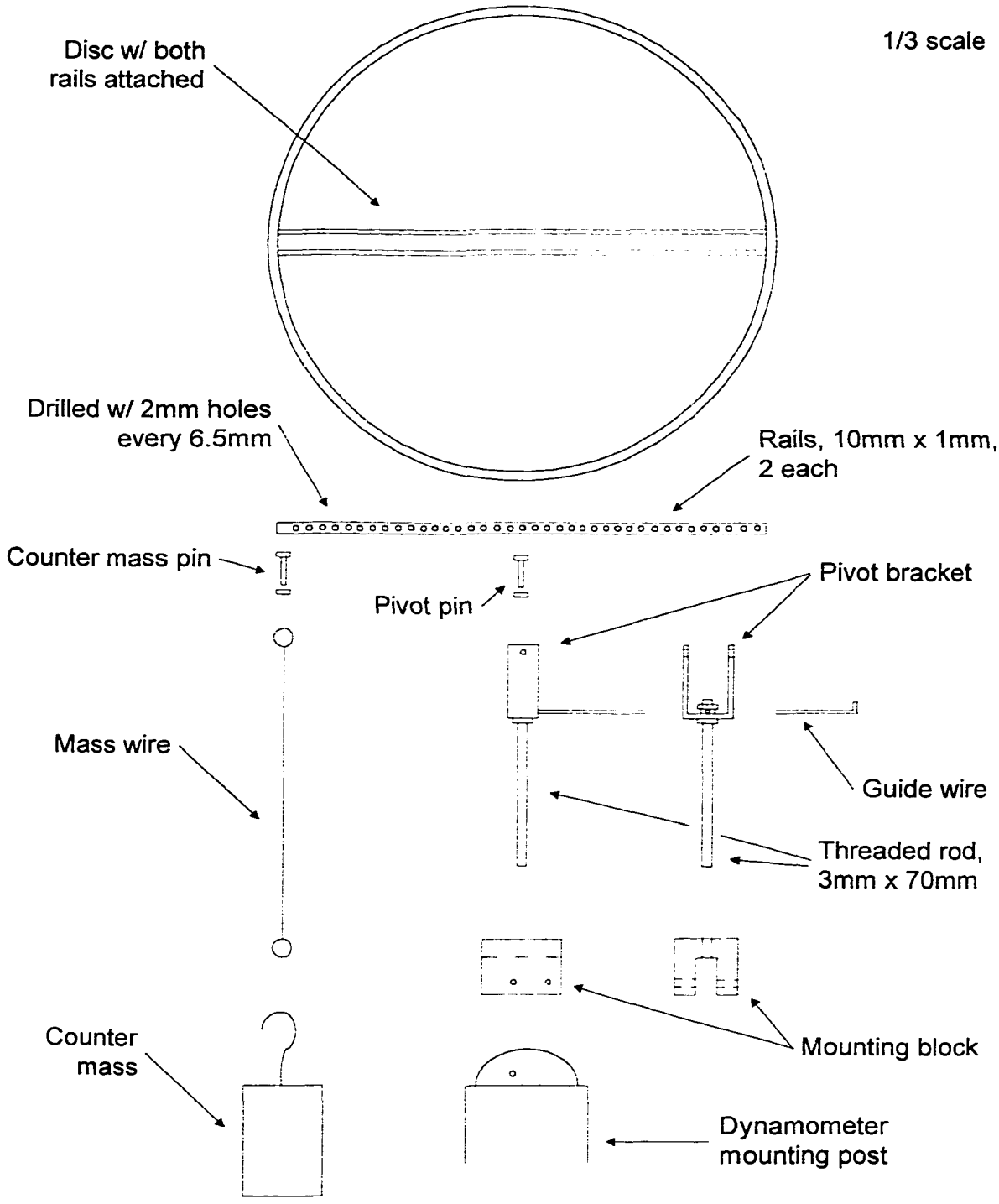

Figure 3.4 Center of lift assembly diagram.

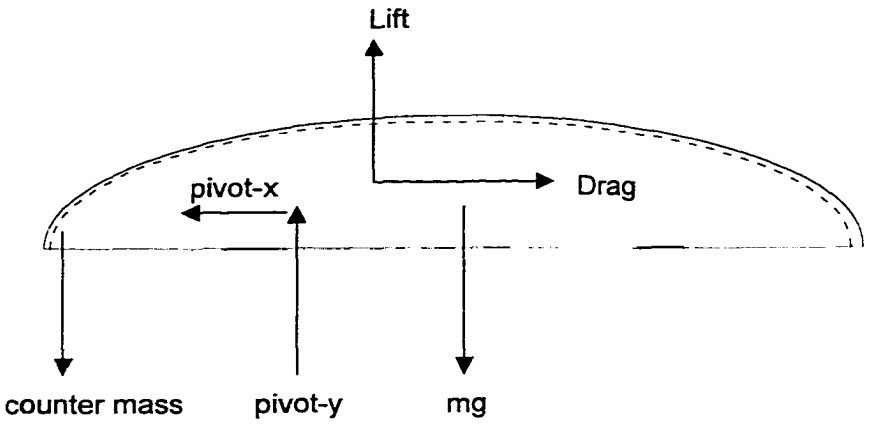

Figure 3.5 Center of lift free body diagram.

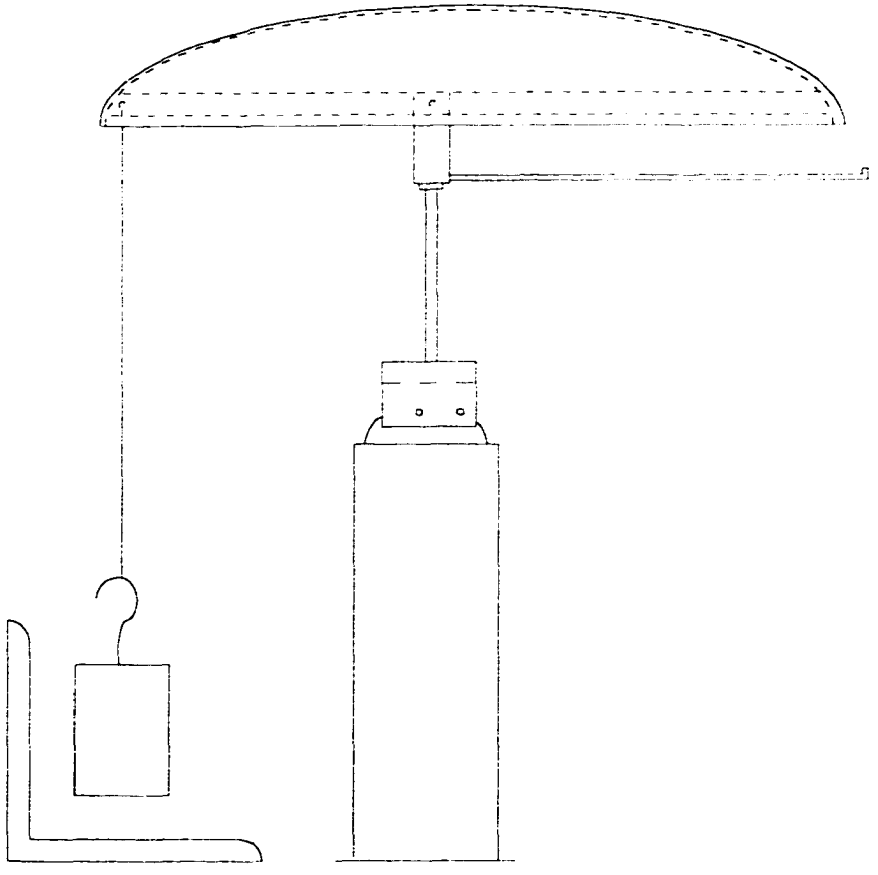

Figure 3.6 Center of lift test section setup.

6. Repeat steps 4 and 5 until the disc shows a clear forward or backward flipping tendency.
7. Return the wind tunnel to idle.
8. Increment the pivot point and adjust the counter mass accordingly.
9. Repeat steps 2 through 8 until all the pivot points are tested.

3.5 TUFT TEST SET-UP

The third experiment was to determine the boundary layer upon a non-rotating, free-flying disc. Three different discs are again compared in this experiment. Each was covered with rows of one-inch thread tufts. The experimental setup was much the same as the one used in the lift and drag test, utilizing the aluminum mounting block fastened securely to the mounting post of the force dynamometer. A threaded steel rod, 70mm long and 6mm in diameter extended from the top of the aluminum block. The top of the rod was drilled and tapped to fit a 2mm-diameter screw. A corresponding 2mm hole was drilled in the top of each disc. A thin steel washer was placed upon the top of the rod and the test disc was placed on top of the washer. The entire assembly was held together by the 2mm set screw. The mounting block was designed to allow changes in the angle of attack by pivoting upon a fastening screw. Minimum and maximum angles of attack were –20 degrees and +20 degrees respectively. Figure 3.7 shows a schematic diagram of the tuft test mount assembly (this diagram is not to scale). A schematic diagram of the assembly setup within the wind tunnel test section is shown in Figure 3.8.

Once the setup was complete, the experiment was ready to begin. The following is the procedure used to secure the information uncovered by this experiment.

Procedure:

1. Set the Angle Of Attack (AOA) on the disc by measuring the distance from the bottom of the test section to the leading and trailing edge of the disc and tightening the mounting block set screw at the desired AOA.
2. Turn on the wind tunnel and allow 10 minutes for the turbine to warm up. NOTE: Failure to allow an appropriate warm up time can result in a large hysteresis.
3. Set the wind tunnel to the starting velocity (4.0 Hz).
4. Observe, record, and photograph the tuft response to the velocity.
5. Increment the velocity (I used 4.0 Hz increments).
6. Repeat steps 4 and 5 until the test is complete.

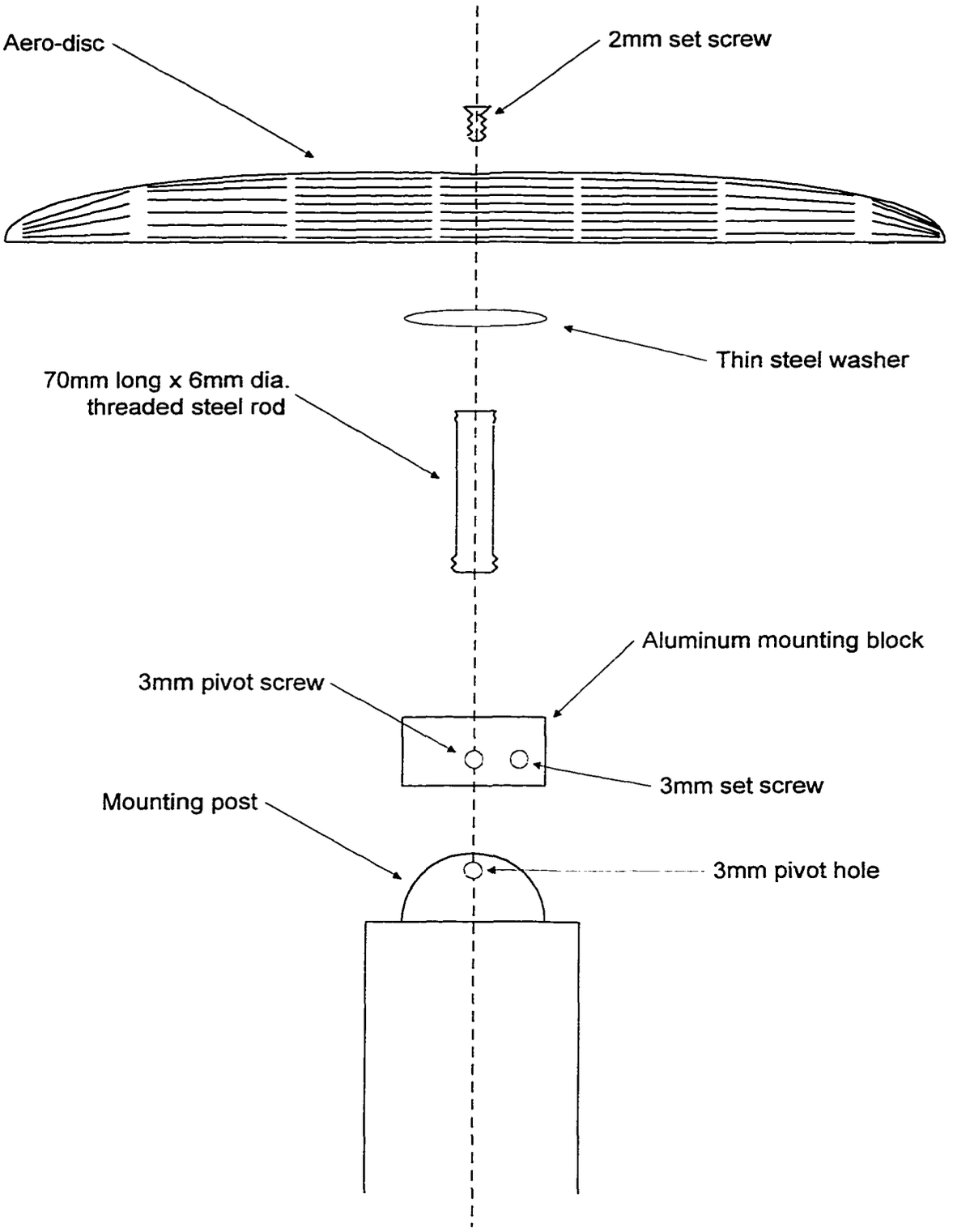

Figure 3.7 Tuft test assembly.

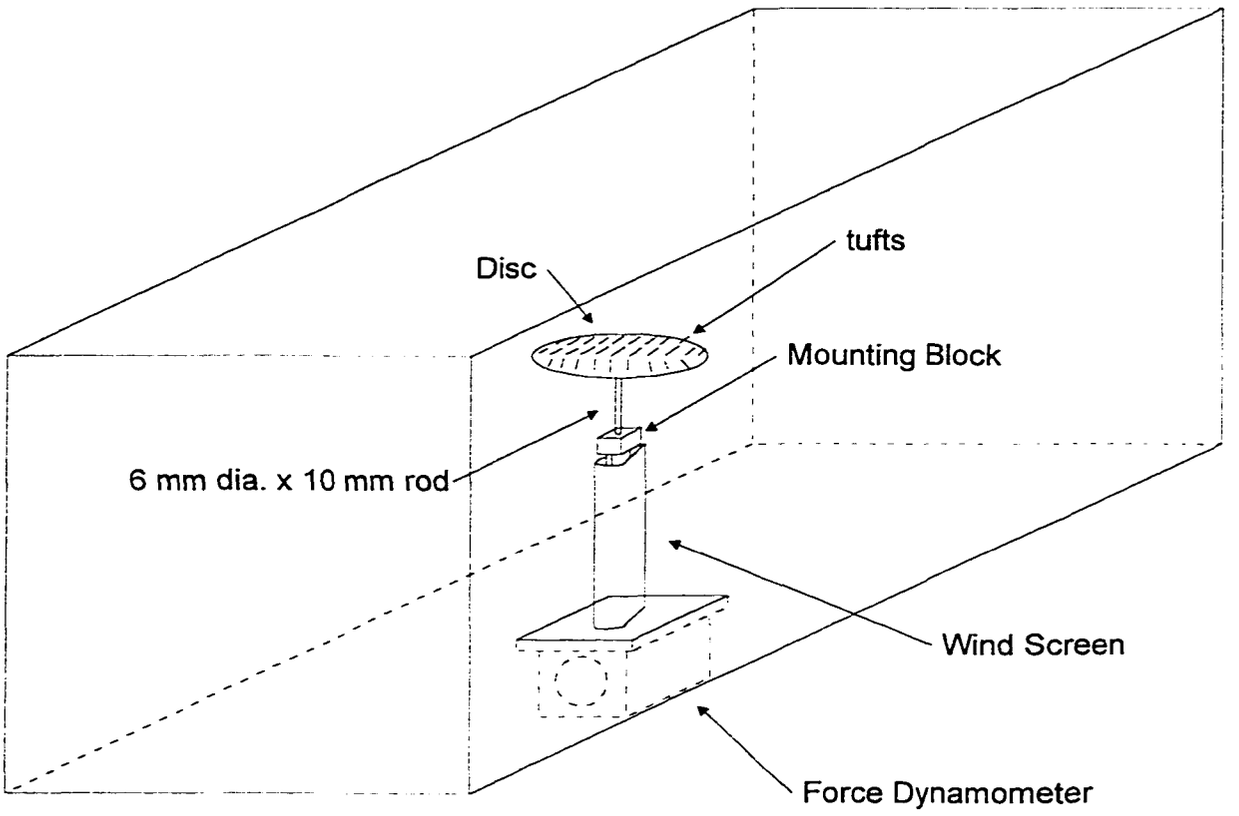

Figure 3.8 Tuft test setup in test section.

3.6 SMOKE TEST SET-UP

In the fourth and final test, smoke visualization was used to image the boundary layer and wake of a rotating free-flying disc. A color video camera and a 35mm camera were used to record these images. Two tests were conducted: the first was at 0° AOA and lasted 2 minutes and 57 seconds, the second was at a positive AOA and lasted 2 minutes and 30 seconds.

For these experiments the tip speed ratio for a hand-thrown disc was matched at 0.4378 but the Reynolds number was not. The reason is simple; a 1:3 scale aluminum disc was machined specifically for this experiment. Due to its smaller diameter, a larger than usual velocity is required to match the Reynolds number. However, higher

velocities come with greater difficulties. The first difficulty is the second requirement for dynamic similitude, the tip speed ratio. Higher linear velocities require higher angular velocities to match the tip speed ratio. If the Reynolds number is matched then the angular velocity required is enormous and was beyond the ability of the facility to provide it. The second difficulty was the flow visualization. Higher velocities thin the smoke stream and disperse it more quickly. Smoke equipment requires a high-pressure reservoir to inject smoke with a larger mass flow rate. Furthermore, a tunnel that produces extremely low turbulence intensities at high velocities would have to be utilized. A Reynolds number of 33,153 was used (approximately one-fifth the number for a hand-thrown conventional disc).

The video camera was mounted outside of the test section just behind and slightly above the disc. The camera was attached via a coaxial cable to a SVHS videocassette recorder and color TV monitor. The hand-held 35mm camera was located just ahead of and slightly above the disc. To illuminate the smoke within the tunnel two external light sources were mounted above the test section and a non-reflective background was taped to the far side of the test section. The videocassette used was TDK Extra High Grade (EHG), while the 35mm film used was fujicolor ASA 800.

The disc was made of aluminum, 110mm in diameter, and fabricated with a bearing seated in the underside. A steel rod 70mm long and 5mm in diameter was press fit into the inner race of the bearing and held fast with Loc-tite™ sealant. The top of the disc was drilled and tapped to allow the threaded end of a 2.5mm steel dowel. The dowel, 250mm in length, extended up through the Plexiglas of the wind tunnel test section. A Black & Decker™ variable speed drill, set to 180 rpm, was fitted to the top of the dowel. The

70mm long steel rod was threaded into the mounting block, which was attached to the force dynamometer's mount point.

The smoke generator and smoke rake, both manufactured by Aerolab, were mounted atop the wind tunnel with the smoke rake inserted through a slot in the top of the test section. The smoke rake was held 300mm from the leading edge of the disc and manually manipulated vertically and horizontally to capture the streamlines above, below and around the spinning disc. Several photographs, a videotape, and personal observations were recorded. Figure 3.9 shows the assembly of the disc test apparatus. A diagram of the interior test section setup is shown in Figure 3.10. Figure 3.11 shows a diagram of the exterior test section setup.

Procedure:

1. Set the disc in the test apparatus within the wind tunnel.
2. Turn on the wind tunnel and allow adequate time for it to warm up.
3. Set the wind tunnel to the test velocity.
4. Turn the video monitor on and press record on the VCR.
5. Turn the pressure on the smoke generator up to 30 psi.
6. When oil begins leaking from the tip of the smoke rake, turn on the smoke generator's heater.
7. Wait 45 seconds or until smoke begins.
8. Start the drill (to rotate disc).
9. Move the smoke rake horizontally and vertically to capture the streamlines around the disc.

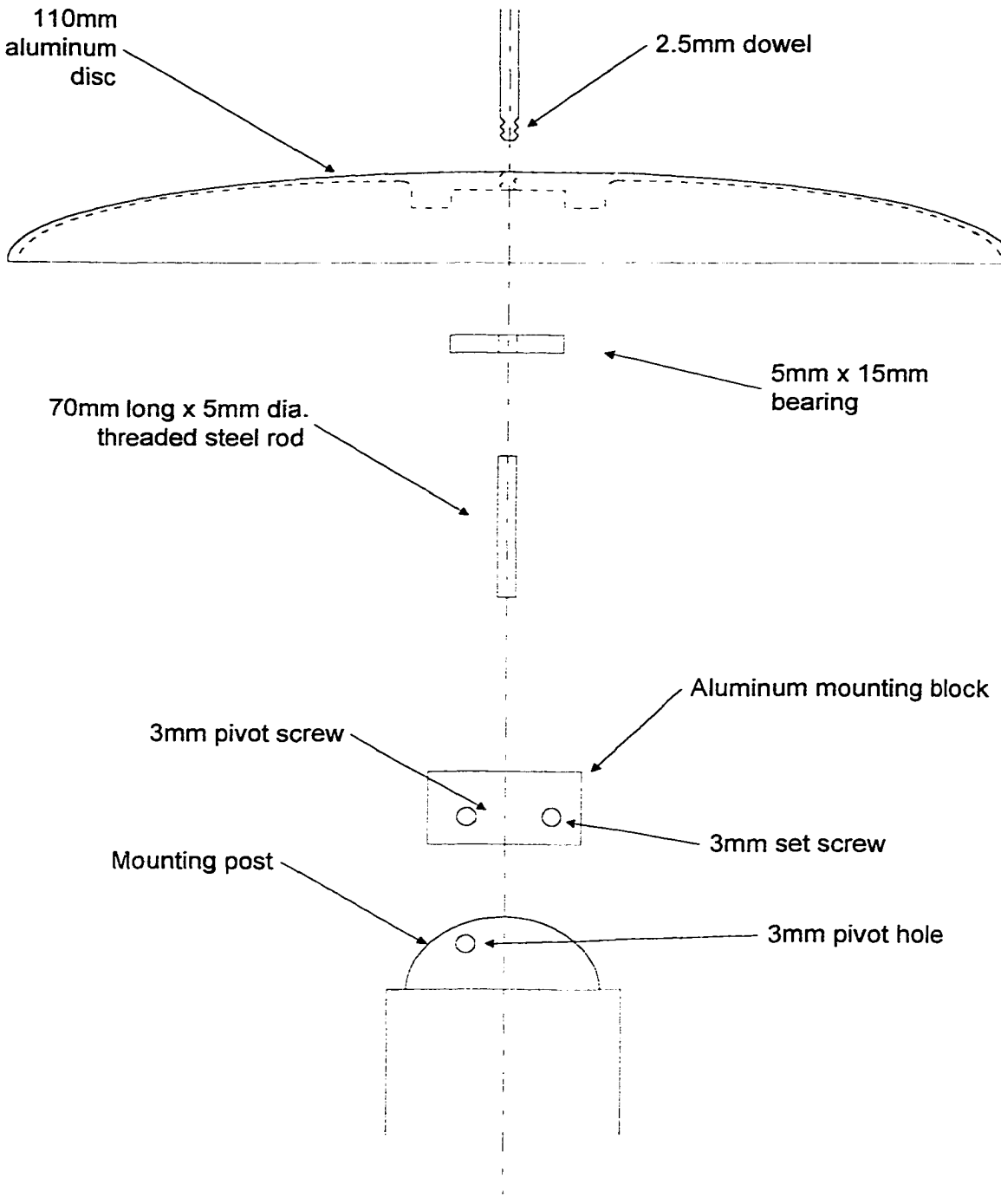

Figure 3.9 Assembly of apparatus for spinning disc test.

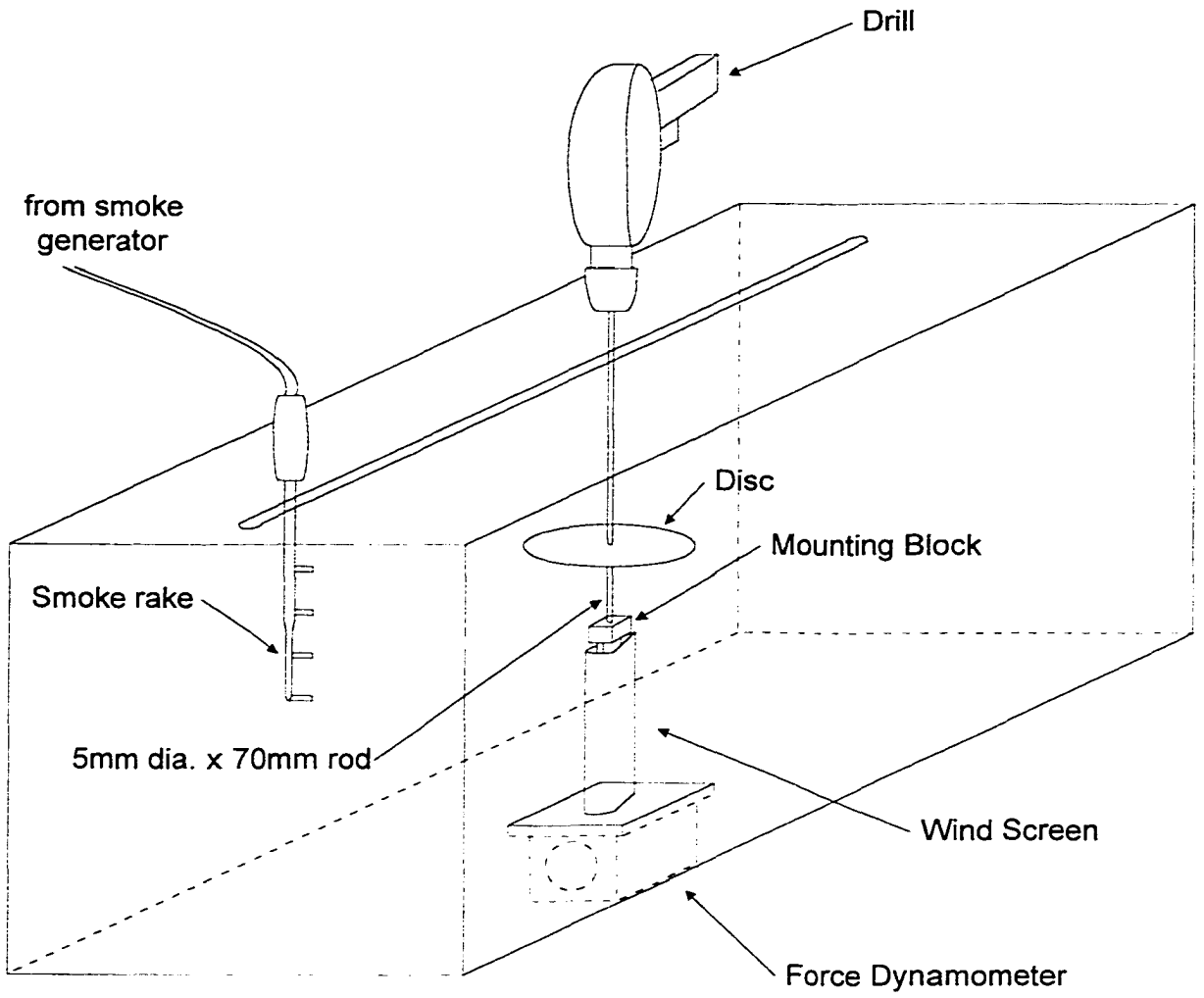

Figure 3.10 Wind tunnel setup for smoke visualization.

10. Photograph the streamlines and record observations.

11. Turn heater on smoke generator off.

12. When smoke rake cools, turn down the smoke generator pressure.

13. Adjust the angle of attack.

14. Repeat steps 5 through 13 until done.

CHAPTER 4

EXPERIMENTAL ANALYSIS

4.1 LIFT AND DRAG ANALYSIS

The data recorded in Appendix B was used to determine the lift and drag coefficients, the lift to drag ratio, the effects of velocity and angle of attack, and the effects of the disc contour and leading edge.

The raw value for lift was converted into a dimensionless coefficient using the well-known coefficient of lift equation given in Anderson [25].

$$C_L = \frac{2LRT}{PSV^2} \qquad \text{[EQ. 4.1]}$$

where L is the raw lift value, R is the gas constant, T is the absolute temperature, P is pressure, S is the planform area of the airfoil, and V is the velocity.

Similarly, the raw value for drag is converted using its corresponding equation in Anderson.

$$C_D = \frac{2DRT}{PA_fV^2} \qquad \text{[EQ. 4.2]}$$

where D is the raw drag value and A_f is the projected frontal area.

Tables 4.1 through 4.9 show the coefficients of lift and drag for each disc by Reynolds number.

Disc 'A'			Disc 'B'			Disc 'C'		
Reynolds number	C_L	C_D	Reynolds number	C_L	C_D	Reynolds number	C_L	C_D
42,170	-0.1388	0.0000	43,077	0.0000	0.0000	39,044	-0.0830	0.0000
93,680	-0.0432	-0.0288	94,484	-0.0425	-0.0283	85,639	-0.0345	0.0000
154,957	-0.0317	-0.0211	156,287	-0.0363	-0.0208	141,656	-0.0063	-0.0189
216,578	-0.0243	-0.0189	218,437	-0.0292	-0.0186	197,988	0.0032	-0.0162
275,940	-0.0300	-0.0166	278,309	-0.0294	-0.0180	252,255	0.0080	-0.0159
331,129	-0.0324	-0.0173	333,971	-0.0296	-0.0182	302,706	0.0097	-0.0166
386,317	-0.0331	-0.0170	389,633	-0.0326	-0.0184	353,157	0.0183	-0.0163
441,505	-0.0325	-0.0163	445,295	-0.0326	-0.0166	403,608	0.0241	-0.0163

Table 4.1, Coefficients of lift and drag at -20° AOA

Disc 'A'			Disc 'B'			Disc 'C'		
Reynolds number	C_L	C_D	Reynolds number	C_L	C_D	Reynolds number	C_L	C_D
42,170	-0.0694	0.0000	43,077	0.0000	0.0000	39,044	-0.0830	0.0000
93,680	-0.0288	-0.0288	94,484	-0.0283	-0.0283	85,639	-0.0172	0.0000
154,957	-0.0264	-0.0211	156,287	-0.0311	-0.0208	141,656	0.0063	-0.0126
216,578	-0.0216	-0.0189	218,437	-0.0266	-0.0159	197,988	0.0097	-0.0129
275,940	-0.0266	-0.0166	278,309	-0.0262	-0.0164	252,255	0.0120	-0.0159
331,129	-0.0289	-0.0162	333,971	-0.0273	-0.0159	302,706	0.0180	-0.0152
386,317	-0.0297	-0.0161	389,633	-0.0301	-0.0167	353,157	0.0244	-0.0152
441,505	-0.0306	-0.0150	445,295	-0.0313	-0.0160	403,608	0.0304	-0.0148

Table 4.2, Coefficients of lift and drag at -15° AOA

Disc 'A'			Disc 'B'			Disc 'C'		
Reynolds number	C_L	C_D	Reynolds number	C_L	C_D	Reynolds number	C_L	C_D
42,170	-0.0694	0.0000	43,077	-0.0682	0.0000	39,044	-0.0830	0.0000
93,680	0.0000	-0.0288	94,484	0.0000	0.0283	85,639	0.0000	0.0000
154,957	0.0053	-0.0211	156,287	0.0000	-0.0259	141,656	0.0189	-0.0126
216,578	0.0000	-0.0162	218,437	-0.0027	-0.0186	197,988	0.0194	-0.0129
275,940	-0.0216	-0.0166	278,309	-0.0115	-0.0180	252,255	0.0219	-0.0139
331,129	-0.0243	-0.0150	333,971	-0.0159	-0.0159	302,706	0.0263	-0.0138
386,317	-0.0263	-0.0136	389,633	-0.0175	-0.0150	353,157	0.0335	-0.0142
441,505	-0.0273	-0.0137	445,295	-0.0192	-0.0153	403,608	0.0366	-0.0140

Table 4.3, Coefficients of lift and drag at -10° AOA

Disc 'A'			Disc 'B'			Disc 'C'		
Reynolds number	C_L	C_D	Reynolds number	C_L	C_D	Reynolds number	C_L	C_D
42,170	-0.0694	0.0000	43,077	0.0000	0.0000	39,044	-0.1661	0.0000
93,680	0.0000	-0.0144	94,484	0.0000	-0.0142	85,639	-0.0517	0.0000
154,957	0.0053	-0.0158	156,287	0.0052	-0.0156	141,656	-0.0063	-0.0126
216,578	0.0108	-0.0135	218,437	0.0080	-0.0133	197,988	0.0194	-0.0129
275,940	0.0150	-0.0133	278,309	0.0098	-0.0147	252,255	0.0239	-0.0120
331,129	0.0185	-0.0127	333,971	0.0102	-0.0136	302,706	0.0291	-0.0138
386,317	0.0195	-0.0119	389,633	0.0109	-0.0142	353,157	0.0356	-0.0142
441,505	0.0208	-0.0117	445,295	0.0115	-0.0141	403,608	0.0412	-0.0140

Table 4.4, Coefficients of lift and drag at -5° AOA

Disc 'A'			Disc 'B'			Disc 'C'		
Reynolds number	C_L	C_D	Reynolds number	C_L	C_D	Reynolds Number	C_L	C_D
42,170	-0.0694	0.0000	43,077	0.0000	0.0000	39,044	-0.3322	0.0000
93,680	0.0000	0.0000	94,484	0.0142	-0.0142	85,639	-0.1035	0.0000
154,957	0.0158	-0.0106	156,287	0.0208	-0.0104	141,656	-0.0126	-0.0126
216,578	0.0216	-0.0108	218,437	0.0213	-0.0106	197,988	0.0194	-0.0129
275,940	0.0233	-0.0100	278,309	0.0213	-0.0098	252,255	0.0279	-0.0120
331,129	0.0289	-0.0116	333,971	0.0239	-0.0102	302,706	0.0360	-0.0138
386,317	0.0314	-0.0119	389,633	0.0292	-0.0117	353,157	0.0447	-0.0142
441,505	0.0338	-0.0111	445,295	0.0339	-0.0134	403,608	0.0467	-0.0140

Table 4.5, Coefficients of lift and drag at 0° AOA

Disc 'A'			Disc 'B'			Disc 'C'		
Reynolds number	C_L	C_D	Reynolds number	C_L	C_D	Reynolds number	C_L	C_D
42,170	0.0000	0.0000	43,077	0.0000	0.0000	39,044	-0.3322	0.0000
93,680	0.0288	-0.0144	94,484	0.0283	-0.0142	85,639	-0.0690	-0.0517
154,957	0.0369	-0.0158	156,287	0.0259	-0.0104	141,656	0.0000	-0.0316
216,578	0.0352	-0.0135	218,437	0.0239	-0.0106	197,988	0.0259	-0.0227
275,940	0.0349	-0.0133	278,309	0.0245	-0.0115	252,255	0.0319	-0.0179
331,129	0.0382	-0.0127	333,971	0.0273	-0.0114	302,706	0.0401	-0.0180
386,317	0.0433	-0.0136	389,633	0.0301	-0.0142	353,157	0.0478	-0.0173
441,505	0.0429	-0.0124	445,295	0.0332	-0.0134	403,608	0.0498	-0.0163

Table 4.6, Coefficients of lift and drag at 5° AOA

Disc 'A'			Disc 'B'			Disc 'C'		
Reynolds number	C_L	C_D	Reynolds number	C_L	C_D	Reynolds number	C_L	C_D
42,170	0.0000	0.0000	43,077	0.0000	-0.0682	39,044	-0.3322	-0.0830
93,680	0.0432	-0.0144	94,484	0.0425	-0.0283	85,639	-0.0345	-0.0345
154,957	0.0369	-0.0106	156,287	0.0363	-0.0156	141,656	0.0253	-0.0253
216,578	0.0406	-0.0108	218,437	0.0319	-0.0133	197,988	0.0356	-0.0227
275,940	0.0483	-0.0133	278,309	0.0376	-0.0131	252,255	0.0359	-0.0199
331,129	0.0532	-0.0139	333,971	0.0375	-0.0136	302,706	0.0457	-0.0194
386,317	0.0577	-0.0144	389,633	0.0376	-0.0150	353,157	0.0518	-0.0193
441,505	0.0540	-0.0143	445,295	0.0371	-0.0141	403,608	0.0568	-0.0187

Table 4.7, Coefficients of lift and drag at 10° AOA

Disc 'A'			Disc 'B'			Disc 'C'		
Reynolds number	C_L	C_D	Reynolds number	C_L	C_D	Reynolds number	C_L	C_D
42,170	0.0000	0.0000	43,077	0.0000	-0.0682	39,044	-0.2491	-0.1661
93,680	0.0432	-0.0144	94,484	0.0850	-0.0283	85,639	-0.0172	-0.0690
154,957	0.0475	0.0000	156,287	0.0623	-0.0208	141,656	0.0379	-0.0379
216,578	0.0406	-0.0027	218,437	0.0532	-0.0186	197,988	0.0453	-0.0259
275,940	0.0483	-0.0067	278,309	0.0458	-0.0147	252,255	0.0438	-0.0219
331,129	0.0543	-0.0069	333,971	0.0511	-0.0159	302,706	0.0526	-0.0208
386,317	0.0586	-0.0102	389,633	0.0492	-0.0175	353,157	0.0589	-0.0193
441,505	0.0527	-0.0117	445,295	0.0454	-0.0166	403,608	0.0654	-0.0187

Table 4.8, Coefficients of lift and drag at 15° AOA

Disc 'A'			Disc 'B'			Disc 'C'		
Reynolds number	C_L	C_D	Reynolds number	C_L	C_D	Reynolds number	C_L	C_D
42,170	0.1388	0.0000	43,077	0.2047	-0.1364	39,044	-0.1661	-0.3322
93,680	0.0721	-0.0288	94,484	0.1134	-0.0425	85,639	0.0000	-0.1035
154,957	0.0580	-0.0211	156,287	0.0778	-0.0259	141,656	0.0505	-0.0505
216,578	0.0487	-0.0162	218,437	0.0744	-0.0213	197,988	0.0518	-0.0324
275,940	0.0599	-0.0166	278,309	0.0703	-0.0180	252,255	0.0518	-0.0239
331,129	0.0775	-0.0162	333,971	0.0682	-0.0170	302,706	0.0595	-0.0221
386,317	0.0832	-0.0170	389,633	0.0676	-0.0184	353,157	0.0660	-0.0203
441,505	0.0839	-0.0169	445,295	0.0659	-0.0179	403,608	0.0739	-0.0187

Table 4.9, Coefficients of lift and drag at 20° AOA

Observing the coefficients of lift for disc 'A', it appears to perform well for all angles at and above 0° AOA. However, in the negative AOA range, it is overshadowed by the stellar performance of disc 'C'. The long slope of disc A's airfoil and its large camber allow it to take advantage of small changes in the AOA and still produce a generous lift. In fact, all of the discs produced a positive lift at -5° AOA.

Disc 'B' gives a strong coefficient of lift above 15° angle of attack. It produced noticeably less lift in the region in between. Which is precisely the region that will get the most use. The cupola upon its airfoil produces significant drag near 0° AOA and only contributes to the lift at higher (above 15°) angles of attack. The result is a poorly designed airfoil.

Disc 'C' generates moderate lift in the positive AOA range but is absolutely dominant in the negative range. Not surprising considering its shape, disc 'C' has a broad flat airfoil with a small camber and sharp lip. Disc 'C' was the only disc to produced a positive lift at -20° AOA.

Considering the coefficient of drag for each disc, disc 'A', with its large camber, produces the most drag in the negative AOA region, but performs well at 0° AOA and excels in the positive AOA region.

Disc 'B' performs poorly at 0° AOA, with its cupola prominent in the flow and adding to the drag. And as might be expected, the disc performs similarly to disc 'A' the further it gets from 0°.

Disc 'C', due to its low camber and sharp lip out performs the others in the negative AOA region and under performs in the positive region.

Disc A, Side View
Whammo Imperial Windjammer disc, 233 mm O.D., 105 grams

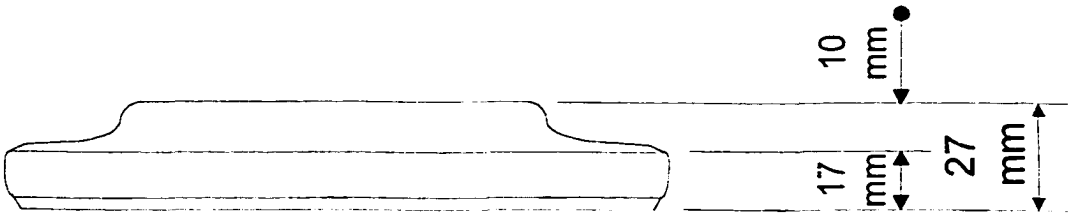

Disc B, Side View
Humphrey Flyer disc, 235 mm O.D., 92 grams

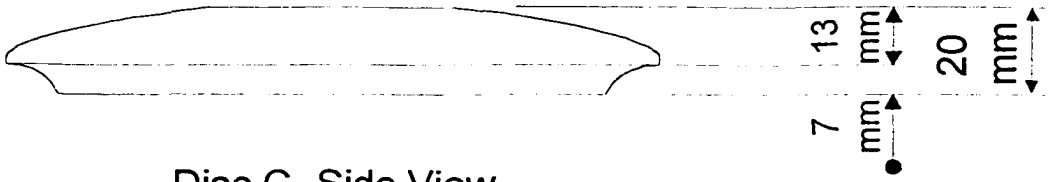

Disc C, Side View
Innova Golf Disc, 213 mm O.D., 176 grams

Figure 4.1. Side view of disc A, disc B, and disc C.

Figures 4.1 shows the profile of the three discs used in the non-spinning disc tests. Figure 4.2 to 4.10 show the lift to drag (L/D) ratio curves for all discs at several angles of attack.

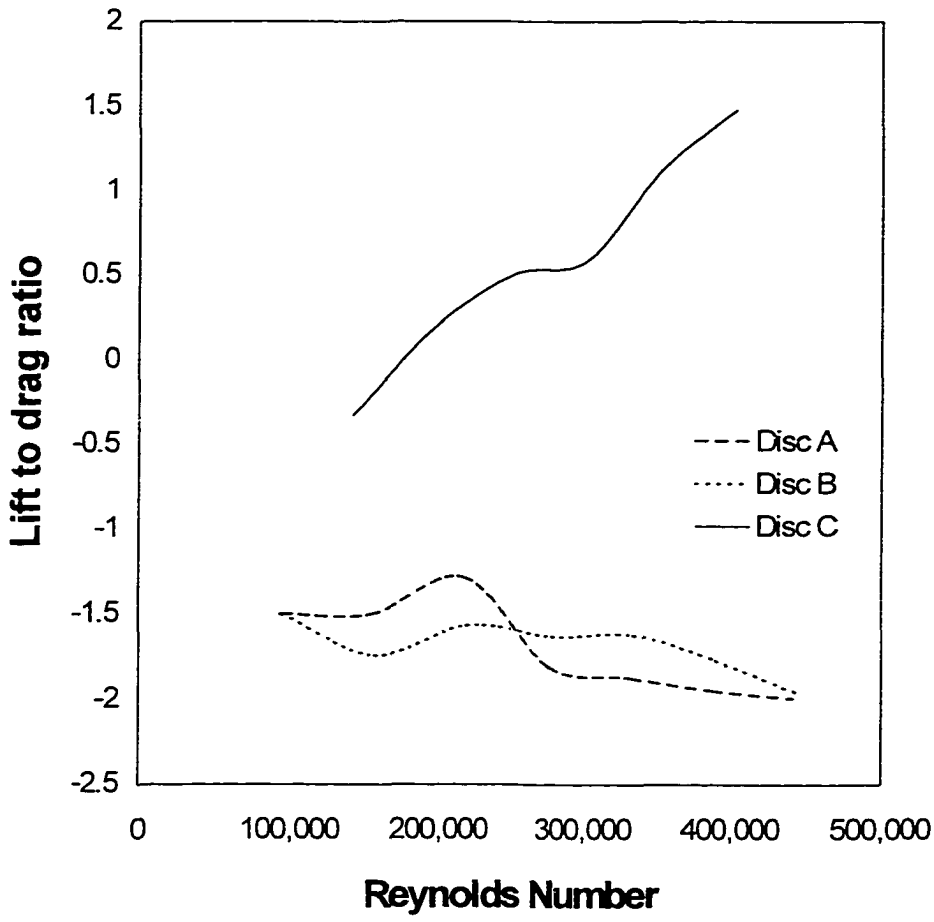

Figure 4.2, Lift to drag ratio at –20 AOA.

As Figure 4.2 shows, Disc C's L/D curve is well above that of the others and was the only disc to produce positive lift at this angle. Disc 'C's large drag was more than enough to offset its lift at lower Reynolds numbers. This phenomenon is also apparent in Figure 4.3, which shows the lift to drag ratios at -15° angle of attack. However, at -10° and -5°, disc 'C's lift does not suffer at lower Reynolds numbers. In Figure 4.2, disc 'A' performs disc 'B' below a Reynolds number of 250,000, and disc 'B' begins to dominate disc 'A' there after.

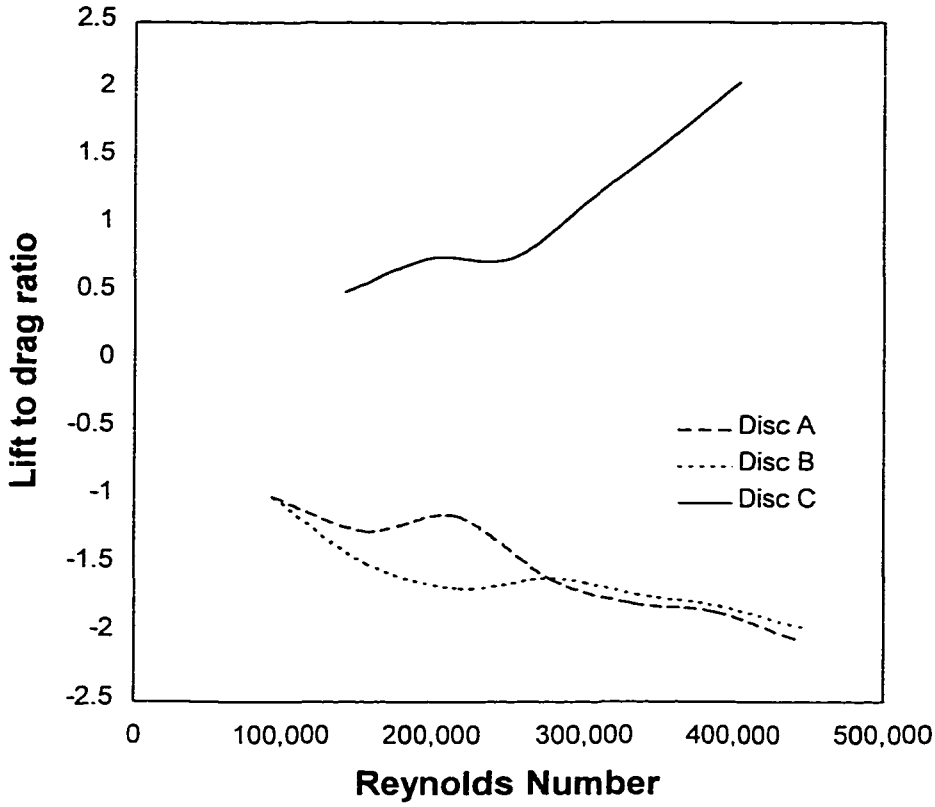

Figure 4.3, Lift to drag ratio at -15° AOA.

At -15° angle of attack, Figure 4.3 shows that the general characteristics from -20° are preserved. Disc 'A' still provides a higher lift to drag ratio below Reynolds numbers of 250,000 than disc 'B' and disc 'B' still dominates at Reynolds numbers above 250,000. Though disc 'C' is generating higher lift to drag ratios and still out-performs the other two discs.

At -10° angle of attack disc 'A' and disc 'B' are both experiencing a transition from positive lift to negative lift and disc 'C's drag is low enough to allow a good lift to drag ratio. These changes are readily apparent in the graph shown in Figure 4.4. Here disc 'A' and disc 'B's lift to drag ratio is suppressed to nearly zero until the Reynolds number reaches 220,000. Disc 'C' is clearly outperforming the other two. The portion of disc

'A's L/D curve that extends up into the positive region is a result of the wind tunnel's signal processor resolution of +/- 0.05 Newtons and the unique aerodynamics associated with the angle of attack. Table 4.3 shows disc 'A's drag was measured as 0.05 Newtons at 2.73 m/s of velocity, Then measured zero for measurements taken at 5.99 m/s and 9.90 m/s. As a result, the third order polynomial regression analysis used to fit the data extends upward into the positive region.

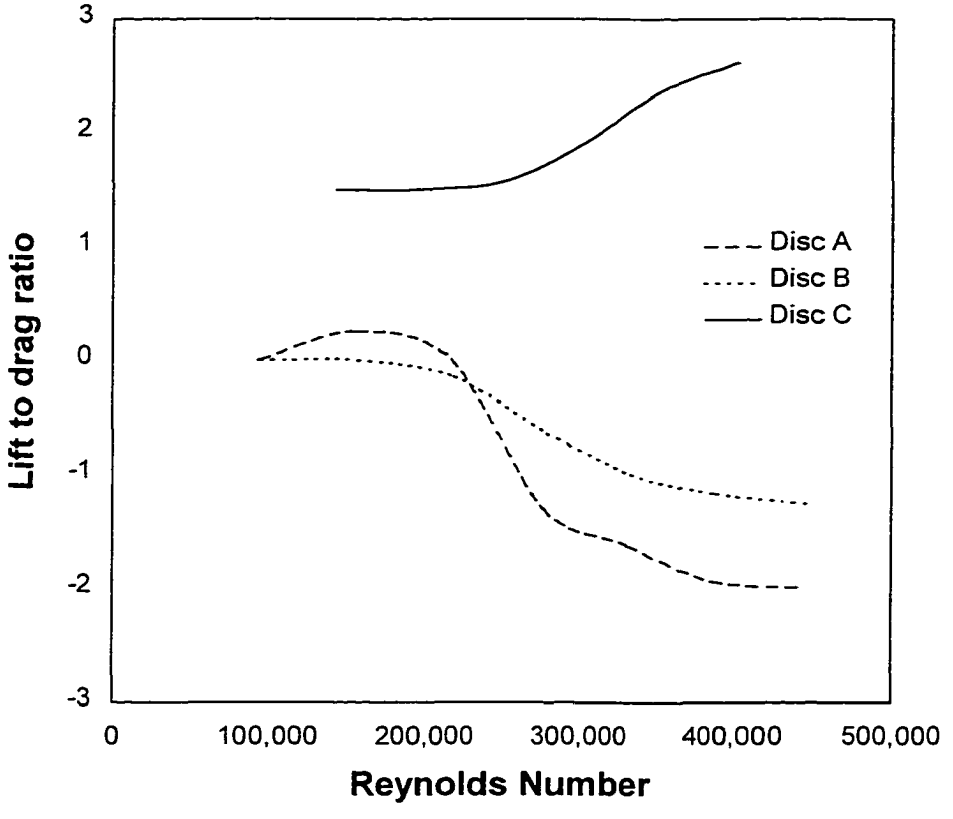

Figure 4.4, Lift to drag ratio at -10° AOA.

In Figure 4.5, which shows the lift to drag ratios at -5°, we see that the cupola of disc 'B' begins to contribute more frontal area to the disc increasing its drag and flattening its L/D curve. Unencumbered by a cupola disc 'A's curve extends upward and disc 'C' with its narrow cross section sees a lower drag and a corresponding increase in its L/D curve.

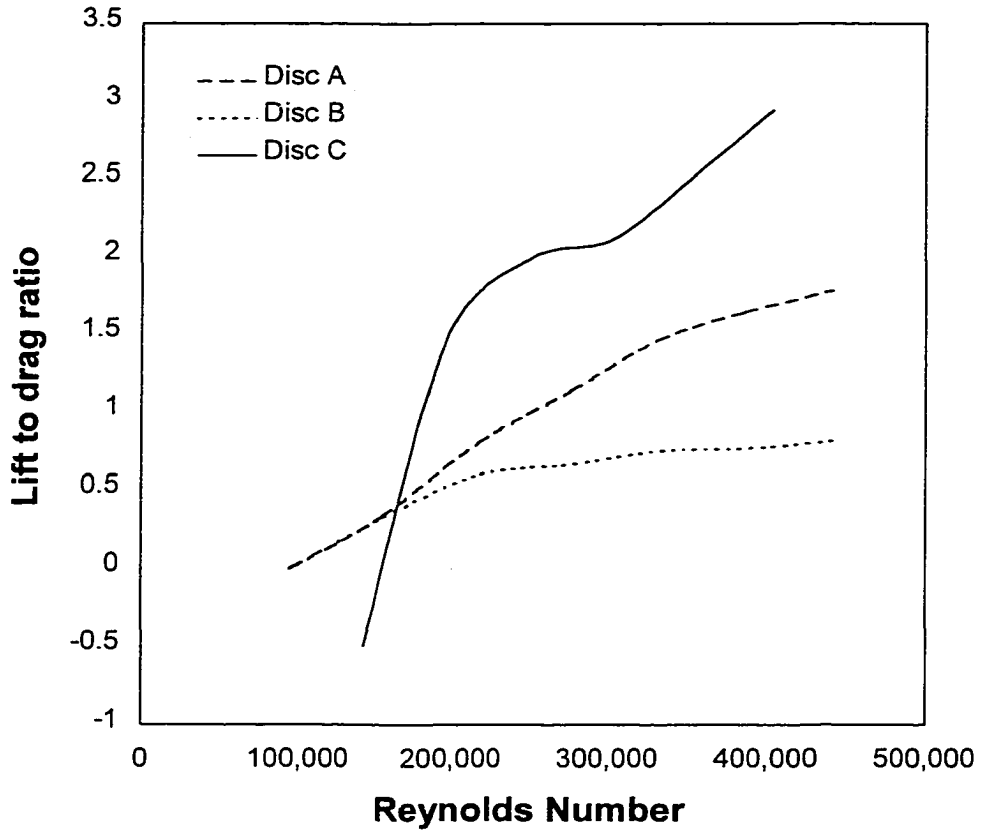

Figure 4.5, Lift to drag ratio at -5° AOA.

Recall that the Reynolds number for a typical hand thrown disc is near 156,000. Consider Figure 4.6, which shows that in the range of a typical hand thrown disc, disc 'B' exhibits a greater lift to drag ratio. However, at Reynolds numbers above that, disc 'C' produces the better lift to drag ratio. A professional disc thrower may take advantage of disc 'C's aerodynamic characteristic in this range by simply throwing the disc harder, where-as a disc thrower of leisure is completely satisfied with disc 'B'. Notice also that disc 'A's lift to drag curve shows intermediate performance for all the Reynolds numbers tested.

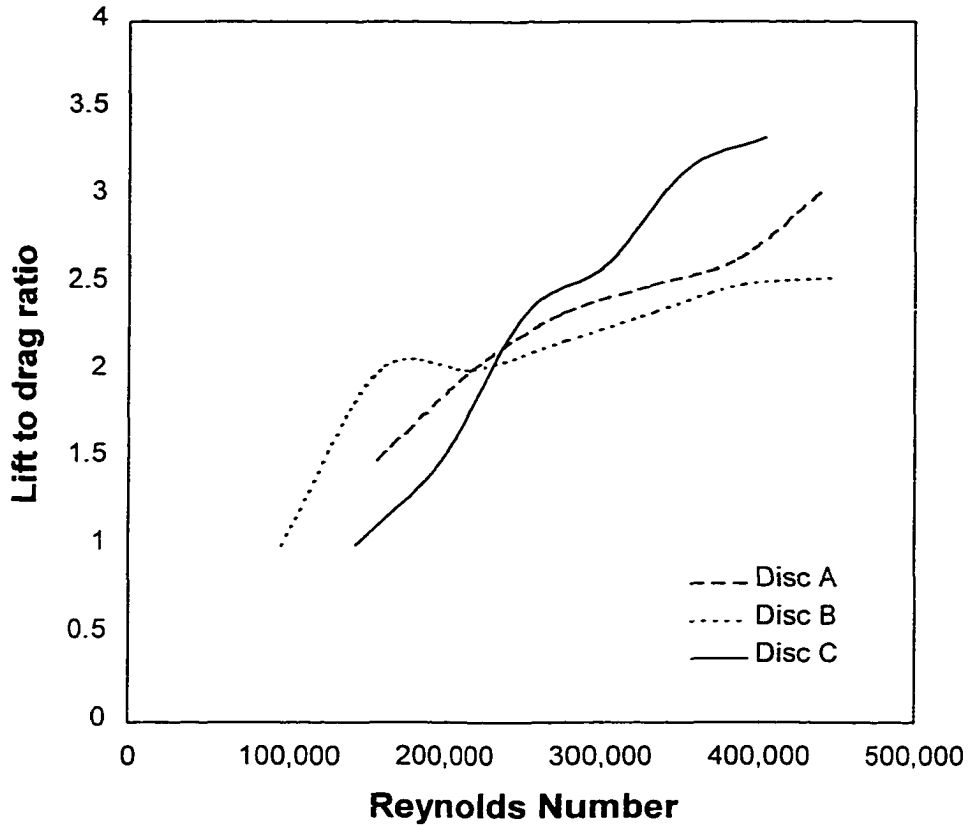

Figure 4.6, Lift to drag ratio at 0° AOA.

As the discs go from 0° to 5° angle of attack, disc 'A' shows a high well-positioned and steady lift to drag curve. Disc 'B' exhibits a unique curve that increases and decreases with Reynolds number. And Disc 'C' begins to the 'see' the parasitic effects of drag lowering its overall lift to drag values.

Figure 4.8 shows the disc lift to drag ratio curves at 10° AOA. Disc 'A' has an exemplary curve with a lift to drag ratio of 4 at its highest point. Disc 'B's curve is lackluster between 1.5 and 3. While disc 'C's curve starts low and builds steadily with increasing velocity. The sharp lip of disc 'C' causes separation, hence, increased drag.

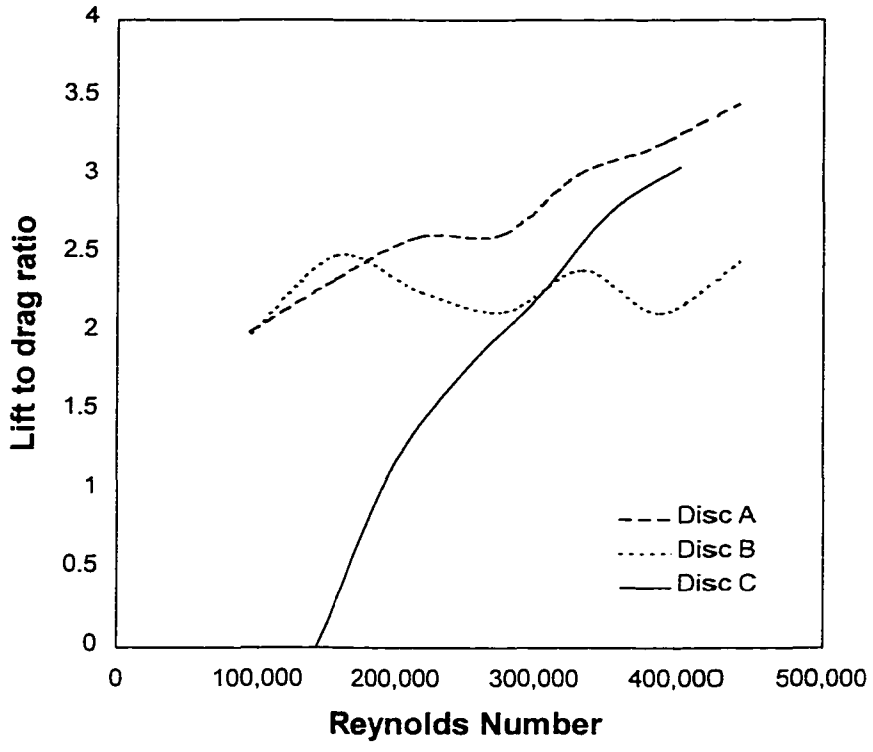

Figure 4.7, Lift to drag ratio at 5° AOA.

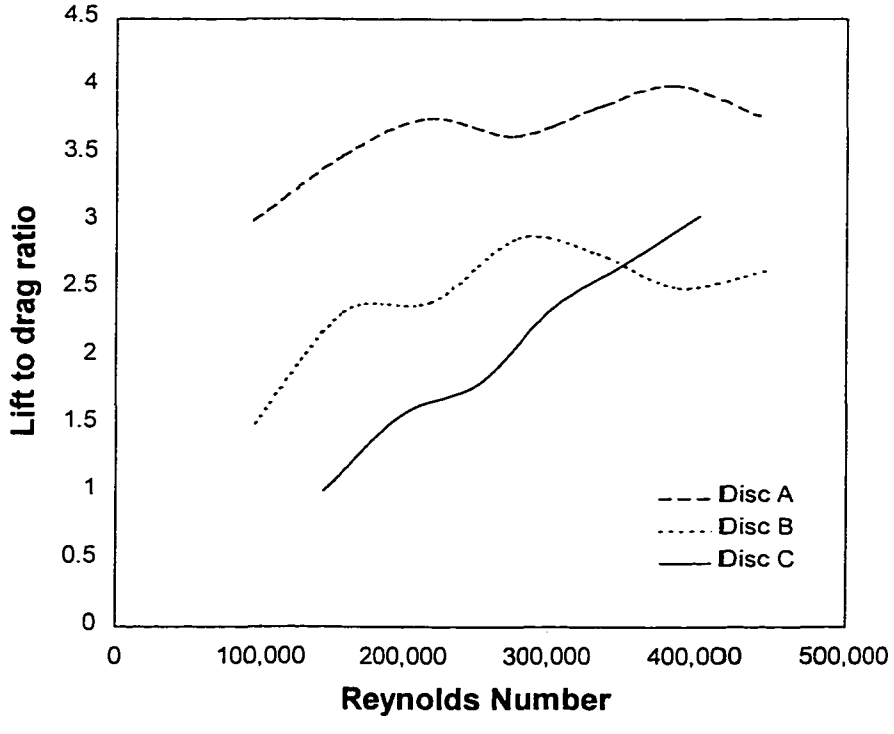

Figure 4.8, Lift to drag ratio at 10° AOA.

In Figure 4.9, disc 'A's curve below a Reynolds number of 250,000 is highly suspect. An extremely low drag measurement and a reasonable lift measurement combined to produce a lift to drag ratio of 47. Omitting the data point does help the regression analysis. But as you can see the result is highly questionable.

For disc 'B', here again, a steady performance occurs in the lift to drag ratio area of 3. Disc 'C' responds well to increases in velocity but suffers from heavy increases in drag.

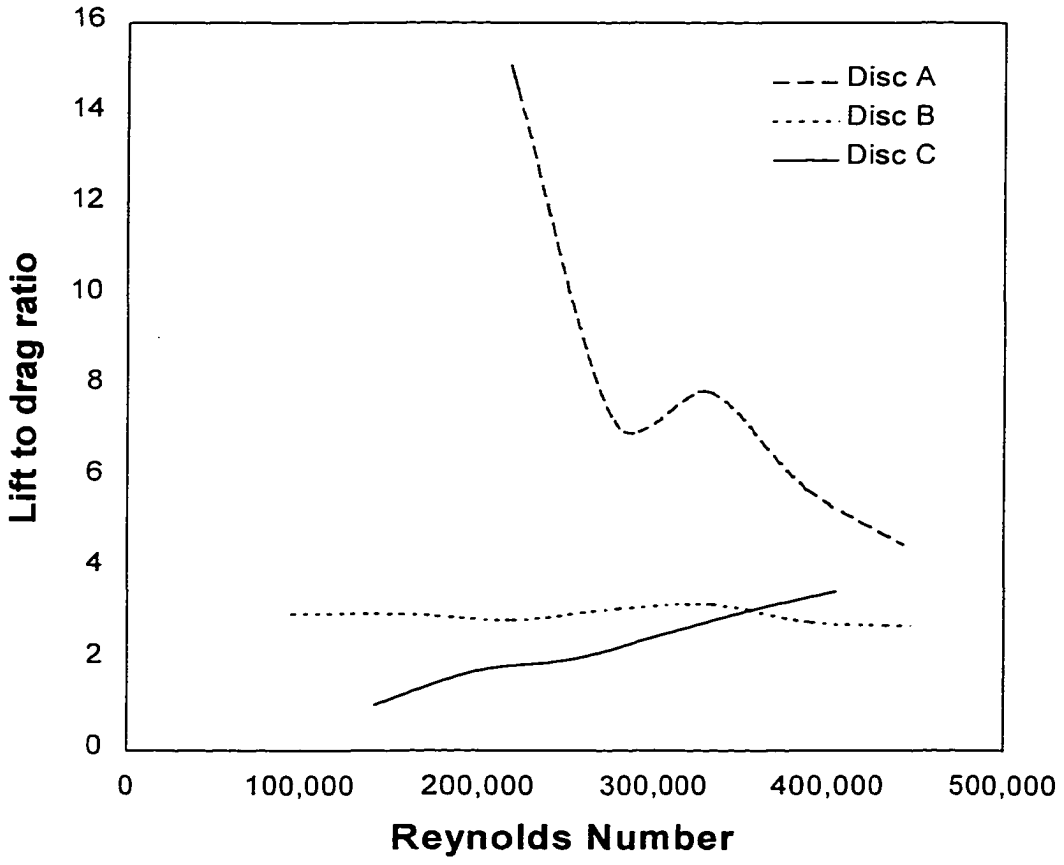

Figure 4.9, Lift to drag ratio at 15° AOA.

Finally in Figure 4.10 we see the lift to drag ratios for all discs at 20° AOA. Discs 'A' and 'B' perform similarly while disc 'C' is depressed by its increased drag values.

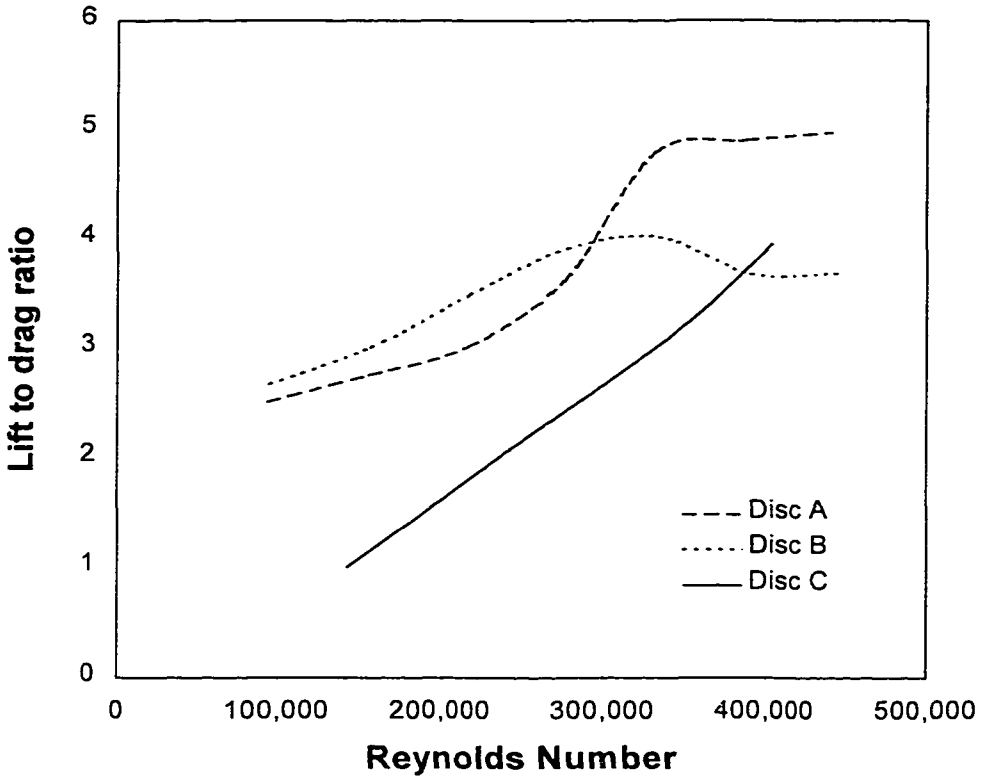

Figure 4.10, Lift to drag ratio at 20° AOA.

4.2 CENTER OF LIFT ANALYSIS

No conclusive results could be determined from the center of lift tests. The Center of lift experiments showed that the lifting moment on a disc is a function of its angle of attack, velocity, and shape. The magnitude and location of the center of lift changes rapidly with changes in angle of attack. As the angle of attack changes from zero, a corrective drag force is introduced that changes the overall pitching moment of the disc.

If one examines the initial response of the disc as it moves from 0° AOA, then a tendency to rotate to a positive or negative AOA orientation will indicate, at least, upon which side of the pivot the lifting force is acting. However, if the lifting force is a

function of velocity, it is then moving either forward or backward with increases in velocity. Under such conditions the only thing that can be determined from observations of the initial response of the disc is which side of the pivot the lifting force is acting on at a given Reynolds number.

Several times during these tests the disc would pitch to assume a negative AOA, then remain fixed. In this situation the moment created by the lift is equal to the moment produced by the drag. This can only occur if the lift is acting behind the pivot. With the recorded velocity and AOA the drag force can be calculated. Hence, the magnitude of the lift force is known. A caveat: since the disc's AOA is not zero, then we cannot infer that the lift's magnitude or location would be the same at zero.

In Chapter 5, a series of measures to correct the deficiencies of this experiment will be presented.

From the center of lift experiments performed:

1. That the center of lift at low velocity is behind the mid-chord point.
2. That the center of lift moves forward with increasing velocity to some point ahead of the mid-chord.
3. That the center of lift is angle of attack sensitive. At small positive AOA the center of lift moves forward and at small negative AOA the center of lift moves rearwards.
4. That the magnitude of the pitching moment increases with increased velocity.
5. At velocities less than 20 m/s, the center of lift was never ahead of the 95/235 chord point.

6. That the domed cupola atop disc 'B' affects the center of lift at small positive and negative AOA. NOTE: this observed effect is most notable between Reynolds numbers of 115,000 and 117,000 and may have been drag/lift interactions.

4.3 TUFT AND SMOKE TEST ANALYSIS

The tuft and smoke tests are combined in this analysis to characterize and compare the boundary layer and wake of a spinning and non-spinning disc. For the non-spinning discs, the effects of contour and angle of attack are analyzed. Photographs were taken to document the observed phenomena.

Each of the non-spinning discs exhibited differences in the boundary layer. The boundary layer differences are related to the contour and lip (leading edge) differences between the discs tested. In addition, changes in the boundary layer were noted for positive, negative and neutral angles of attack for each disc. The differences between the discs aside, each of the discs did experience similarities in aerodynamic behavior. At 0° AOA, all the discs had completely separated and detached boundary layers on their lower (concave) surface.

For these tests, the wind tunnel started at idle (3.41 m/s) and the velocity was increased in incremental stages. All other parameters were held constant. As an aerodynamic characteristic developed, it was observed and noted.

The first characteristic to develop is typically the mid-chord 'wing-tip' vorticies. For disc 'A', at a neutral AOA, these vorticies were observed at a Reynolds number of 64,034. For disc 'B', the same vorticies developed at Reynolds number 53,388. For disc 'C' they developed at a Reynolds number of 74,360. Figure 4.11 shows theses vorticies.

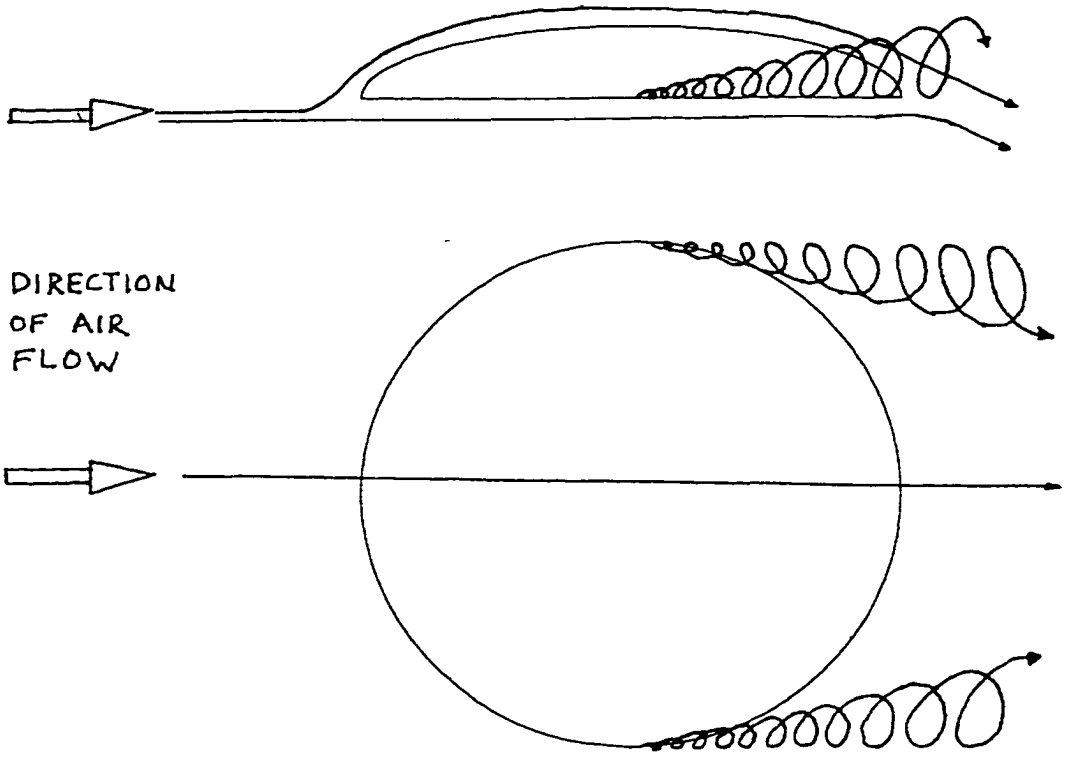

Figure 4.11 Mid-chord vorticies

Considering how AOA affects the development of these vorticies, for disc 'A' at positive angles of attack the mid-chord vorticies develop at lower Reynolds numbers and at negative angles of attack at higher Reynolds numbers. This characteristic is identical for disc 'B' but not for disc 'C'. Disc 'C', at 10° angle of attack, developed the mid-chord vorticies at a slightly higher Reynolds number (83,868 Re).

The second observed characteristic is turbulence in the boundary layer on the upper surface. At 0° AOA, disc 'A's first observed boundary layer turbulence was at a Reynolds number of 173,618. This is above the average Reynolds number for a typical hand thrown disc. So, if thrown at neutral AOA by an average typical human, the disc does not experience turbulence in its upper surface boundary layer. For disc 'B', the cupola developed turbulence on its rear sloping surface at Re = 82,039, while the upper surface proper did not develop turbulence until Re = 115,073. The cupola atop disc 'B'

had a large effect on the disc's overall aerodynamics. Finally, disc 'C' with its much smaller camber did not develop turbulence in its upper surface boundary layer until Re = 190,297, significantly higher than the other discs.

Looking at the AOA effects, for all three discs at positive angles of attack the turbulence develops at lower Reynolds number, while at negative angles of attack, with the exception of disc 'C', the turbulence develops at higher Reynolds numbers. Disc 'C' did not develop any turbulence in its upper surface boundary layer at negative angles of attack for the Reynolds numbers tested. It is probable that disc 'C' does develop turbulence at some Reynolds number above those that were tested.

Another interesting characteristic of discs is the tendency for the streamlines to curve in at the rear and follow the contour of the disc. On disc 'A' this characteristic occurs at higher Reynolds numbers for positive AOA and at lower Reynolds numbers for negative AOA. On disc 'B' this phenomena occurs at higher Reynolds numbers in general, not occurring until Re = 262,085 compared to disc 'A's development at Re = 189,506. Like disc 'A', this characteristic also occurs at lower Reynolds numbers given a negative AOA. However, at positive angles of attack, this phenomena did not develop in the experiments for disc 'B' over the Reynolds numbers tested. Again it is highly probable that this would have occurred at some Reynolds number higher than what was tested. Oddly enough, on disc 'C' this tendency for streamlines to curve in at the rear of a disc only presented itself at the 0° angle of attack inclination. At both positive and negative angles of attack this characteristic, due to disc 'C's low camber and sharp lip, did not develop. Figure 4.12 shows a drawing of streamlines curving in at the rear of a disc.

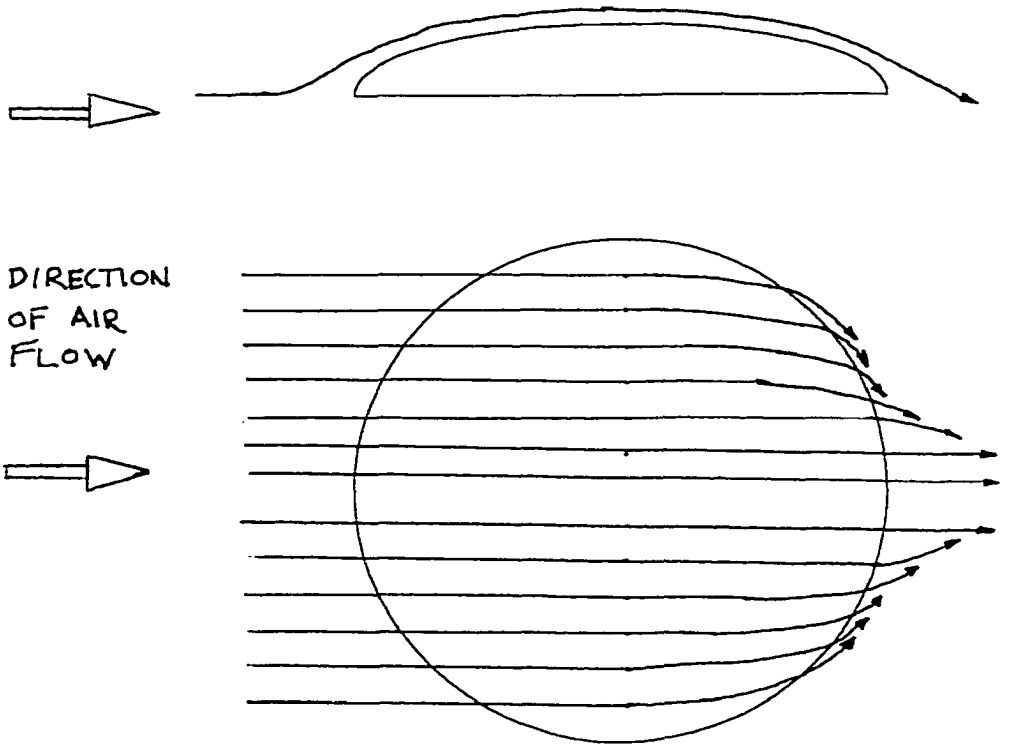

Figure 4.12 Streamlines curving in on a disc

Correlating some of the differences between boundary layer and disc contour we see that disc 'A', the standard recreational airborne disc, at neutral AOA had a boundary layer on the upper surface that remained entirely attached while its lower surface was completely detached and stagnant. At small positive AOA, the mid-chord vorticies would curl up over the edge of the disc and shed from the cambered portion of the upper surface. At negative AOA, streamlines impacting the leading edge would curl back, away from the center of the disc, to drop off of the leading edge and curl up under the disc.

For disc 'B', a disc similar to the standard recreational disc with addition of a cupola on its upper surface, we see that vorticity quickly leads to separation on the rear slope of the cupola. This zone of separation grows with increasing velocity to encompass the entire rear of the airfoil. Furthermore, at positive AOA we see this turbulence and

separation occurring at lower Reynolds numbers and, not surprisingly, at negative AOA the turbulence occurs at higher Reynolds numbers and the separation does not occur. However the streamline curl back phenomena observed with disc 'A' does occur. The curl back phenomenon is an extension of the streamline tendency to move away from the centerline of the disc. It was only noticed on the higher cambered airfoils and is related to the 3-D relieving effect.

Disc 'C' is a golf disc with a low camber and sharp lip. At 0° AOA, it showed no unusual aerodynamic characteristics. But at positive AOA, the sharp lip of the disc trips the boundary layer to cause turbulence and separation. At negative AOA, the upper surface remains laminar throughout the test and the sharp lip develops complete circumferential vorticity shedding. In addition, the vorticity in the tufts at the rear of the disc showed a downwash which increased with velocity. That is, the angle at which the tufts extended from the rear of the disc changed as the velocity changed. Figure 4.13 shows the circumferential vortex shedding when disc C is at negative AOA.

The smoke results compare nicely with the tuft results. The smoke tests show conclusively that the upper surface boundary layer is entirely attached at 0° AOA. In the concave region of the cambered disc, the flow is entirely detached and separated. The smoke clearly showed an upwash in the streamlines just ahead of contact with the disc and a downwash in the wake of the disc. Also illuminated in detail are the mid-chord vorticies, which have a large effect on the wake of a disc.

The mid-chord vorticies compress or channel the streamlines on the central upper surface of the disc. In the wake, the mid-chord vorticies tend to "roll-up". In fact, this roll-up effect begins at the point of generation and the vorticies appear to be 'climbing'

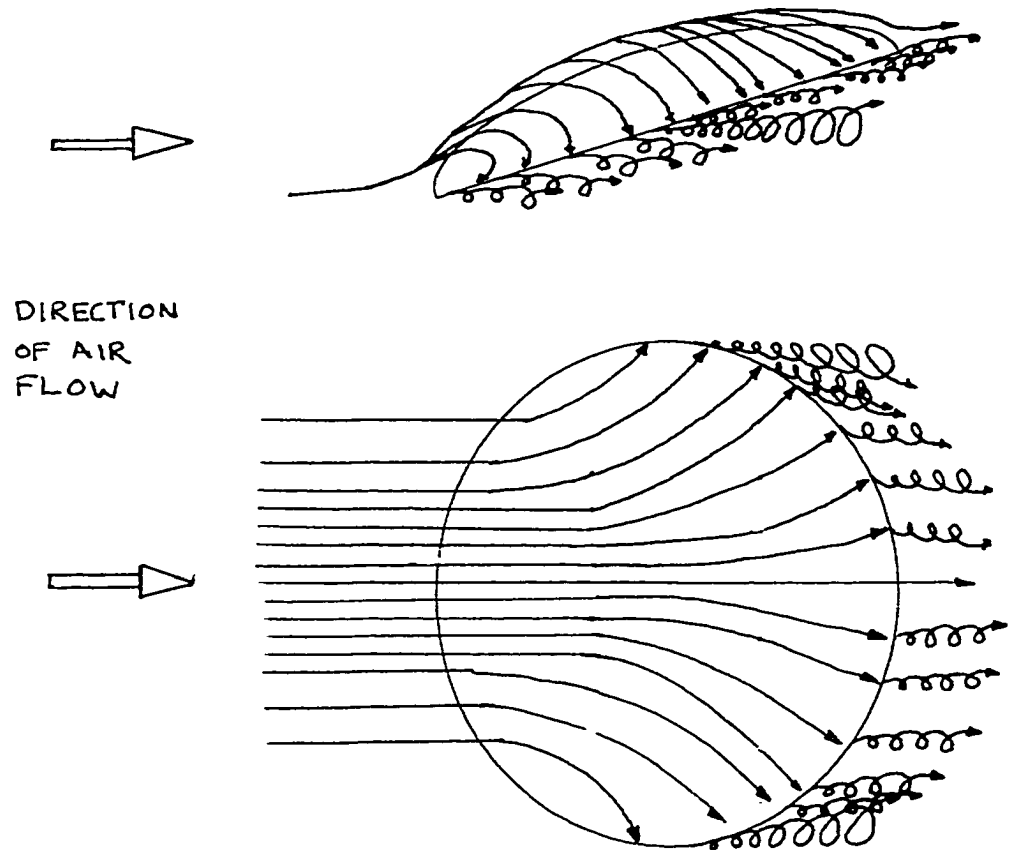

Figure 4.13 Circumferential vortex shedding

the cambered sides of the airfoil. This allows a thin band of streamlines beneath the vortices to follow the contour of the disc and curve in at the rear, hence the curving in effect observed in the tuft tests.

No effect of spin was observed in the boundary layer of an airborne disc. All of the aerodynamic characteristics observed in the non-spinning disc were also observed in the spinning disc. This is an interesting finding. It says that aerodynamic visualization tests can be conducted on non-spinning discs with reasonable results being obtained for the case of a spinning disc.

CHAPTER 5

CONCLUSION

5.1 THE BIG PICTURE

An experimental evaluation of the aerodynamic characteristics of airborne discs has been made to see the effects of airfoil contour, airfoil camber, and spin. The motivation for these experiments was the lack of published and available literature on the subject. The primary objective was to understand the aerodynamic structures (mid-chord vorticies, zones of laminar, turbulent, and separated flow) which developed in the flight of discs. The secondary objective was to determine the effect of angle of attack and velocity on the structures.

In pursuit of these objectives, experiments were conducted on the lift and drag of static discs of differing contour and camber. Experiments were also conducted on the location of the center of lift for static discs of differing contour and camber, and on the boundary of static discs using tufts and photography for differing contour and camber. Experiments included a single spinning disc of general contour using smoke and photography.

The study shows that the airfoil camber and contour contributes greatly to the lift and drag characteristics of discs. Further, the airfoil camber and contour have some effect on the magnitude and location of the center of lift and hence, the pitching moment. Many of the aerodynamic characteristics can be correlated directly to the

boundary layer structures illuminated in the tuft and smoke tests. This study also shows that spin has no effect on the development or location of these structures.

1) The cupola on disc 'B' does not provide any additional lift but does create additional drag.
2) Larger cambered airfoils generate larger lifts at lower velocities.
3) Larger cambered airfoils generate a positive lift over a longer range of angles of attack.
4) The center of lift is velocity and angle of attack dependent.
5) The center of lift is behind the geometric center of a disc at low velocities and moves forward to a point ahead of the geometric center with increasing velocity, provided the disc is at a constant zero degree angle of attack.
6) The grooves on the surface of a disc do not trip the boundary layer to turbulence and serve no useful aerodynamic purpose.
7) The lip and contour of a disc greatly affect the development of the boundary layer above and below the disc.
8) The lip and contour of a disc have some effect on the location and magnitude of the center of lift.
9) All discs generate mid-chord 'wing-tip' vorticies.
10) The magnitude of the mid-chord vorticies influences the flow at the rear and in the wake of airborne discs.
11) At zero degree angle of attack, the upper surface of a disc is entirely attached and laminar over the range of Reynolds numbers tested.

12) At zero degree angle of attack, the lower 'concave' surface is entirely detached and separated.

13) Cambered discs generate positive lift at small negative angles of attack.

14) The curl back phenomena observed in the tuft tests may be an aerodynamic structure which can indicate when a disc at small negative angle of attack is transitioning from positive lift to negative lift.

15) Spin has no effect on the boundary layer of airborne discs.

6.2 RECOMMENDATIONS

Future work should be done to improve the experiments in several areas. The resolution of the signal processor from which the lift and drag values are read is 0.05 Newtons. This resulted in a loss of accuracy for the low velocity drag values. Future work involving the measurement of drag would be greatly improved by a signal processor with a resolution of 0.01 Newtons.

Productive results from the center of lift experiments were greatly inhibited by the unexpected dependency of the location of the center of lift on velocity. A mechanism which could restrain the disc at specific AOA until the desired test velocity is reached, would be of tremendous benefit to future researchers.

In the lift, drag, and tuft tests, an AOA creep was experienced which became worse with increased velocity and increased AOA. The AOA creep was the result of using plastic experimental discs, which were attached at their geometric center. The plastic of the disc is a non-rigid material, which allows the disc to flex about its

attachment point. Future efforts should fabricate all discs from rigid materials and mount the discs securely.

Several suggestions can also be made to improve the tuft and smoke tests. First, photographs and videotape should be used to document every single observation and detail. Secondly, the positioning of the photography equipment should be improved. In the smoke tests, the photography was made from a single angle which hid some of the observed properties. Third, a bigger model with a finer smoke stream would help in illuminating the smaller details in the boundary layer. Also, higher spin rates would allow spin testing at higher test section velocities.

Future research should consider the study of these discs over a larger range of angle of attack. The apparatus used in this study only allowed a limited range between +20 degree and –20 degree angle of attack.

Most of the attention in this work was focused on the lift, drag, pitching moment, and boundary layer of airborne discs. Similar tests done with a six-degree of freedom force dynamometer would be of great interest.

APPENDIX A

Induced lift and drag from post and mount

July 31, 1997 Thursday 9:15 am

Wind Tunnel Reading In hertz	Drag in lbf (+/- 0.005)	Lift in lbf (+/- 0.05)
OFF	-00.00	-00.01
3.7	-00.00	-00.01
5.0	-00.00	-00.00
10.0	-00.01	00.05
15.0	-00.03	00.14
20.0	-00.05	00.28
25.0	-00.07	00.44
30.0	-00.10	00.62
35.0	-00.13	00.89
40.0	-00.16	01.27
45.0	-00.20	01.75
50.0	-00.25	02.36
54.3 MAX VEL.	-00.30	03.03
4.0	-00.01	00.10
OFF	-00.01	00.09

Table A.1 Parasitic drag and lift of dynamometer post and mount

Due to hysteresis in the force dynamometer accuracy is limited to +/- 0.005 lbf in drag and +/- 0.05 lbf in lift.

APPENDIX B

EXPERIMENTAL DATA

LIFT AND DRAG RESULTS

Test AL1

Disc A — Lift and Drag Test

Diameter: 233mm — AOA: -20°

Ambient Air Temperature: 22.1 C — Ambient Air Pressure: 96,012 Pa

Reynolds Number	Velocity (m/s)	Lift (Newtons)	Drag (Newtons)
42,710	02.73	-00.10	00.00
93,680	05.99	-00.15	-00.10
154,957	09.90	-00.30	-00.20
216,578	13.83	-00.45	-00.35
275,940	17.63	-00.90	-00.50
331,129	21.15	-01.40	-00.75
386,317	24.68	-01.95	-01.00
441,505	28.20	-02.50	-01.25

Table A.2 Lift and drag test, disc A, -20 Deg.

Test AL2

Disc A — Lift and Drag Test

Diameter: 233mm — AOA: -15°

Ambient Air Temperature: 22.1 C — Ambient Air Pressure: 96,012 Pa

Reynolds Number	Velocity (m/s)	Lift (Newtons)	Drag (Newtons)
42,710	02.73	-00.05	00.00
93,680	05.99	-00.10	-00.10
154,957	09.90	-00.25	-00.20
216,578	13.83	-00.40	-00.35
275,940	17.63	-00.80	-00.50
331,129	21.15	-01.25	-00.70
386,317	24.68	-01.75	-00.95
441,505	28.20	-02.35	-01.15

Table A.3 Lift and drag test, disc A, -15 Deg.

Test AL3

Disc A Lift and Drag Test

Diameter: 233mm AOA: -10°

Ambient Air Temperature: 22.1 C Ambient Air Pressure: 96,012 Pa

Reynolds Number	Velocity (m/s)	Lift (Newtons)	Drag (Newtons)
42,710	02.73	-00.05	00.00
93,680	05.99	00.00	-00.10
154,957	09.90	00.05	-00.20
216,578	13.83	00.00	-00.30
275,940	17.63	-00.65	-00.50
331,129	21.15	-01.05	-00.65
386,317	24.68	-01.55	-00.80
441,505	28.20	-02.10	-01.05

Table A.4 Lift and drag test, disc A, -10 Deg.

Test AL4

Disc A Lift and Drag Test

Diameter: 233mm AOA: -5°

Ambient Air Temperature: 22.1 C Ambient Air Pressure: 96,012 Pa

Reynolds Number	Velocity (m/s)	Lift (Newtons)	Drag (Newtons)
42,710	02.73	-00.05	00.00
93,680	05.99	00.00	-00.05
154,957	09.90	00.05	-00.15
216,578	13.83	00.20	-00.25
275,940	17.63	00.45	-00.40
331,129	21.15	00.80	-00.55
386,317	24.68	01.15	-00.70
441,505	28.20	01.60	-00.90

Table A.5 Lift and drag test, disc A, -5 Deg.

Test AL5

Disc A — Lift and Drag Test

Diameter: 233mm — AOA: 0°

Ambient Air Temperature: 22.1 C — Ambient Air Pressure: 96,012 Pa

Reynolds Number	Velocity (m/s)	Lift (Newtons)	Drag (Newtons)
42,710	02.73	-00.05	00.00
93,680	05.99	00.00	00.00
154,957	09.90	00.15	-00.10
216,578	13.83	00.40	-00.20
275,940	17.63	00.70	-00.30
331,129	21.15	01.25	-00.50
386,317	24.68	01.85	-00.70
441,505	28.20	02.60	-00.85

Table A.6 Lift and drag test, disc A, 0 Deg.

Test AL6

Disc A — Lift and Drag Test

Diameter: 233mm — AOA: 5°

Ambient Air Temperature: 22.1 C — Ambient Air Pressure: 96,012 Pa

Reynolds Number	Velocity (m/s)	Lift (Newtons)	Drag (Newtons)
42,710	02.73	00.00	00.00
93,680	05.99	00.10	-00.05
154,957	09.90	00.35	-00.15
216,578	13.83	00.65	-00.25
275,940	17.63	01.05	-00.40
331,129	21.15	01.65	-00.55
386,317	24.68	02.55	-00.80
441,505	28.20	03.30	-00.95

Table A.7 Lift and drag test, disc A, 5 Deg.

Test AL7

Disc A | Lift and Drag Test

Diameter: 233mm | AOA: 10°

Ambient Air Temperature: 22.1 C | Ambient Air Pressure: 96,012 Pa

Reynolds Number	Velocity (m/s)	Lift (Newtons)	Drag (Newtons)
42,710	2.73	00.00	00.00
93,680	5.99	00.15	-00.05
154,957	9.90	00.35	-00.10
216,578	13.83	00.75	-00.20
275,940	17.63	01.45	-00.40
331,129	21.15	02.30	-00.60
386,317	24.68	03.40	-00.85
441,505	28.20	04.15	-01.10

Table A.8 Lift and drag test, disc A, 10 Deg.

Test AL8

Disc A Lift and Drag Test

Diameter: 233mm AOA: 15°

Ambient Air Temperature: 22.1 C Ambient Air Pressure: 96,012 Pa

Reynolds Number	Velocity (m/s)	Lift (Newtons)	Drag (Newtons)
42,710	02.73	00.00	00.00
93,680	05.99	00.15	-00.05
154,957	09.90	00.45	00.00
216,578	13.83	00.75	-00.05
275,940	17.63	01.45	-00.20
331,129	21.15	02.35	-00.30
386,317	24.68	03.45	-00.60
441,505	28.20	04.05	-00.90

Table A.9 Lift and drag test, disc A, 15 Deg.

Test AL9

Disc A | Lift and Drag Test

Diameter: 233mm | AOA: 20°

Ambient Air Temperature: 22.1 C | Ambient Air Pressure: 96,012 Pa

Reynolds Number	Velocity (m/s)	Lift (Newtons)	Drag (Newtons)
42,710	02.73	00.10	00.00
93,680	05.99	00.25	-00.10
154,957	09.90	00.55	-00.20
216,578	13.83	00.90	-00.30
275,940	17.63	01.80	-00.50
331,129	21.15	03.35	-00.70
386,317	24.68	04.90	-01.00
441,505	28.20	06.45	-01.30

Table A.10 Lift and drag test, disc A, 20 Deg.

Test BL1

Disc B Lift and Drag Test

Diameter: 235mm AOA: -20°

Ambient Air Temperature: 22.1 C Ambient Air Pressure: 96,012 Pa

Reynolds Number	Velocity (m/s)	Lift (Newtons)	Drag (Newtons)
43,077	2.73	00.00	00.00
94,484	5.99	-00.15	-00.10
156,287	9.90	-00.35	-00.20
218,437	13.83	-00.55	-00.35
278,309	17.63	-00.90	-00.55
333,971	21.15	-01.30	-00.80
389,633	24.68	-01.95	-01.10
445,295	28.20	-02.55	-01.30

Table A.11 Lift and drag test, disc B, -20 Deg.

Test BL2

Disc B Lift and Drag Test

Diameter: 235mm AOA: -15°

Ambient Air Temperature: 22.1 C Ambient Air Pressure: 96,012 Pa

Reynolds Number	Velocity (m/s)	Lift (Newtons)	Drag (Newtons)
43,077	2.73	00.00	00.00
94,484	5.99	-00.10	-00.10
156,287	9.90	-00.30	-00.20
218,437	13.83	-00.50	-00.30
278,309	17.63	-00.80	-00.50
333,971	21.15	-01.20	-00.70
389,633	24.68	-01.80	-01.00
445,295	28.20	-02.45	-01.25

Table A.12 Lift and drag test, disc B, -15 Deg.

Test BL3

Disc B Lift and Drag Test

Diameter: 235mm AOA: -10°

Ambient Air Temperature: 22.1 C Ambient Air Pressure: 96,012 Pa

Reynolds Number	Velocity (m/s)	Lift (Newtons)	Drag (Newtons)
43,077	2.73	-00.05	00.00
94,484	5.99	00.00	-00.10
156,287	9.90	00.00	-00.25
218,437	13.83	-00.05	-00.35
278,309	17.63	-00.35	-00.55
333,971	21.15	-00.70	-00.70
389,633	24.68	-01.05	-00.90
445,295	28.20	-01.50	-01.20

Table A.13 Lift and drag test, disc B, -10 Deg.

Test BL4

Disc B Lift and Drag Test

Diameter: 235mm AOA: -5°

Ambient Air Temperature: 22.1 C Ambient Air Pressure: 96,012 Pa

Reynolds Number	Velocity (m/s)	Lift (Newtons)	Drag (Newtons)
43,077	2.73	00.00	00.00
94,484	5.99	00.00	-00.05
156,287	9.90	00.05	-00.15
218,437	13.83	00.15	-00.25
278,309	17.63	00.30	-00.45
333,971	21.15	00.45	-00.60
389,633	24.68	00.65	-00.85
445,295	28.20	00.90	-01.10

Table A.14 Lift and drag test, disc B, -5 Deg.

Test BL5

Disc B Lift and Drag Test

Diameter: 235mm AOA: 0°

Ambient Air Temperature: 22.1 C Ambient Air Pressure: 96,012 Pa

Reynolds Number	Velocity (m/s)	Lift (Newtons)	Drag (Newtons)
43,077	2.73	00.00	00.00
94,484	5.99	00.05	-00.05
156,287	9.90	00.20	-00.10
218,437	13.83	00.40	-00.20
278,309	17.63	00.65	-00.30
333,971	21.15	01.05	-00.45
389,633	24.68	01.75	-00.70
445,295	28.20	02.65	-01.05

Table A.15 Lift and drag test, disc B, 0 Deg.

Test BL6

Disc B — Lift and Drag Test

Diameter: 235mm — AOA: 5°

Ambient Air Temperature: 22.1 C — Ambient Air Pressure: 96,012 Pa

Reynolds Number	Velocity (m/s)	Lift (Newtons)	Drag (Newtons)
43,077	2.73	00.00	00.00
94,484	5.99	00.10	-00.05
156,287	9.90	00.25	-00.10
218,437	13.83	00.45	-00.20
278,309	17.63	00.75	-00.35
333,971	21.15	01.20	-00.50
389,633	24.68	01.80	-00.85
445,295	28.20	02.60	-01.05

Table A.16 Lift and drag test, disc B, 5 Deg.

Test BL7

Disc B Lift and Drag Test

Diameter: 235mm AOA: 10°

Ambient Air Temperature: 22.1 C Ambient Air Pressure: 96,012 Pa

Reynolds Number	Velocity (m/s)	Lift (Newtons)	Drag (Newtons)
43,077	2.73	00.00	-00.05
94,484	5.99	00.15	-00.10
156,287	9.90	00.35	-00.15
218,437	13.83	00.60	-00.25
278,309	17.63	01.15	-00.40
333,971	21.15	01.65	-00.60
389,633	24.68	02.25	-00.90
445,295	28.20	02.90	-01.10

Table A.17 Lift and drag test, disc B, 10 Deg.

Test BL8

Disc B Lift and Drag Test

Diameter: 235mm AOA: 15°

Ambient Air Temperature: 22.1 C Ambient Air Pressure: 96,012 Pa

Reynolds Number	Velocity (m/s)	Lift (Newtons)	Drag (Newtons)
43,077	2.73	00.00	-00.05
94,484	5.99	00.30	-00.10
156,287	9.90	00.60	-00.20
218,437	13.83	01.00	-00.35
278,309	17.63	01.40	-00.45
333,971	21.15	02.25	-00.70
389,633	24.68	02.95	-01.05
445,295	28.20	03.55	-01.30

Table A.18 Lift and drag test, disc B, 15 Deg.

Test BL9

Disc B Lift and Drag Test

Diameter: 235mm AOA: 20°

Ambient Air Temperature: 22.1 C Ambient Air Pressure: 96,012 Pa

Reynolds Number	Velocity (m/s)	Lift (Newtons)	Drag (Newtons)
43,077	2.73	00.15	-00.10
94,484	5.99	00.40	-00.15
156,287	9.90	00.75	-00.25
218,437	13.83	01.40	-00.40
278,309	17.63	02.15	-00.55
333,971	21.15	03.00	-00.75
389,633	24.68	04.05	-01.10
445,295	28.20	05.15	-01.40

Table A.19 Lift and drag test, disc B, 20 Deg.

Test CL1

Disc C Lift and Drag Test

Diameter: 213mm AOA: -20°

Ambient Air Temperature: 22.1 C Ambient Air Pressure: 96,012 Pa

Reynolds Number	Velocity (m/s)	Lift (Newtons)	Drag (Newtons)
39,044	02.73	-00.05	00.00
85,639	05.99	-00.10	00.00
141,656	09.90	-00.05	-00.15
197,988	13.83	00.05	-00.25
252,255	17.63	00.20	-00.40
302,706	21.15	00.35	-00.60
353,157	24.68	00.90	-00.80
403,608	28.20	01.55	-01.05

Table A.20 Lift and drag test, disc C, -20 Deg.

Test CL2

Disc C Lift and Drag Test

Diameter: 213mm AOA: -15°

Ambient Air Temperature: 22.1 C Ambient Air Pressure: 96,012 Pa

Reynolds Number	Velocity (m/s)	Lift (Newtons)	Drag (Newtons)
39,044	02.73	-00.05	00.00
85,639	05.99	-00.05	00.00
141,656	09.90	00.05	-00.10
197,988	13.83	00.15	-00.20
252,255	17.63	00.30	-00.40
302,706	21.15	00.65	-00.55
353,157	24.68	01.20	-00.75
403,608	28.20	01.95	-00.95

Table A.21 Lift and drag test, disc C, -15 Deg.

Test CL3

Disc C Lift and Drag Test

Diameter: 213mm AOA: -10°

Ambient Air Temperature: 22.1 C Ambient Air Pressure: 96,012 Pa

Reynolds Number	Velocity (m/s)	Lift (Newtons)	Drag (Newtons)
39,044	02.73	-00.05	00.00
85,639	05.99	00.00	00.00
141,656	09.90	00.15	-00.10
197,988	13.83	00.30	-00.20
252,255	17.63	00.55	-00.35
302,706	21.15	00.95	-00.50
353,157	24.68	01.65	-00.70
403,608	28.20	02.35	-00.90

Table A.22 Lift and drag test, disc C, -10 Deg.

Test CL4

Disc C Lift and Drag Test

Diameter: 213mm AOA: -5°

Ambient Air Temperature: 22.1 C Ambient Air Pressure: 96,012 Pa

Reynolds Number	Velocity (m/s)	Lift (Newtons)	Drag (Newtons)
39,044	02.73	-00.10	00.00
85,639	05.99	-00.15	00.00
141,656	09.90	00.05	-00.10
197,988	13.83	00.30	-00.20
252,255	17.63	00.60	-00.30
302,706	21.15	01.05	-00.50
353,157	24.68	01.75	-00.70
403,608	28.20	02.65	-00.90

Table A.23 Lift and drag test, disc C, -5 Deg.

Test CL5

Disc C Lift and Drag Test

Diameter: 213mm AOA: 0°

Ambient Air Temperature: 22.1 C Ambient Air Pressure: 96,012 Pa

Reynolds Number	Velocity (m/s)	Lift (Newtons)	Drag (Newtons)
39,044	02.73	-00.20	00.00
85,639	05.99	-00.30	00.00
141,656	09.90	-00.10	-00.10
197,988	13.83	00.30	-00.20
252,255	17.63	00.70	-00.30
302,706	21.15	01.30	-00.50
353,157	24.68	02.20	-00.70
403,608	28.20	03.00	-00.90

Table A.24 Lift and drag test, disc C, 0 Deg.

Test CL6

Disc C Lift and Drag Test

Diameter: 213mm AOA: 5°

Ambient Air Temperature: 22.1 C Ambient Air Pressure: 96,012 Pa

Reynolds Number	Velocity (m/s)	Lift (Newtons)	Drag (Newtons)
39,044	02.73	-00.20	00.00
85,639	05.99	-00.20	-00.15
141,656	09.90	00.00	-00.25
197,988	13.83	00.40	-00.35
252,255	17.63	00.80	-00.45
302,706	21.15	01.45	-00.65
353,157	24.68	02.35	-00.85
403,608	28.20	03.20	-01.05

Table A.25 Lift and drag test, disc C, 5 Deg.

Test CL7

Disc C Lift and Drag Test

Diameter: 213mm AOA: 10°

Ambient Air Temperature: 22.1 C Ambient Air Pressure: 96,012 Pa

Reynolds Number	Velocity (m/s)	Lift (Newtons)	Drag (Newtons)
39,044	02.73	-00.20	-00.20
85,639	05.99	-00.10	-00.30
141,656	09.90	00.20	-00.40
197,988	13.83	00.55	-00.50
252,255	17.63	00.90	-00.60
302,706	21.15	01.65	-00.80
353,157	24.68	02.55	-01.00
403,608	28.20	03.65	-01.20

Table A.26 Lift and drag test, disc C, 10 Deg.

Test CL8

Disc C Lift and Drag Test

Diameter: 213mm AOA: 15°

Ambient Air Temperature: 22.1 C Ambient Air Pressure: 96,012 Pa

Reynolds Number	Velocity (m/s)	Lift (Newtons)	Drag (Newtons)
39,044	02.73	-00.15	-00.10
85,639	05.99	-00.05	-00.20
141,656	09.90	00.30	-00.30
197,988	13.83	00.70	-00.40
252,255	17.63	01.10	-00.55
302,706	21.15	01.90	-00.75
353,157	24.68	02.90	-00.95
403,608	28.20	04.20	-01.20

Table A.27 Lift and drag test, disc C, 15 Deg.

Test CL9

Disc C Lift and Drag Test

Diameter: 213mm AOA: 20°

Ambient Air Temperature: 22.1 C Ambient Air Pressure: 96,012 Pa

Reynolds Number	Velocity (m/s)	Lift (Newtons)	Drag (Newtons)
39,044	02.73	-00.10	-00.05
85,639	05.99	00.00	-00.10
141,656	09.90	00.40	-00.20
197,988	13.83	00.80	-00.35
252,255	17.63	01.30	-00.50
302,706	21.15	02.15	-00.70
353,157	24.68	03.25	-00.95
403,608	28.20	04.75	-01.20

Table A.28 Lift and drag test, disc C, 20 Deg.

CENTER OF LIFT RESULTS

Test AP1 6/1/97 10:00 am

Disc 'A' Center of lift experiment

Outside diameter: 235 mm Mass w/ rails: 214.9 g

Ambient air temperature: 24.35 C Ambient air pressure: 717.91 mm of Hg

Distance of pivot from leading edge: 44 mm (1.75 inches)

Counter mass on disc: 115.7 g

Reynolds #:	Comments:
53,388	@ 3.41 m/s (5.0 Hz), the disc experiences small oscillations.
57,615	@ 3.68 m/s (5.4 Hz), the disc lifts from retaining rod and bounces against it.
64,034	@ 4.09 m/s (6.0 Hz), the disc lifts and remains off of the retaining rod.
74,524	@ 4.76 m/s (6.6 Hz), the amplitude of the oscillations is increasing. The disc lifts for a moment then bounces downward sharply.
79,690	@ 5.09 m/s (6.9 Hz), a pattern develops. More momentary lifts followed by downward bounces.
85,483	@ 5.46 m/s (7.3 Hz), same pattern as above broken by periods of stability.
156,249	@ 9.98 m/s (12.1 Hz), the disc moves between to states, one oscillating and one stable.
176,289	@ 11.26 m/s (13.2 Hz), the disc lifts its rear higher.
194,920	@ 12.45 m/s (14.4 Hz), the disc becomes extremely unstable. Bouncing hard back and forth against the bump stops.

NOTE: Lift is behind the pivot throughout the entire test.

Test AP2 6/3/97 10:40 am

Disc 'A' Center of lift experiment

Outside diameter: 235 mm Mass of disc w/ rails: 214.9 g

Ambient air temperature: 23.80 C Ambient air pressure: 704.54 mm of Hg

Distance of pivot from leading edge: 52 mm (2.0625 inches)

Counter mass on disc: 243.9 g (hanging 19 mm from the leading edge)

Reynolds #:	Comments:
64,034	@ 4.09 m/s (6.0 Hz), the disc lifts from the retaining wire and assumes a negative AOA.
65,101	@ 4.16 m/s (6.1 Hz), the disc starts to oscillate. Amplitude is small.
72,138	@ 4.61 m/s (6.5 Hz), the disc continues to oscillate at increasingly negative angles of attack.
NOTE:	Lift is behind the pivot throughout the entire test.

Figure A.1 Center of lift test apparatus, disc A.

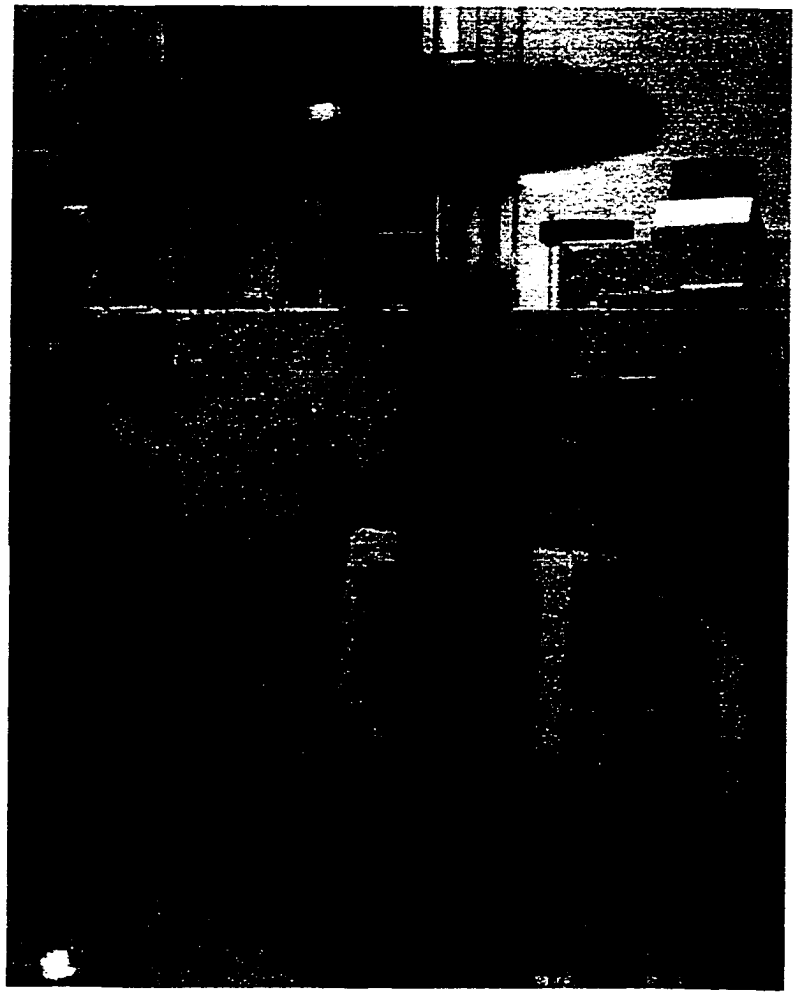

Figure A.2 Center of lift test, side view of apparatus, disc A.

Test AP3 6/3/97 10:00 am

Disc 'A' Center of lift experiment

Outside diameter: 235 mm Mass of disc w/ rails: 214.9 g

Ambient air temperature: 23.80 C Ambient air pressure: 704.54 mm of Hg

Distance of pivot from leading edge: 79 mm (3.125 inches)

Counter mass on disc: 520.4 g (hanging 19 mm from the leading edge)

Reynolds #:	Comments:
40,053	@ 2.56 m/s (4.3 Hz), the disc experiences small oscillations at a slightly negative AOA.
71,028	@ 4.54 m/s (6.4 Hz), the disc will stop oscillating for a moment and then continue. Amplitude and frequency are constant.
116,155	@ 7.42 m/s (9.1 Hz), slight increase in amplitude.
126,836	@ 8.10 m/s (9.9 Hz), interrupted oscillation behavior continues, disc is close to lifting. The mass may be too great.
191,811	@ 12.25 m/s (14.2 Hz), amplitude increases slightly.
209,999	@ 13.41 m/s (15.0 Hz), brief moments of stability interrupt the oscillations.
280,080	@ 17.89 m/s (20.3 Hz), behavior continues unabated. AOA is still negative.

NOTE: Lift is behind the pivot throughout the entire test.

Test AP4	6/3/97	11:30 am
Disc 'A'		Center of lift experiment
Outside diameter: 235 mm		Mass of disc w/ rails: 214.9 g
Ambient air temperature: 23.80 C		Ambient air pressure: 704.54 mm of Hg

Distance of pivot from leading edge: 95 mm (3.75 inches)

Counter mass on disc: 27.6 g (hanging 19 mm from the leading edge)

Reynolds #:	Comments:
58,698	@ 3.75 m/s (5.5 Hz), the disc pitches forward.
NOTE:	Lift is behind the pivot throughout the entire test.

Test AP5 6/3/97 1:00 p.m.

Disc 'A' Center of lift experiment

Outside diameter: 235 mm Mass of disc w/ rails: 214.9 g

Ambient air temperature: 23.80 C Ambient air pressure: 704.54 mm of Hg

Distance of pivot from leading edge: 95 mm (3.75 inches)

Counter mass on disc: 24.0 g (hanging 19 mm from the leading edge)

Identical to test AP4 except the counter mass is lighter.

Reynolds #:	Comments:
71,028	@ 4.54 m/s (6.4 Hz), The back of the disk is bouncing down on the wire without coming off of it. The lighter counter mass does not completely balance the mass moment of the disc. The center of lift, behind the pivot, is not strong enough at this velocity to overcome the mass moment. As a result the disc bounces on the retaining wire.
104,667	@ 6.69 m/s (8.2 Hz), The disc is off the wire. The unaccounted mass moment of the disc is equalized.
112,325	@ 7.18 m/s (8.8 Hz), the center of list is behind the pivot.
130,680	@ 8.35 m/s (10.2 Hz), the disc pitches forward.

Test AP6 6/6/97 11:00 am

Disc 'A' Center of lift experiment

Outside diameter: 235 mm Mass of disc w/ rails: 214.9 g

Ambient air temperature: 23.4 C Ambient air pressure: 708.33 mm of Hg

Distance of pivot from leading edge: 101.6 mm (4.0 inches)

Counter mass on disc: 19.3 g (hanging 19 mm from the leading edge)

Reynolds #:	Comments:
72,138	@ 4.61 m/s (6.5 Hz), The disc is bouncing on the wire. The center of lift is behind the pivot point.
79,690	@ 5.09 m/s (6.9 Hz), The disc has lifted from the wire. The center of lift is near the pivot point.
83,141	@ 5.31 m/s (7.1 Hz), the disc has pitched forward.

Test AP7 6/6/97 11:50 am

Disc 'A' Center of lift experiment

Outside diameter: 235 mm Mass of disc w/ rails: 214.9 g

Ambient air temperature: 23.4 C Ambient air pressure: 708.33 mm of Hg

Distance of pivot from leading edge: 101.6 mm (4.0 inches)

Counter mass on disc: 15.7 g (hanging 19 mm from the leading edge)

NOTE: *Experiment is identical to AP6 except that the counter mass is lighter.*

Reynolds #:	Comments:
75,653	@ 4.83 m/s (6.7 Hz), the disc is bouncing on its retaining wire.
83,141	@ 5.31 m/s (7.1 Hz), the bouncing is increasing in frequency and force.
86,654	@ 5.53 m/s (7.4 Hz), continued increases in bouncing force.
94,851	@ 6.06 m/s (8.1 Hz), the disc is very near to pitching forward.
108,496	@ 6.93 m/s (8.5 Hz), the disc pitches forward.

Test AP8 6/6/97 1:00 p.m.

Disc 'A' Center of lift experiment

Outside diameter: 235 mm Mass of disc w/ rails: 214.9 g

Ambient air temperature: 23.4 C Ambient air pressure: 708.33 mm of Hg

Distance of pivot from leading edge: 108 mm (4.25 inches)

Counter mass on disc: 10.9 g (hanging 19 mm from the leading edge)

Reynolds #:	Comments:
69,918	@ 4.47 m/s (6.3 Hz), the center of lift may be acting through the pivot.
71,028	@ 4.54 m/s (6.4 Hz), the disc lifts from the retaining wire and bounces gently.
74,524	@ 4.76 m/s (6.6 Hz), the disc lifts from the retaining wire and remains lifted.
76,782	@ 4.90 m/s (6.8 Hz), the disc pitches forward.
NOTE:	It is possible that the center of lift moves backward with increasing velocity. At 4.5 m/s the center of lift appeared to be acting through the center of the pivot. At 4.54 m/s the center of lift is behind the pivot.

Test AP9 6/6/97 1:10 p.m.

Disc 'A' Center of lift experiment

Outside diameter: 235 mm Mass of disc w/ rails: 214.9 g

Ambient air temperature: 23.4 C Ambient air pressure: 708.33 mm of Hg

Distance of pivot from leading edge: 108 mm (4.25 inches)

Counter mass on disc: 7.7 g (hanging 19 mm from the leading edge)

NOTE: *Experiment is identical to AP8 except that the counter mass is lighter.*

Reynolds #:	Comments:
108,496	@ 6.93 m/s (8.5 Hz), The disc is oscillating slowly back and forth.
111,049	@ 7.10 m/s (8.7 Hz), The disc lifts and then settles back down.
112,326	@ 7.18 m/s (8.8 Hz), The disc experiences some hard oscillations.
113,602	@ 7.26 m/s (8.9 Hz), The disc pitches forward.
NOTE:	The pitching moment is angle of attack sensitive. As the disc oscillates forward and backward, so too does the center of lift. When the center of lift is near the pivot, changes in angle of attack may move the center of lift back and forth across the pivot point causing hard oscillations.

Test AP10 6/6/97 1:40 p.m.

Disc 'A' Center of lift experiment

Outside diameter: 235 mm Mass of disc w/ rails: 214.9 g

Ambient air temperature: 23.4 C Ambient air pressure: 708.33 mm of Hg

Distance of pivot from leading edge: 114 mm (4.50 inches)

Counter mass on disc: 2.0 g (hanging 19 mm from the leading edge)

Reynolds #:	Comments:
64,034	@ 4.09 m/s (6.0 Hz), a steady disc just starts to lift.
68,808	@ 4.40 m/s (6.2 Hz), the disc pitches forward.

Test AP11 6/6/97 2:10 p.m.

Disc 'A' Center of lift experiment

Outside diameter: 235 mm Mass of disc w/ rails: 214.9 g

Ambient air temperature: 23.4 C Ambient air pressure: 708.33 mm of Hg

Distance of pivot from leading edge: 114 mm (4.50 inches)

Counter mass on disc: 0 g (No counter mass!)

NOTE: *Experiment is identical to AP10 except that there is no counter mass.*

Reynolds #:	Comments:
71,028	@ 4.54 m/s (6.4 Hz), the disc lifts away from the retaining wire and remains steady.
90,167	@ 5.75 m/s (7.7 Hz), the disc is steady.
108,496	@ 6.93 m/s (8.5 Hz), the disc lifts again.
111,049	@ 7.10 m/s (8.7 Hz), the disc pitches forward.
NOTE:	The center of lift is behind the pivot throughout the entire test.

Test AP12 6/9/97 9:00 a.m.

Disc 'A' Center of lift experiment

Outside diameter: 235 mm Mass of disc w/ rails: 214.9 g

Ambient air temperature: 23.0 C Ambient air pressure: 712.30 mm of Hg

Distance of pivot from leading edge: 121 mm (4.75 inches)

Counter mass on disc: 5.6 g (hanging 19 mm from the leading edge)

Reynolds #:	Comments:
64,034	@ 4.09 m/s (6.0 Hz), the disc pitches forward.
NOTE:	The pivot is now past the geometric center of the disc. It seems unlikely that the center of lift is behind the geometric center of the disc. The counter mass may be influencing the pitching direction of the disc. Subsequent test will use lighter masses at the same pivot point.

Test AP13 6/9/97 9:10 a.m.

Disc 'A' Center of lift experiment

Outside diameter: 235 mm Mass of disc w/ rails: 214.9 g

Ambient air temperature: 23.0 C Ambient air pressure: 712.30 mm of Hg

Distance of pivot from leading edge: 121 mm (4.75 inches)

Counter mass on disc: 3.0 g (exactly neutralizes the mass moment of the disc)

NOTE: *Experiment is identical to AP12 except that the counter mass is lighter.*

Reynolds #:	Comments:
34,465	@ 2.20 m/s (3.7 Hz), the disc pitches forward. The wind tunnel is at its lowest speed.

Test AP14 6/9/97 9:20 am

Disc 'A' Center of lift experiment

Outside diameter: 235 mm Mass of disc w/ rails: 214.9 g

Ambient air temperature: 23.0 C Ambient air pressure: 712.30 mm of Hg

Distance of pivot from leading edge: 121 mm (4.75 inches)

Counter mass on disc: 12.8 g

NOTE: *Experiment is identical to AP12 except that the counter mass is larger.*

Reynolds #:	Comments:
69,918	@ 4.47 m/s (6.3 Hz), the disc begins small oscillations.
75,653	@ 4.83 m/s (6.7 Hz), center of lift seems to be ahead of pivot.
79,690	@ 5.09 m/s (6.9 Hz), oscillations get stronger.
94,851	@ 6.06 m/s (8.1 Hz), oscillations continue to increase in strength.
113,602	@ 7.26 m/s (8.9 Hz), as the disc bounced on the retaining wire, it began to lift at the rear inducing a slight negative AOA. For a moment the disc hovered one half an inch off the wire then flipped forward. The disc stayed forward until the wind tunnel velocity was reduced and the mass moment overcame the lifting moment about the pivot. In this experiment, the center of lift was definitely behind the geometric center of the disc.
NOTE:	This shows the center of lift is very sensitive to AOA. The implication is that at positive angles the center of lift would be forward of the geometric center and at negative angles the center of lift would be behind the geometric center. This throws into question the validity of these experiments as the AOA changes in the course of them.

Test AP15 6/9/97 10:20 am

Disc 'A' Center of lift experiment

Outside diameter: 235 mm Mass of disc w/ rails: 214.9 g

Ambient air temperature: 23.0 C Ambient air pressure: 712.30 mm of Hg

Distance of pivot from leading edge: 121 mm (4.75 inches)

Counter mass on disc: 12.8 g

NOTE: *Experiment is identical to AP14 except that the retaining wire is bent down such that it cannot interfere with the test. Starting AOA is positive because the counter mass is not sufficient to neutralize the mass moment.*

Reynolds #:	Comments:
83,141	@ 5.31 m/s (7.1 Hz), the disc is vibrating slightly, the center of lift is ahead of geometric center.
131,961	@ 8.43 m/s (10.3 Hz), behavior is unchanged.
154,958 – 223,999	@ 9.90 to 14.30 m/s (12.0 – 16.0 Hz), the rear of the disc is pushing the retaining wire down. Center of lift is definitely ahead of the geometric center.
242,199	@ 15.47 m/s (17.3 Hz), oscillations begin to occur, disc is still forcing the retaining wire down.
248,347	@ 15.86 m/s (18.0 Hz), the oscillations become stronger but the disc never lifts from the wire.
NOTE:	This shows a relationship between the center of lift and the angle of attack. However, it is not enough to say that positive AOA moves the center of lift forward of the geometric center and that negative AOA moves the center of lift behind the geometric center. Because the drag force is contributing to the pitching moment at all angles of attack except zero degrees, in which the drag force acts through the geometric center of the disc.

Test AP16 6/9/97 11:00 am

Disc 'A' Center of lift experiment

Outside diameter: 235 mm Mass of disc w/ rails: 214.9 g

Ambient air temperature: 23.0 C Ambient air pressure: 712.30 mm of Hg

Distance of pivot from leading edge: 121 mm (4.75 inches)

Counter mass to balance disc: 12.8 g

NOTE: *Experiment is identical to AP15 except that we are using a thin rod to constrain the disc to 0 degrees AOA.*

Reynolds #:	Comments:
53,388	@ 3.41 m/s (5.0 Hz), the disc flips backward when the rod is lifted.
64,034	@ 4.09 m/s (6.0 Hz), the disc flips backward when the rod is lifted.
81,970	@ 5.24 m/s (7.0 Hz), the disc flips backward when the rod is lifted.
93,680	@ 5.99 m/s (8.0 Hz), the disc flips backward when the rod is lifted.
108,496	@ 6.93 m/s (8.5 Hz), vibrations begin in disc. Experiment halted.
NOTE:	This center of lift is clearly ahead of the geometric center at 0° AOA.

Test BP1 6/12/97 9:20 am

Disc 'B' Center of lift experiment

Outside diameter: 235mm Mass of disc w/ rails: 111.7g

Distance of pivot from leading edge: 40mm (1.5625 inches)

Counter mass to balance disc: 338g

Reynolds #:	Comments:
37,262	@ 2.38 m/s (4.0 Hz), Disc is at a slightly negative angle of attack.
93,781	@ 5.99 m/s (8.0 Hz), Disc is experiencing very small oscillations in pitch while maintaining the same general AOA.
116,169	@ 7.42 m/s (9.1 Hz), Oscillation amplitude, while still small, has increased.
128,225	@ 8.19 m/s (10.0 Hz), Oscillation amplitude, while still small, increases again.
142,785	@ 9.12 m/s (11.1 Hz), The center of lift is definitely acting on the rear of the disc, behind the pivot.
188,031	@ 12.01 m/s (14.0 Hz), The disc is again oscillating. The amplitude has been slowly increasing. The bottom of the disc is nearly touching the retaining wire at the lowest point of oscillation.
237,975	@ 15.20m/s (17.0 Hz), It is apparent that the frequency of oscillation is also increasing with the velocity.
248,308	@ 15.86 m/s (18.0 Hz), Oscillation amplitude and frequency are still increasing.
262,085	@ 16.74 m/s (19.0 Hz), The disc oscillation has increased such that it is now bouncing against the retaining wire.
275,941	@ 17.63 m/s (20.0 Hz), Oscillation amplitude and frequency are still increasing.
289,797	@ 18.51 m/s (21.0 Hz), Oscillation amplitude and frequency are still increasing.

303,574	@ 19.39 m/s (22.0 Hz), Oscillation amplitude and frequency are still increasing.
Author's Note:	It is obvious that the center of lift is pressing up on the disc behind the pivot. As the disc pitches forward the drag force increases with the angle of attack. Resulting in a large counter-moment which rotates the disc down. I believe, and it seems intuitively obvious, that the magnitude of the forward pitching moment is smaller for increased angles of attack. The result is the observed oscillating motion in which at maximum forward pitch (negative angle of attack) the drag force dominates the disc response and the disc counter rotates down to bounce against the retaining wire were the lift force dominates and rotates the disc forward. The increasing amplitude and frequency observed are consistent with the stronger lift and drag forces expected with the increased velocity.

Test BP2 6/12/97 9:45 am

Disc 'B' Center of lift experiment

Outside diameter: 235mm Mass of disc w/ rails: 111.7g

Distance of pivot from leading edge: 59mm (2.3125 inches)

Counter mass to balance disc: 143.5g

Reynolds #:	Comments
82,039	@ 5.24 m/s (7.0 Hz), Disc is off of the wire and at a slightly negative angle of attack.
87,675	@ 5.60 m/s (7.5 Hz), Disc is experiencing very small oscillations in pitch while maintaining the same general AOA.
93,781	@ 5.99 m/s (8.0 Hz), Oscillation amplitude, while still small, has increased.
108,498	@ 6.93 m/s (8.5 Hz), Oscillation amplitude, while still small, increases again.
115,073	@ 7.34 m/s (9.0 Hz), The disc experiences occasional popping in its oscillations as if a periodic perturbation, perhaps a resonance, is increasing the lift.
134,800	@ 8.61 m/s (10.5 Hz), The disc's oscillation are clearly experiencing a resonant increase followed by a damping decrease. It appears that two oscillations are overlaid one another. When damped the oscillations are so small as to be barely detectable and the disc seems stable at a negative AOA (approx. –5 degrees).
164,077	@ 10.48 m/s (12.5 Hz) The disc oscillation continues to increase in amplitude and frequency.
188,031	@ 12.01 m/s (14.0 Hz), The increases in amplitude and frequency have continued and the disc is bouncing against the retaining wire.
209,950	@ 13.41 m/s (15.0 Hz), Increases in velocity continue to increase amplitude and frequency.
232,338	@ 14.84 m/s (16.6 Hz), Oscillations are much harder.

237,975	@ 15.20 m/s (17.0 Hz), Frequency has increased.
251,126	@ 16.04 m/s (18.2 Hz), Frequency has increased.
262,085	@ 16.74 m/s (19.0 Hz), On-going oscillations.
268,974	@ 17.18 m/s (19.5 Hz), The disc is pitching back and forth very hard.
275,941	@ 17.63 m/s (20.0 Hz), Test aborted due to the increasingly violent behavior of the disc.

Author's Note: The same phenomena here as in the previous experiment BP1.

Test BP3 6/12/97 10:15 am

Disc 'B' Center of lift experiment

Outside diameter: 235mm Mass of disc w/ rails: 111.7g

Distance of pivot from leading edge: 78mm (3.0625inches)

Counter mass to balance disc: 66g

Reynolds #:	Comments:
82,039	@ 5.24 m/s (7.0 Hz), Disc is stable just above the retaining wire.
87,675	@ 5.60 m/s (7.5 Hz), Disc is experiencing very small oscillations.
93,781	@ 5.99 m/s (8.0 Hz), Oscillation amplitude, while still small, has increased.
115,073	@ 7.35 m/s (9.0 Hz), The disc occasionally pitches forward to assume a position, seemingly stable yet, at an increased negative angle of attack. Then pitches back to just above the wire. The more I observe this behavior, as in the last experiment and now in this one, I think it is related to the domed cupola on the surface of the disc.
125,406	@ 8.01 m/s (9.8 Hz), Oscillation amplitude, while still small, increases again.
134,800	@ 8.61 m/s (10.5 Hz), The frequency and amplitude continue to increase with velocity.
141,376	@ 9.03 m/s (11.0 Hz) The frequency and amplitude continue to increase with velocity.
149,517	@ 9.55 m/s (11.6 Hz), The increases in amplitude and frequency have continued and the disc is bouncing against the retaining wire.
156,249	@ 9.98 m/s (12.1 Hz), The disc has assumed an even greater angle of attack and appears ready to pitch fully forward. It is most unusual how it seems to remain relatively fixed in place, barring the tiny oscillations. The pitching moments sensitivity to angle of attack and to the cupola's effects on the aerodynamics is must be the cause of this.

162,825	@ 10.40 m/s (12.4 Hz), Oscillations amplitude and frequency continue to increase with velocity.
166,113	@ 10.61 m/s (12.6 Hz), The disc looks very close to pitching forward.
169,870	@ 10.85 m/s (12.8 Hz), Oscillations amplitude and frequency continue to increase with velocity.
180,829	@ 11.55 m/s (13.5 Hz), The disc is reaching -20° AOA at its highest point and is oscillating about a -10° AOA.
188,031	@ 12.01 m/s (14.0 Hz), The disc has begun to hit the retaining wire with increased force.
194,920	@ 12.45 m/s (14.4 Hz), The disc is oscillating about some negative AOA, approximately -12°. The interesting thing is that the angle about which it is oscillating appears to increase with velocity.
218,248	@ 13.94 m/s (15.6 Hz), The amplitude and frequency continue to increase.
223,884	@ 14.30 m/s (16.0 Hz), The amplitude and frequency continue to increase.
243,924	@ 15.58 m/s (17.5 Hz), Occasionally the disc pitches up and pauses for several seconds at about -20°.
253,787	@ 16.21 m/s (18.4 Hz), Oscillations amplitude and frequency continue to increase with velocity. The oscillations are pitching the disc forward and backward very quickly.
264,903	@ 16.92 m/s (19.2 Hz), The disc is oscillating without the occasional pauses I saw before.
275,941	@ 17.63 m/s (20.0 Hz), The experiment is halted.
Author's Note:	The strange oscillating behavior is likely due to the center of lift starting behind the pivot point and moving forward and closer to, but not ahead of, the pivot point with increased velocity and increased AOA. The pitch forward and pause behavior occurs when the lift and drag moments about the pivot point are equal.

Test BP4 6/12/97 10:45 am

Disc 'B' Center of lift experiment

Outside diameter: 235mm Mass of disc w/ rails: 111.7g

Distance of pivot from leading edge: 90mm (3.5625 inches)

Counter mass to balance disc: 35.5g

Reynolds #:	Comments:
82,039	@ 5.24 m/s (7.0 Hz), Disc is stable just above the retaining wire.
87,675	@ 5.60 m/s (7.5 Hz), Disc moves a little further from the wire.
93,781	@ 5.99 m/s (8.0 Hz), Disc pitches slightly forward to assume a small negative AOA.
109,750	@ 7.01 m/s (8.6 Hz), The first noticeable oscillations occur. The disc is oscillating about a negative AOA (approx. -3°).
117,421	@ 7.50 m/s (9.2 Hz), The disc began to pitch fully forward but stopped at a -45° AOA. It stayed at -45° for a while, then came back to level flight, and returned to -45° AOA. It has huge amplitude but a small frequency.
122,745	@ 7.84 m/s (9.6 Hz), Hanging on at -45° AOA. Small amplitude oscillations. Seems to be stable at -45°.
138,714	@ 8.86 m/s (10.8 Hz) The AOA has increased slightly.
173,800	@ 11.05 m/s (13.0 Hz), The AOA has decreased slightly.
202,435	@ 12.93 m/s (14.7 Hz), The frequency and amplitude have increased.
222,475	@ 14.21 m/s (15.9 Hz), No change in disc behavior.
255,197	@ 16.30 m/s (18.5 Hz), The disc amplitude has increased and the disc is oscillating about an angle greater than -45°.
270,383	@ 17.27 m/s (19.6 Hz), No change in disc behavior.

284,161	@ 18.15 m/s (20.6 Hz), Again the disc goes back to level flight and returns to oscillating about an angle greater than -45°.
286,979	@ 18.33 m/s (20.8 Hz), The changes in pitch attitude are continuing at 5 second intervals.
304,983	@ 19.48 m/s (22.1 Hz), The frequency is increasing rapidly now.
314,534	@ 20.09 m/s (22.8 Hz), The AOA is less than -45° now. The drag force is beginning to dominate the response by moving the AOA toward level flight.
354,614	@ 22.65 m/s (25.7 Hz), The behavior continues. Test is halted.

Author's Note: This experiment was repeated to ensure the exhibited behavior was not an aberration.

Test BP5 6/18/97 10:00 am

Disc 'B' Center of lift experiment

Outside diameter: 235mm Mass of disc w/ rails: 111.7g

Distance of pivot from leading edge: 98mm (3.875 inches)

Counter mass to balance disc: 21g

Reynolds #:	Comments:
56,519	@ 3.61 m/s (5.3 Hz), Disc is lightly bouncing against the retaining wire.
58,711	@ 3.75 m/s (5.5 Hz), The disc bounces high and flips forward.

Test BP6 6/18/97 10:30 am

Disc 'B' Center of lift experiment

Outside diameter: 235mm Mass of disc w/ rails: 111.7g

Distance of pivot from leading edge: 98mm (3.875 inches)

Counter mass to balance disc: 25.1g

Reynolds #:	Comments
46,029	@ 2.94 m/s (4.6 Hz), Disc is pressing against wire. Center of lift is ahead of pivot.

Test BP7 6/18/97 11:00 am

Disc 'B' Center of lift experiment

Outside diameter: 235mm Mass of disc w/ rails: 111.7g

Distance of pivot from leading edge: 105mm (4.125 inches)

Counter mass to balance disc: 15.1g

Reynolds #:	Comments:
64,034	@ 4.09 m/s (6.0 Hz), The disc lifts one-quarter inch from the wire and holds steady.
75,620	@ 4.83 m/s (6.7 Hz), The gap between the disc and the wire grows another quarter of an inch. The disc is stable.
79,690	@ 5.09 m/s (6.9 Hz), The disc pitches forward.

Test BP8 6/18/97 11:30 am

Disc 'B' Center of lift experiment

Outside diameter: 235mm Mass of disc w/ rails: 111.7g

Distance of pivot from leading edge: 110mm (4.3125 inches)

Counter mass to balance disc: 7.7g

Reynolds #:	Comments:
40,080	@ 2.56 m/s (4.3 Hz), The disc pitches forward.

Test BP9 6/18/97 12:00 pm

Disc 'B' Center of lift experiment

Outside diameter: 235mm Mass of disc w/ rails: 111.7g

Distance of pivot from leading edge: 116mm (4.5625 inches)

Counter mass to balance disc: 4.1g

Reynolds #:	Comments:
42,428	@ 2.71 m/s (4.4 Hz), The disc pitches forward.

Test BP10 6/18/97 1:30 pm

Disc 'B' Center of lift experiment

Outside diameter: 235mm Mass of disc w/ rails: 111.7g

Distance of pivot from leading edge: 122mm (4.8125 inches)

Counter mass to balance disc: 3.4g hanging from the rear of the disc.

Reynolds #:	Comments
62,938	@ 4.02 m/s (5.9 Hz), The disc bounces lightly for several seconds then pitches forward.

Test BP11 6/18/97 2:00 pm

Disc 'B' Center of lift experiment

Outside diameter: 235mm Mass of disc w/ rails: 111.7g

Distance of pivot from leading edge: 122mm (4.8125 inches)

Counter mass to balance disc: 2.2g hanging from the rear.

Identical to BP10 except the counter-mass has changed.

Reynolds #:	Comments:
39,141	@ 2.50 m/s (4.2 Hz), The disc pitches forward.

Test BP12 6/18/97 2:30 pm

Disc 'B' Center of lift experiment

Outside diameter: 235mm Mass of disc w/ rails: 111.7g

Distance of pivot from leading edge: 122mm (4.8125 inches)

Counter mass to balance disc: 2.8g hanging from the rear.

Identical to BP10 except counter-mass has changed.

Reynolds #:	Comments:
42,428	@ 2.71 m/s (4.4 Hz), Disc is pushing against wire. Center of lift is ahead

Test BP13 6/18/97 3:00 pm

Disc 'B' Center of lift experiment

Outside diameter: 235mm Mass of disc w/ rails: 111.7g

Distance of pivot from leading edge: 122mm (4.8125 inches)

Counter mass to balance disc: 6.7g hanging from the rear.

Identical to BP10 except counter-mass has changed.

Reynolds #:	Comments:
61,842	@ 3.95 m/s (5.8 Hz), The disc pitches forward.

Test BP14 6/18/97 3:30 pm

Disc 'B' Center of lift experiment

Outside diameter: 235mm Mass of disc w/ rails: 111.7g

Distance of pivot from leading edge: 122mm (4.8125 inches)

Counter mass to balance disc: 11.4g hanging from the rear.

Identical to BP10 except that the counter-mass has changed.

Reynolds #:	Comments
90,023	@ 5.75 m/s (97.7 Hz), The disc pitches forward.

Test BP15 6/18/97 4:00 pm

Disc 'B' Center of lift experiment

Outside diameter: 235mm Mass of disc w/ rails: 111.7g

Distance of pivot from leading edge: 122mm (4.8125 inches)

Counter mass to balance disc: 15.1g hanging from the rear.

Identical to BP10 except that the counter-mass has changed.

Reynolds #:	Comments:
115,073	@ 7.35 m/s (9.0 Hz), The disc pitches forward.

Test BP16 6/18/97 4:30 pm

Disc 'B' Center of lift experiment

Outside diameter: 235mm Mass of disc w/ rails: 111.7g

Distance of pivot from leading edge: 122mm (4.8125 inches)

Counter mass to balance disc: 18.8g hanging from the rear.

Identical to BP10 except that the counter-mass has changed.

Reynolds #:	Comments:
118,831	@ 7.59 m/s (9.3 Hz), The disc begins vibrating.
129,477	@ 8.27 m/s (10.1 Hz), The disc pitches forward.

Test BP17 6/18/97 5:00 pm

Disc 'B' Center of lift experiment

Outside diameter: 235mm Mass of disc w/ rails: 111.7g

Distance of pivot from leading edge: 122mm (4.8125 inches)

Counter mass to balance disc: 22.5g hanging from the rear.

Identical to BP10 except that the counter-mass has changed.

Reynolds #:	Comments:
134,800	@ 8.61 m/s (10.5 Hz), The disc is vibrating and bouncing against the retaining wire.
149,517	@ 9.55 m/s (11.6 Hz), The disc pitches forward.
Author's note:	The center of lift is ahead of the pivot. When the disc is level it causes the disc to rotate backward and contact the retaining wire. As the velocity increases, the disc bounces harder until the bouncing force pitches the disc so far forward that the lift changes direction and pushes down on the disc with enough force to pitch it the rest of the way forward.

Test BP18 6/20/97 9:10 am

Disc 'B' Center of lift experiment

Outside diameter: 235mm Mass of disc w/ rails: 111.7g

Distance of pivot from leading edge: 127mm (5 inches)

Counter mass to balance disc: 12g hanging from the rear.

Reynolds #:	Comments
34,444	@ 2.20 m/s (3.7 Hz), The disc oscillated back and forth for 20 seconds then pitched forward.

Test BP19 6/20/97 9:45 am

Disc 'B' Center of lift experiment

Outside diameter: 235mm Mass of disc w/ rails: 111.7g

Distance of pivot from leading edge: 127mm (5 inches)

Counter mass to balance disc: 14.7g hanging from the rear.

Identical to BP18 except that the counter mass has changed.

Reynolds #:	Comments:
64,034	@ 4.09 m/s (6.0 Hz), The disc pitches forward.

Test BP20 6/20/97 10:15 am

Disc 'B' Center of lift experiment

Outside diameter: 235mm Mass of disc w/ rails: 111.7g

Distance of pivot from leading edge: 127mm (5 inches)

Counter mass to balance disc: 18.4g hanging from the rear.

Identical to BP18 except that the counter mass has changed.

Reynolds #:	Comments:
105,993	@ 6.77 m/s (8.3 Hz). The disc pitches forward.
Author's note:	There was no movement before the disc pitched.

Test BP21 6/20/97 11:00 am

Disc 'B' Center of lift experiment

Outside diameter: 235mm Mass of disc w/ rails: 111.7g

Distance of pivot from leading edge: 127mm (5 inches)

Counter mass to balance disc: 22.1g hanging from the rear.

Identical to BP18 except that the counter mass has changed.

Reynolds #:	Comments:
113,664	@ 7.26 m/s (8.9 Hz), The disc starts to vibrate.
123,997	@ 7.92 m/s (9.7 Hz), The disc pitches forward.

Test BP22 6/22/97 11:30 am

Disc 'B' Center of lift experiment

Outside diameter: 235mm Mass of disc w/ rails: 111.7g

Distance of pivot from leading edge: 133mm (5.25 inches)

Counter mass to balance disc: 19.8g hanging from the rear.

Reynolds #:	Comments
48,534	@ 3.10 m/s (4.7 Hz), The disc pitches forward.

Test BP23 6/22/97 12:00 pm

Disc 'B' Center of lift experiment

Outside diameter: 235mm Mass of disc w/ rails: 111.7g

Distance of pivot from leading edge: 133mm (5.25 inches)

Counter mass to balance disc: 23.5g hanging form the rear.

Identical to BP22 except that the counter mass has changed.

Reynolds #:	Comments:
79,690	@ 5.09 m/s (6.9 Hz), The disc pitches forward.

Test BP24 6/22/97 2:00 pm

Disc 'B' Center of lift experiment

Outside diameter: 235mm Mass of disc w/ rails: 111.7g

Distance of pivot from leading edge: 140mm (5.5 inches)

Counter mass to balance disc: 28.6g hanging from the rear.

Reynolds #:	Comments:
112,411	@ 7.18 m/s (8.8 Hz), Disc bounces very lightly on wire. Movement is 1/32nd of an inch.
113,664	@ 7.26 m/s (8.9 Hz), Disc flips forward.

Test BP25 6/22/97 2:30 pm

Disc 'B' Center of lift experiment

Outside diameter: 235mm Mass of disc w/ rails: 111.7g

Distance of pivot from leading edge: 140mm (5.5 inches)

Counter mass to balance disc: 36.3g hanging from the rear.

Identical to BP24 except that the counter mass has changed.

Reynolds #:	Comments
125,406	@ 8.01 m/s (9.8 Hz), Disc is pressing against wire. Center of lift is ahead of pivot.

Test BP26 6/22/97 3:00 pm

Disc 'B' Center of lift experiment

Outside diameter: 235mm Mass of disc w/ rails: 111.7g

Distance of pivot from leading edge: 144mm (5.6875 inches)

Counter mass to balance disc: 42.2g hanging from the rear.

Reynolds #:	Comments:
37,262-169,870	@ 2.38 m/s – 10.85 m/s (4.0 – 12.8 Hz), Completely stable disc. No vibrations. No changes. Still 0 degrees AOA.
172,219	@ 11.00 m/s (12.9 Hz), Frisbee pitches forward to wire. *Lift is in front of pivot.*

Test BP27 6/22/97 3:30 pm

Disc 'B' Center of lift experiment

Outside diameter: 235mm Mass of disc w/ rails: 111.7g

Distance of pivot from leading edge: 152mm (6 inches)

Counter mass to balance disc: 61.4g hanging from the rear.

Reynolds #:	Comments:
154,997	@ 9.90 m/s (12.0 Hz), Disc is pushing against wire. Center of lift is ahead of the pivot. The disc began experiment against wire and it is likely that the disc would have flipped backward much earlier if not constrained by the wire.

Test CP1 8/5/97 9:30 am

Disc 'C' Center of lift experiment

Outside diameter: 213mm Mass of disc w/ rails: 194.8g

Distance of pivot from leading edge: 54mm (2.125 inches)

Counter mass to balance disc: 584.4g

Counter mass hung 35mm (1.375 inches) from leading edge.

Reynolds #:	Comments:
175,256	@ 12.35 m/s (14.3 Hz), The disc is pitching backward lightly, pressing on the retaining wire.
275,154	@ 19.39 m/s (22.0 Hz), The disc is still resting on the wire but appears to not have a strong pitching force in either direction.
337,741	@ 23.80 m/s (27.0 Hz), Lifts off the wire then settles back on to it. Test aborted.

Test CP2 8/5/97 9:50 am

Disc 'C' Center of lift experiment

Outside diameter: 213mm Mass of disc w/ rails: 194.8g

Distance of pivot from leading edge: 54mm (2.125 inches)

Counter mass to balance disc: 584.4g

Counter mass hung 35mm (1.375 inches) from leading edge.

Same as CP1 except that the retaining wire is removed.

Reynolds #:	Comments:
162,485	@ 11.45 m/s (13.4 Hz), The disc is beginning to oscillate and has lift behind the pivot.
196,543	@ 13.85 m/s (15.5 Hz), Pitches forward slightly to assume a negative AOA. Lift and drag moments are balanced.
251,461	@ 17.72 m/s (20.1 Hz), More lifting at the rear indicating a stronger lift force positioned behind the pivot point.

Test CP3 8/5/97 10:15 am

Disc 'C' Center of lift experiment

Outside diameter: 213mm Mass of disc w/ rails: 194.8g

Distance of pivot from leading edge: 63.5mm (2.5 inches)

Counter mass to balance disc: 292.2g

Counter mass hung 35mm (1.375 inches) from leading edge.

Reynolds #:	Comments:
65,420	@ 4.61 m/s (6.5 Hz). The rear of the disc lifts approximately 1 degree indicating a center of lift behind the pivot.
104,302	@ 7.35 m/s (9.0 Hz). The disc is oscillating about a small, negative angle of attack.
153,970	@ 10.85 m/s (12.8 Hz), The rear continues to oscillate and lift. Now at approximately –10 degrees AOA.
250,113	@ 17.63 m/s (20.0 Hz), The rear of the disc lifts higher and the amplitude of oscillation increases sharply. The disc appears to be bouncing between –60 and 0 degrees AOA. The behavior continues for ~10 seconds then the disc pitches fully forward.

Test CP4 8/5/97 10:30 am

Disc 'C' Center of lift experiment

Outside diameter: 213mm Mass of disc w/ rails: 194.8g

Distance of pivot from leading edge: 63.5mm (2.5 inches)

Counter mass to balance disc: 290.0g

Counter mass hung 35mm (1.375 inches) from leading edge.

Rerun of CP3 with counter mass of 290.0g

Reynolds #:	Comments:
85,996	@ 6.06 m/s (8.1 Hz), Lifted from the wire to approximately –10 degrees. Exhibits very small oscillations but otherwise steady.
185,190	@ 13.05 m/s (14.8 Hz), From 8.1 Hz The magnitude of the AOA is gradually increasing (more negative) as is the amplitude of oscillation. The center of lift is clearly behind the pivot. Test aborted.

Test CP5 8/6/97 10:10 am

Disc 'C' Center of lift experiment

Outside diameter: 213mm Mass of disc w/ rails: 194.8g

Distance of pivot from leading edge: 76mm (3.0 inches)

Counter mass to balance disc: 153.1g

Counter mass hung 35mm (1.375 inches) from leading edge.

Reynolds #:	Comments:
52,222	@ 3.68 m/s (5.4 Hz), The disc pitches completely forward. The center of lift is behind the pivot.

Test CP6 8/6/97 10:30 am

Disc 'C' Center of lift experiment

Outside diameter: 213mm Mass of disc w/ rails: 194.8g

Distance of pivot from leading edge: 89mm (3.5 inches)

Counter mass to balance disc: 75.8g

Counter mass hung 35mm (1.375 inches) from leading edge.

Reynolds #:	Comments:
57,047	@ 4.02 m/s (5.9 Hz), The disc pitches completely forward. The center of lift is behind the pivot.

Test CP7 8/6/97 10:45 am

Disc 'C' Center of lift experiment

Outside diameter: 213mm Mass of disc w/ rails: 194.8g

Distance of pivot from leading edge: 102mm (4.0 inches)

Counter mass to balance disc: 26.6g

Counter mass hung 35mm (1.375 inches) from leading edge.

Reynolds #:	Comments:
33,774	@ 2.38 m/s (4.0 Hz), The disc pitches completely forward. The center of lift is behind the pivot.

Test CP8 8/6/97 11:00 am

Disc 'C' Center of lift experiment

Outside diameter: 213mm Mass of disc w/ rails: 194.8g

Distance of pivot from leading edge: 106mm (4.1875 inches)

Counter mass to balance disc: 2.3g

Counter mass hung 35mm (1.375 inches) from leading edge.

Reynolds #:	Comments:
175,256	@ 12.35 m/s (6.4 Hz), The disc pitches completely forward.
NOTE:	If the center of lift at low velocity is behind the mid-chord point and moves forward with increasing velocity. Then when the pivot is at or just slightly ahead the mid-chord point the disc will still pitch forward. Because a small lifting force behind the pivot will push the rear of the disc up and rotate the disc's center of mass forward of the pivot where the additional counter mass adds the forward pitching moment.

Test CP9 8/6/97 11:25 am

Disc 'C' Center of lift experiment

Outside diameter: 213mm Mass of disc w/ rails: 194.8g

Distance of pivot from leading edge: 113mm (4.4375 inches)

Counter mass to balance disc: 4.2g

Counter mass hung from the rear of the disc, or 197mm (7.75 inches) from leading edge.

Reynolds #:	Comments:
250,113	Up to 17.63 m/s (20.0 Hz), The disc is extremely AOA sensitive. The disc exhibited a tendency to pitch backward indicating a center of lift ahead of the pivot.

Test CP10 8/6/97 11:55 am

Disc 'C' Center of lift experiment

Outside diameter: 213mm Mass of disc w/ rails: 194.8g

Distance of pivot from leading edge: 121mm (4.75 inches)

Counter mass to balance disc: 29g

Counter mass hung from the rear of the disc, or 197mm (7.75 inches) from leading edge.

Reynolds #:	Comments:
175,256	Up to 17.63 m/s (20.0 Hz), At the low velocities (3.7 Hz to 5.0 Hz) the disc tended to pitch forward. In the middle velocities (5.0 Hz to 17.0 Hz) the disc tended to pitch backward. In the high velocities (17.0 Hz and above) the disc is again tending to pitch forward. But even at 20.0 Hz, the disc has not fully pitched either direction.

Test CP11 8/6/97 12:20 pm

Disc 'C' Center of lift experiment

Outside diameter: 213mm Mass of disc w/ rails: 194.8g

Distance of pivot from leading edge: 125mm (4.9375 inches)

Counter mass to balance disc: 53g

Counter mass hung from the rear of the disc, or 197mm (7.75 inches) from leading edge.

Reynolds #:	Comments:
71,079	@ 4.54 m/s (6.4 Hz), The disc pitches backward indicating a center of lift ahead of the pivot. I decide to increase velocity to see if behavior is consistent.
202,928	Up to 14.30 m/s (16.0 Hz), The backward pitching behavior is consistent at all velocities between 6.4 Hz and 16.0 Hz. Therefore the center of lift is ahead of the pivot regardless of its dependence on velocity.

TUFT TEST RESULTS

Test AT1	6/19/97	12:20 p.m.
Disc 'A'	Tuft test	0 degree AOA
Ambient air temperature:		Ambient air pressure:

Reynolds Number	Comments
64,034	@ 4.09 m/s (6.0 Hz), vortices building on the sides at bottom of disc and from the middle rear at bottom of disc.
128,117-142,045	@ 8.18 to 9.07 m/s (10.0-11.0 Hz), shows well-developed vortices at sides and rear of disc.
173,618	@ 11.09 m/s (13.0 Hz), small vibrations in tufts on top surface of disc. Vibrations appear to increase with velocity.
189,506	@ 12.10 m/s (14.0 Hz), Disc shows streamlines curving in at rear and breaking off.
275,941	@ 17.63 m/s (20.0 Hz), Disc is showing visible mechanical vibrations.
	Throughout the experiment the upper surface boundary layer remained attached, while the lower surface was entirely separated and stagnant. The bottom edge of disc generated many vortices. Surface ridges atop disc appear to introduce turbulence to the boundary layer.

Test AT2	6/19/97	1:20 p.m.
Disc 'A'	Tuft test	9.33 degrees AOA
L.E. 11-3/8 inches from ground		T.E. 9-7/8 inches from ground
Ambient air temperature:		Ambient air pressure:

Reynolds Number	Comments
53,388	@ 3.41 m/s (5.0 Hz), vortices from middle to rear edge with small turbulence in rows 2-3 on surface.
114,878	@ 7.34 m/s (9.0 Hz), Turbulence in 2nd row of tufts from front. Vorticinal shedding begins at the bottom lip of the disc and extends from the sides and rear. On the extreme sides the vortices tend to curl up around the body of the disc. On the sides the tufts curl out. In the rear the tufts are straight back and rotating.
142,045	@ 9.07 m/s (11.0 Hz), in the 2nd row, and few are lifted from the surface of the disc. Indicating separation at that point.
173,618	@ 11.09 m/s (13.0 Hz), in the 2nd row, one tuft is moving in a clockwise directional vortex (viewed from the front), indicating an adverse pressure gradient which may cause separation. The vortex near the centerline of the disc and lower toward the sides of the disc also indicate separation. Tufts on the entire top surface showing signs of light turbulence.
209,999	@ 13.42 m/s (15.0 Hz), tufts on rear edge are bending inward. Vortex is shedding from rear right edge.
248,347	@ 15.86 m/s (18.0 Hz), small mechanical vibration showing in disc. Vortices are clearly evident in 2nd and 3rd row (on left side). The front underside of disc is showing strong vortex generation. These vortices are impacting the underbody of the disc, perhaps causing the mechanical vibration.
275,941	@ 17.63 m/s (20.0 Hz), strong mechanical vibrations in disc. Experiment halted.

Test AT3	6/19/97	2:15 p.m.
Disc 'A'	Tuft Test	degree AOA
L.E. 9-3/8 inches from ground		T.E. 12-1/4 inches from ground
Ambient air temperature:		Ambient air pressure:

Reynolds Number	Comments
93,680	@ 6.93 m/s (8.0 Hz), Small vortices along sides at bottom edge with strong vortices at rear edge. The rear underside of disc is separated and recirculating.
114,878	@ 7.34 m/s (9.0 Hz), On the surface, the tufts at the rear are bending outwards while tufts on the lower edge, at the rear, are bending inward and upward. Flow on the top surface is straight back to midpoint in the disc then curves from the center toward the outer edge. Huge vortices are being produced along the rear of the disc. Drag forces must be very high.
142,045	@ 9.07 m/s (11.0 Hz), At the rear of the disc, flow is curling downward from the top surface around the bottom lip to the underside of the disc.
172,618	@ 11.09 m/s (13.0 Hz), Extreme turbulence at the rear of the disc.
248,347	@ 15.86 m/s (18.0 Hz), At the front of the disc, streamlines impacting the middle move upward across the top surface of the disc, while streamlines just off the middle curl back and underneath the front lip.

Test BT1

Disc 'B' Tuft Test 0 degree AOA

L.E. 10-3/16 inches from ground T.E. 10-3/16 inches from ground

Reynolds Number	Comments
53,388	@ 4.09 m/s (5.0 Hz), Slow vorticies begin to develop along the sides, rear of the mid-chord. All other tufts are still.
82,039	@ 5.24 m/s (7.0 Hz), The cupola begins to exhibit vorticinal shedding. The tufts at the rear of the cupola are spinning in vortices. The tufts on the sides at mid-chord also exhibit vorticinal shedding. The bottom is separated and detached. All other tufts are still.

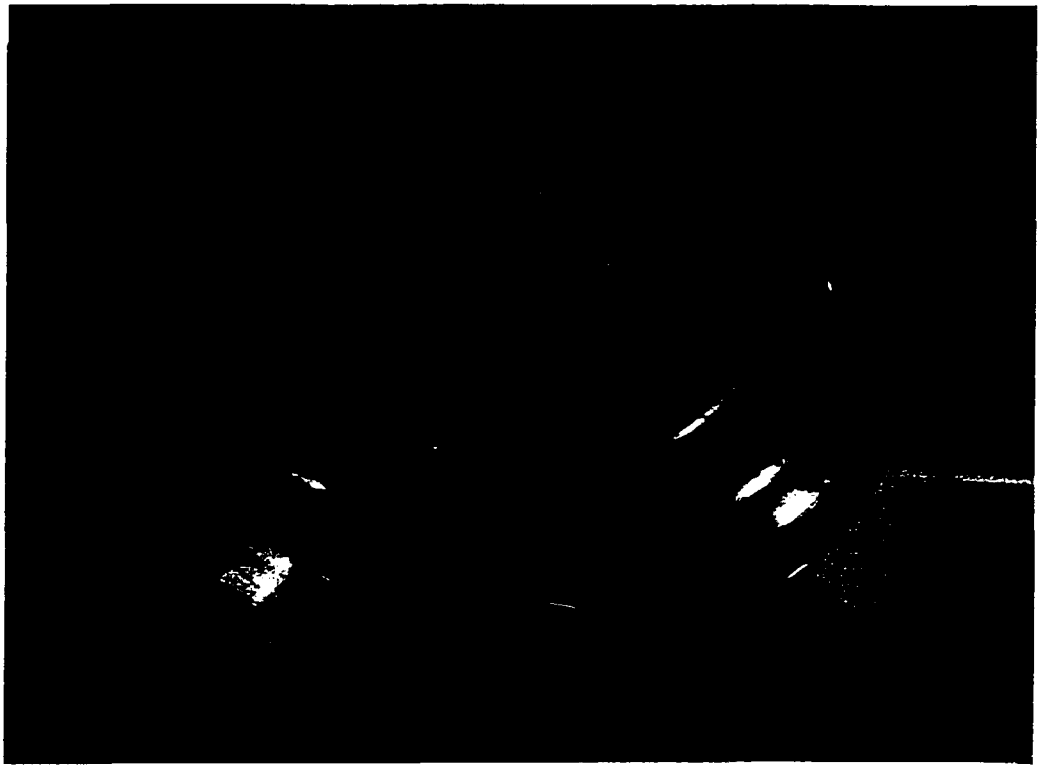

Figure A.3 Tufts at Reynolds number = 115073.

115,073 @ 7.35 m/s (9.0 Hz), The tuft on the 2nd row, 2nd from left shows vorticinal shedding. Occurs at the left side of the base of the cupola. All other tufts remain in their previous states. A photograph is taken to document this flow.

141,376 @ 9.03 m/s (11.0 Hz), The tuft on the 2nd row, 2nd from right shows vorticinal shedding. Occurs at the right side of the base of the cupola. All other tufts remain in their previous states.

154,997 @ 9.90 m/s (12.0 Hz), A diagram showing the present state of the tufts is shown below. NOTE: disc is starting to vibrate upon its mount. This may effect observations at higher velocities.

186,466 @ 11.91 m/s (13.9 Hz), Vorticies appear at the cupola's forward/side surface. 3rd row of tufts, 4th from left side and 5th from right side when viewed from above.

209,950 @ 13.41 m/s (15.0 Hz), Separation at the rear of the cupola. A photograph shows the region of separation. NOTE: Amplitude of disc vibration is increasing with velocity. This may effect observations.

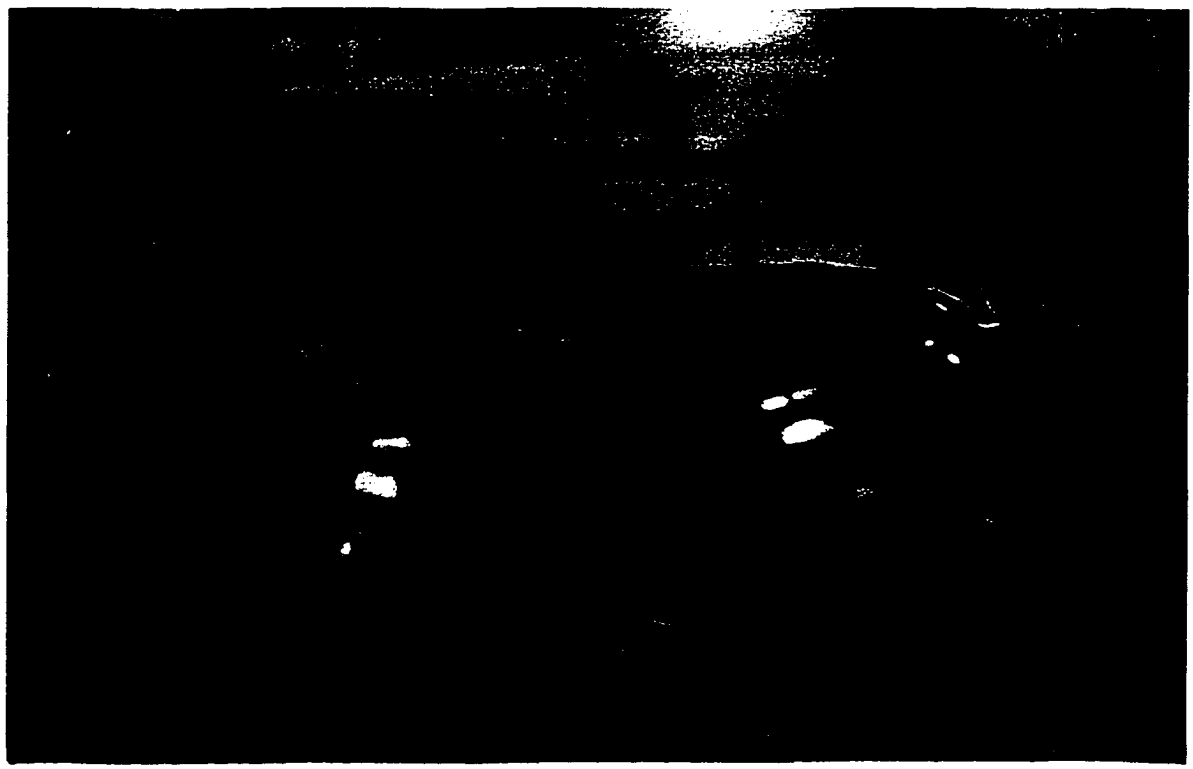

Figure A.4 Tufts at Reynolds Number = 209950.

Figure A.5 Top view at Reynolds Number = 209950.

237,975 @ 15.20 m/s (17.0 Hz), Leading edge tufts showing small vorticinal movements.

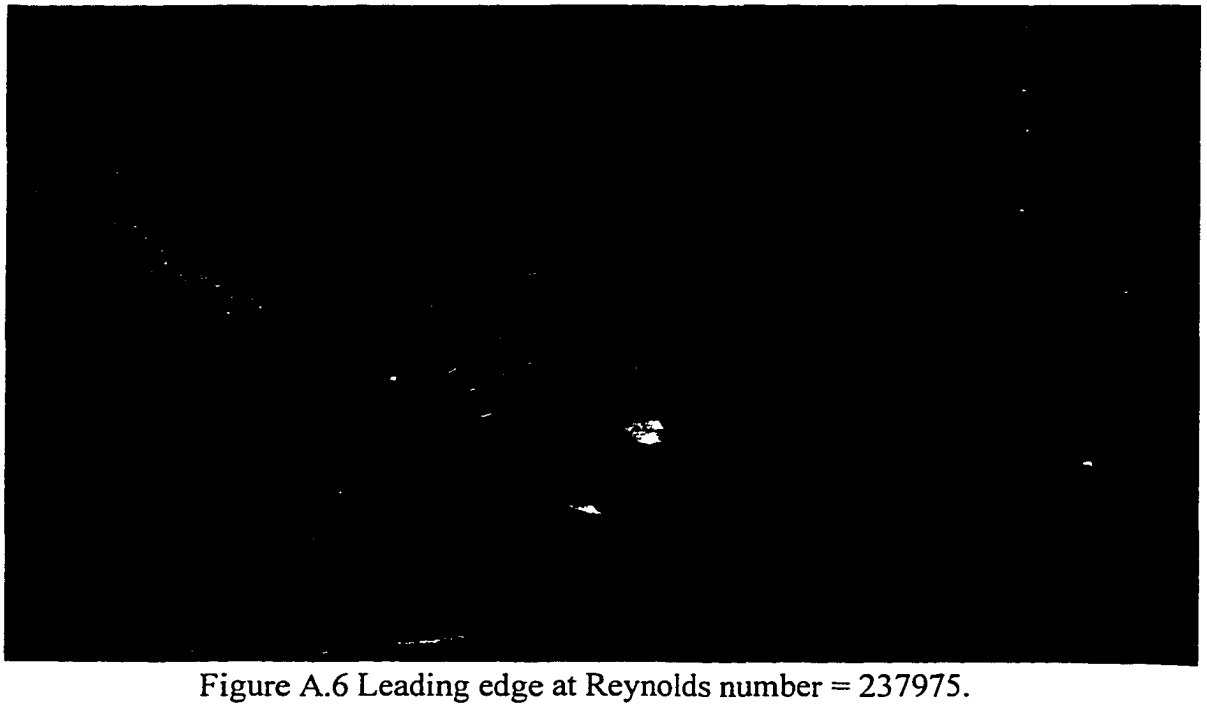

Figure A.6 Leading edge at Reynolds number = 237975.

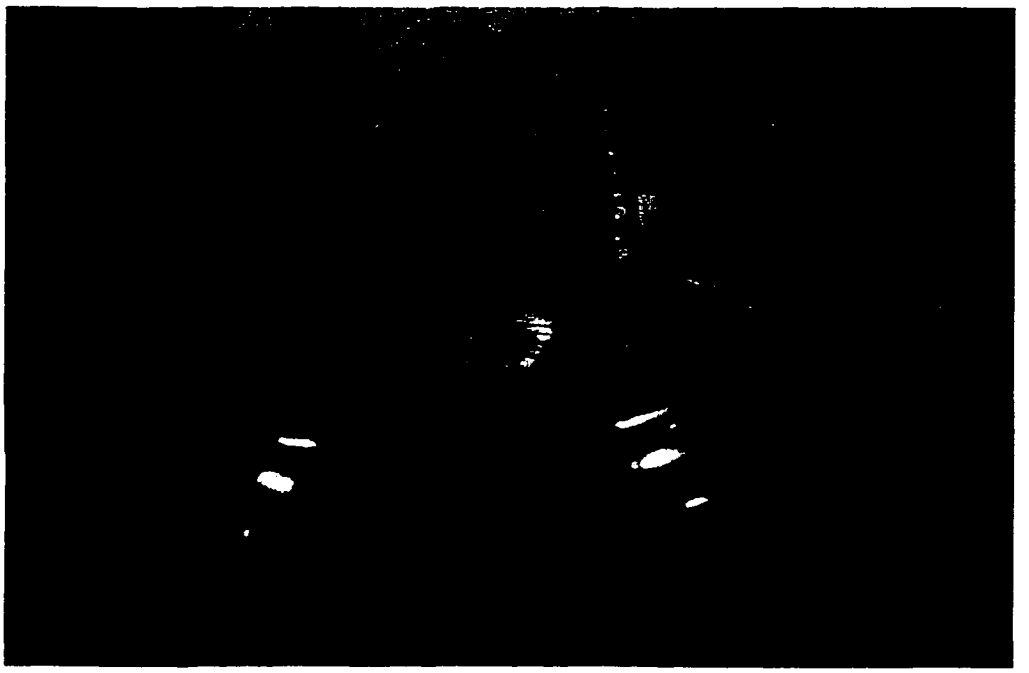

Figure A.7 Trailing edge at Reynolds Number = 237975.

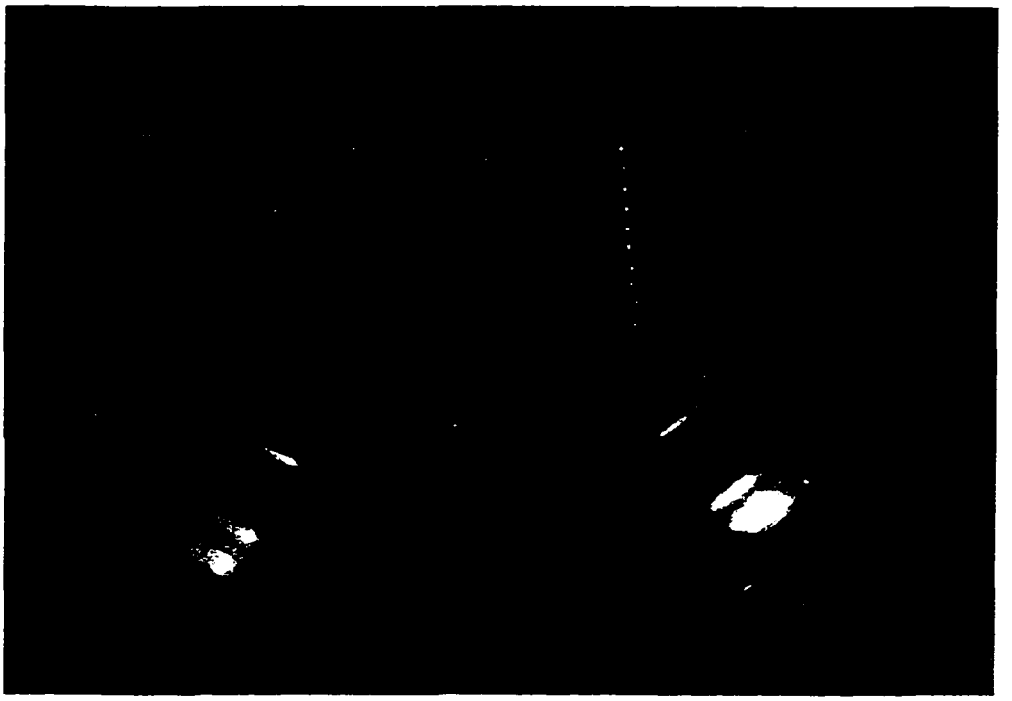

Figure A.8 Top view at Reynolds Number = 237975

262,085 @ 16.74 m/s (19.0 Hz), Stronger vorticies at the leading edge. For that matter, All the vorticies appear to be increasing in strength with increasing velocity. Flow at the rear is turbulent and is curving inward to follow the contour of the disc (first noted this tendency at 15.0 Hz but now it is clearly apparent).

317,352 @ 20.27 m/s (23.0 Hz), The flow is well developed now. Vorticies continue to get stronger and the separated region behind the cupola now extends to the rear of the disc. The disc's vibration at this speed may be influencing the flow. In any case, this velocity is well above what any human can be expected to throw a disc and further investigations into higher velocities will have to be conducted using securely mounted metal discs.

Test BT2

Disc 'B' Tuft Test 9.30 degree AOA

L.E. 11-7/16 inches from ground T.E. 9–15/16 inches from ground

Reynolds Number	Comments
42,428	@ 2.71 m/s (4.4 Hz), The cupola is showing vorticity and turbulence. Also the mid-chord vorticies are developing on the sides of the disc.
109,750	@ 7.01 m/s (8.6 Hz), The rear of the cupola is separated. The front of the cupola is showing vorticity. All of the other upper surface tufts are showing signs of turbulence.
138,714	@ 8.86 m/s (10.8 Hz), The mid-chord vorticies are well developed. The area of separation is increasing with velocity.
202,435	@ 12.93 m/s (14.7 Hz), The entire upper surface is turbulent or separated. There is no sign of streamlines curving in at the rear.

Test BT3

Disc 'B' Tuft Test - degree AOA

L.E. 9-1/2 inches from ground T.E. 12-3/8 inches from ground

Reynolds Number	Comments
82,039	@ 5.24 m/s (7.0 Hz), Vorticity is developing along the side of the disc. Small signs of turbulence near the forward base of the cupola.
122,745	@ 7.84 m/s (9.6 Hz), The forward half of the disc and the top of the cupola show strong turbulence in the boundary layer. The rear of the disc is vorticinal. There is no sign of separation.
173,800	@ 11.05 m/s (13.0 Hz), Streamlines are curving in to follow the contour at the rear of the disc. Lots of vorticity and turbulence on the upper surface. No sign of separation.
209,950	@ 13.41 m/s (15.0 Hz), Streamlines impacting the front of the disc are beginning to curl back just as on disc 'A'. The boundary layer on the upper surface on the disc quickly turns from laminar to turbulent. The rear of the disc has large areas of vorticity generation.

Test CT1 6/2/97 11:00 am

Disc 'C' Tuft Test 0 degree AOA

L.E. 11-1/2 inches from ground T.E. 11-1/2 inches from ground

Reynolds Number	Comments
74,360	@ 5.24 m/s (7.0 Hz), The tufts on the sides at the mid-chord are exhibiting small vorticinal shedding. All other tufts are still.
128,143	@ 9.03 m/s (11.0 Hz), The tufts at the trailing edge are beginning to curve inward and follow the contour of the disc. Small vibrations in the tufts indicate turbulence behind the disc. The entire bottom surface is separated and detached. All other tufts remain in their previous states.

Figure A.9 View of disc at Reynolds number = 128143.

190,297	@ 13.41 m/s (15.0 Hz), Two tufts on the upper surface are showing a very small turbulence. These tufts are in the 4th row, 4th from the left and 5th from the right.
250,113	@ 17.63 m/s (20.0 Hz), The flow is well developed now with no changes from the previous observations. Interestingly, this disc is not experiencing the vibrations disc did at this Reynolds number.

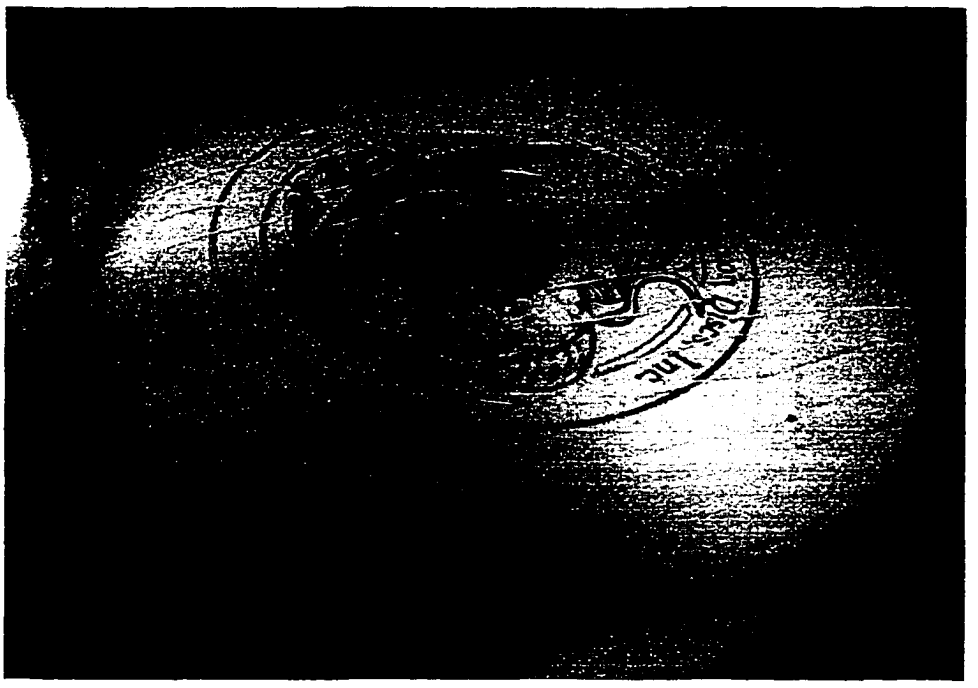

Figure A.10 Top view of disc at Reynolds number = 190297.

350,229 @ 24.68 m/s (28.0 Hz), No changes, the tufts remain very stable on the upper surface indicating a laminar and attached flow. A diagram shows the upper surface of the disc.

NOTE: Following this test I positioned the tufts on the disc straight up and ran the tunnel velocity to 14.3 m/s. The purpose being to see if it would show an increasing boundary layer thickness along the disc's surface. After the test, all of the tufts were aligned straight up for ½ inch and turned flat in the direction of the flow. This would indicate a very quick development of the boundary layer and a constant thickness thereafter. Since no region of separation or turbulence appears, this is in complete agreement with current theory.

Test CT2	6/9/97	11:30 am
Disc 'C'	Tuft Test	10 degree AOA
L.E. 12-1/4 inches from ground		T.E. 10-3/4 inches from ground

Reynolds Number	Comments
74,360	@ 5.24 m/s (7.0 Hz), The tufts on the sides at the mid-chord are exhibiting small vorticinal shedding. All other tufts are still.
116,223	@ 8.19 m/s (10.0 Hz), Side mid-chord tufts exhibiting strong vorticinal shedding. All other tufts remain in their previous states.
156,808	@ 11.05 m/s (13.0 Hz), The vorticity is moving inward from the sides of the disc and creeping forward along the sides of the disc, such that a narrow region of extreme turbulence (12mm in from the edge) exist on the upper surface along both sides. The center band dividing the two regions from leading edge to trailing edge is laminar and attached.
170,431	@ 12.01 m/s (14.0 Hz), Extreme separation, vorticity, and/or turbulence on both sides of the disc. The regions now extend 25mm into the upper surface. The band in the middle is laminar. A diagram of the disc shows the flow over the upper surface.
NOTE:	This test has been terminated due aerodynamic drag increasing the AOA, which undoubtedly effects the flow along the upper surface. This test will be rerun in CT3, once the disc can be mounted securely for the entire velocity region of this test.

Test CT3 6/9/97

Disc 'C' Tuft Test 10 degree AOA

L.E. 12-1/4 inches from ground T.E. 10-3/4 inches from ground

Note: This test is a repeat of CT2. A larger washer was placed in the underside of the mounting and the axial mounting screw was tightened to prevent AOA changes during testing.

Reynolds Number	Comments
83,868	@ 5.91 m/s (7.9 Hz), The tufts on the sides at the mid-chord are exhibiting a small amount of turbulence. All other tufts are still.
103,025	@ 7.26 m/s (8.9 Hz), Side mid-chord tufts exhibiting vorticinal shedding. All other tufts remain in their previous states.
116,223	@ 8.19 m/s (10.0 Hz), The vorticity is stronger. Also the leading edge of the disc has risen approximately 2mm.
126,866	@ 8.94 m/s (10.9 Hz), Vorticity is beginning to move forward from the mid-chord and creep inward from the center. There is no further change in the AOA.
133,110	@ 9.38 m/s (11.4 Hz), The turbulence is at the second row of outside tufts. Regions of separation are developing at the sides.
143,895	@ 10.14 m/s (12.2 Hz), The vorticity is at the second row of outside tufts. Regions of separation are developing at the sides. AOA has changed. The leading edge has risen 5mm.
153,970	@ 10.85 m/s (12.8 Hz), The vorticity is moving inward from the sides of the disc and creeping forward along the sides of the disc. The first row of tufts is show turbulence. The leading edge has risen another 2mm.

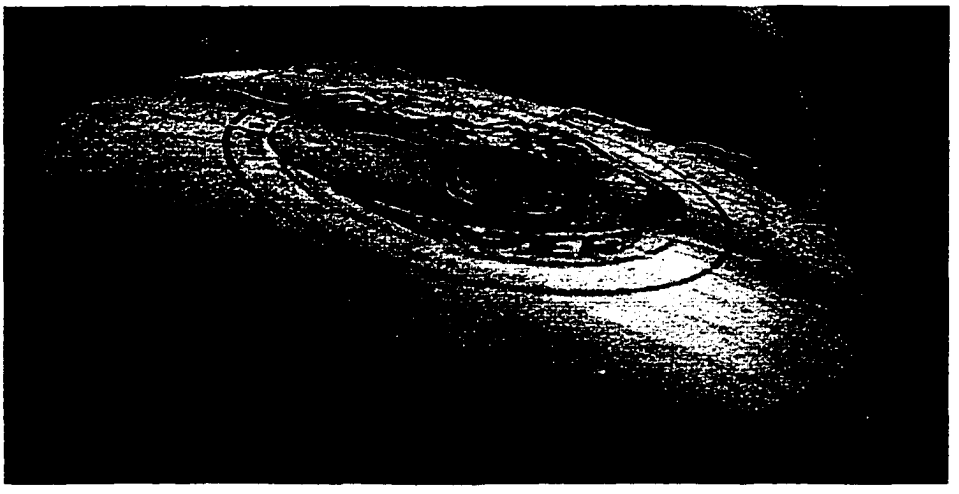

Figure A.11 Top view at Reynolds number = 153970.

169,013 @ 11.91 m/s (13.9 Hz), The areas of separation are growing inward and now extend 25mm in from the sides of the disc. The leading edge has risen an estimated 14mm from its original starting position.

191,576 @ 13.50 m/s (15.1 Hz), All of the tufts on the forward half of the disc's upper surface are showing turbulence and vorticity. The back half is entirely separated with the tufts just laying flat on the disc in the dead air. There was no change in the AOA.

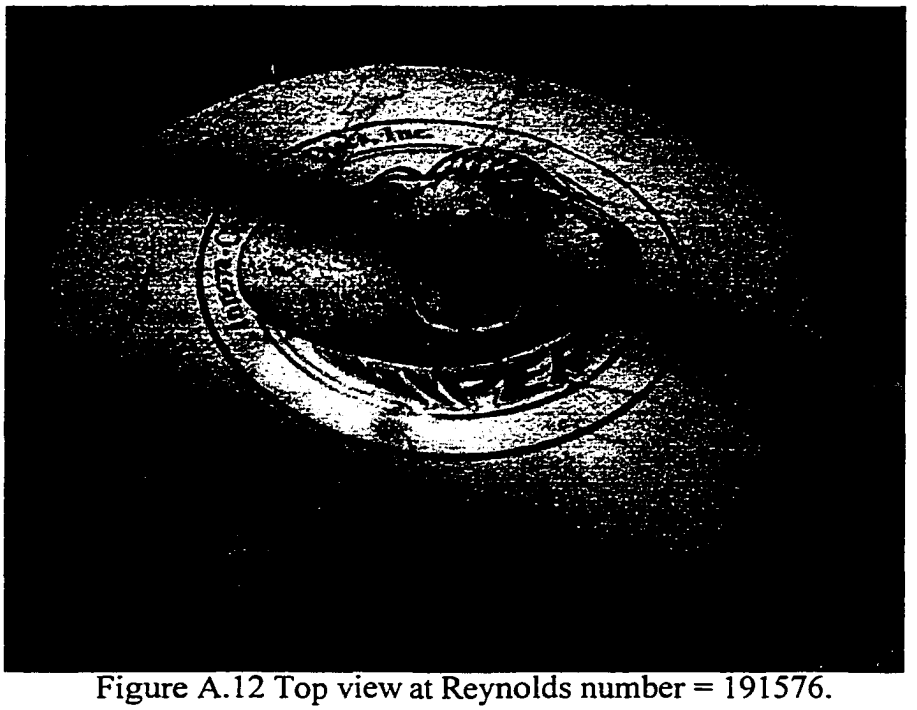

Figure A.12 Top view at Reynolds number = 191576.

Test CT4	6/10/97	9:15 am
Disc 'C'	Tuft Test	-10 degree AOA
L.E. 10-1/2 inches from ground		T.E. 12-11/16 inches from ground

Reynolds Number	Comments
57,047	@ 4.02 m/s (5.9 Hz), The streamlines are laminar over the upper surface, then shed from the trailing edge of the disc. The tufts at the trailing edge indicate a small turbulence. The lower surface (underside) is already separated. All other tufts are still. A diagram shows the streamlines over the surface.
64,426	@ 4.54 m/s (6.4 Hz), There is increasing turbulence in the streamlines. The disc leading edge is starting to show a tendency to push downward making the AOA increasingly negative.
98,343	@ 6.93 m/s (8.5 Hz), Vorticies are shedding from the mid-chord sides of the disc. Turbulence is strong in the trailing edge line of tufts. The leading edge has nosed-down 6mm. A photograph shows the tufts at this velocity.

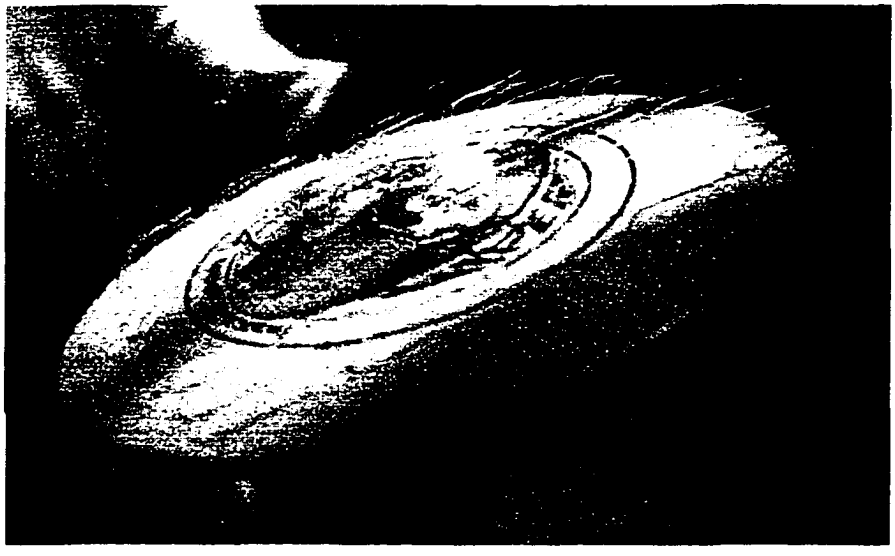

Figure A.13 Top view of disc at Reynolds number = 98343.

109,979	@ 7.75 m/s (9.5 Hz), Vorticies are shedding from the entire circumferential edge. Leading edge has nosed-down 8mm from its starting position.

126,866 @ 8.94 m/s (10.9 Hz), This diagram shows the streamline divergence over the upper surface of the airfoil.

137,935 @ 9.72 m/s (11.8 Hz), No changes in the streamlines or boundary layer is apparent. The leading edge has dropped a total of 14mm.

162,485 @ 11.45 m/s (13.4 Hz), The vorticies shedding from the 1/3 chord to the rear of the disc along the trailing edge appear to be turning downward. This may indicate changes in the downstream wake of the disc. The disc is also beginning to vibrate slightly which may be influencing the flow or causing the effect. The leading is now 19mm lower than its original starting position.

200,374 @ 14.12 m/s (15.8 Hz), The mid-chord vorticies are shedding straight down. The total drop in the leading edge is 25mm. No other changes are apparent in the streamlines. Test is halted.

SMOKE TEST RESULTS

This section consists of two tests performed on an aluminum disc designed to spin in the test section of the wind tunnel. The disc, measuring 108mm in diameter, was spun to match the tip-speed ratio of a Whammo™ Imperial Windjammer disc (disc 'A'), measuring 233mm in diameter. However, the estimated Reynolds number for a hand-thrown disc of 233mm diameter could not be matched using this wind tunnel. Instead, a Reynolds number approximately 1/5 of that was tested.

Both tests were videotaped and photographed. The following tables show the data regarding the experiments and my observations of those experiments. Photographs are displayed to show the observed phenomena.

Figure A.14 Set-up of spinning disc test in wind tunnel.

Test XS1 12/17/98 12:10 pm

Disc 'X' Aluminum Disc Smoke Visualization Test

Ambient air temperature: 22.3 °C Ambient air pressure: 95,027 Pa (712.94mm Hg)

Outside diameter: 108mm Tip Speed Ratio: 0.4378

Angle Of Attack: 0° Reynolds number: 33,153

Observations:

The duration of this test was 2 minutes and 57 seconds. Several important aerodynamic characteristics were observed.

The first is the slight updraft of the streamlines just before they contact the leading edge. This behavior was predicted by Lissaman [9]. The streamlines over the upper surface are laminar and attached. The streamlines on the lower surface are laminar and detached.

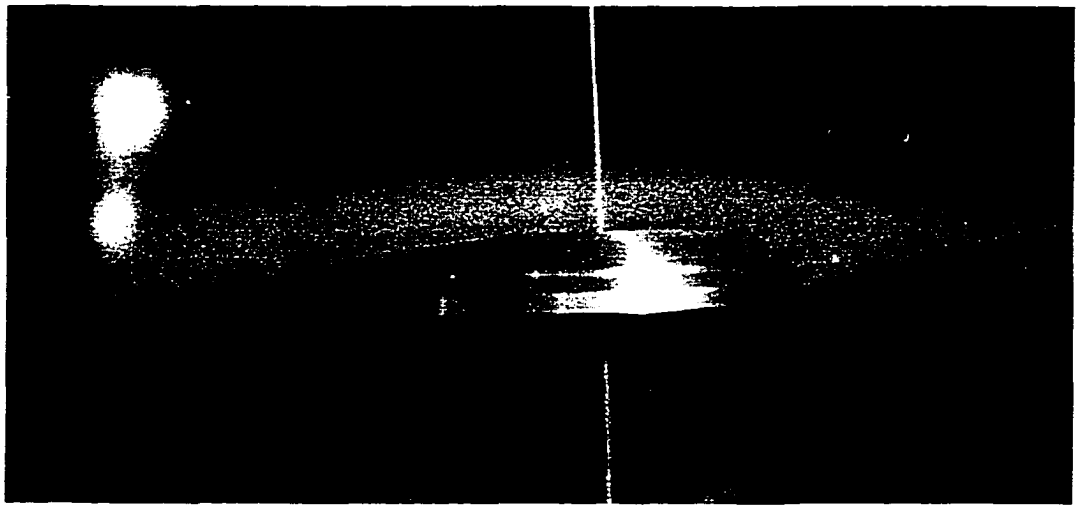

Figure A.15 Laminar top surface of a spinning disc.

The second is the existence of the mid-chord vorticies. These vorticies are very similar to the wingtip vorticies seen in conventional airfoils. They curl upward from the underside of the disc and roll off the lip at the mid-chord point. They are responsible for the majority of the drag experienced by the disc. The observation of these vorticies confirms their existence in the non-spinning tuft tests. The rotation of the disc did not move or change the position of these vorticies.

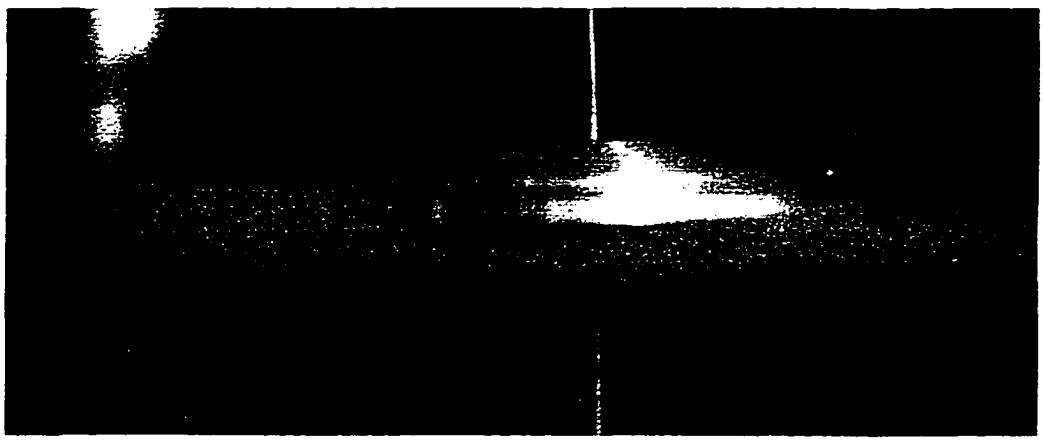

Figure A.16 Detached underside of spinning disc.

The third observation of importance is the down-wash in the trailing wake and the scroll up effect of the mid-chord vorticies in the wake of the disc.

The presence of the upstream uplift and the downstream down-wash, clearly indicate lift.

Test XS2 12/17/98 12:15 pm

Disc 'X' Aluminum Disc Smoke Visualization Test

Ambient air temperature: 22.3 °C Ambient air pressure: 95,027 Pa (712.94mm Hg)

Outside diameter: 108mm Tip Speed Ratio: 0.4378

Angle Of Attack: 5° Reynolds number: 33,153

Observations:

The duration of this test was 2 minutes and 30 seconds. The 5° AOA is representative of the attitude of a typical hand-thrown disc. The observations in the previous test are applicable here as well.

Again, we see the uplift before the streamline contacts the leading edge and the mid-chord vorticies are unchanged in their position or apparent strength.

The trailing wake is more pronounced, with a deeper down-wash but otherwise it is also unchanged.

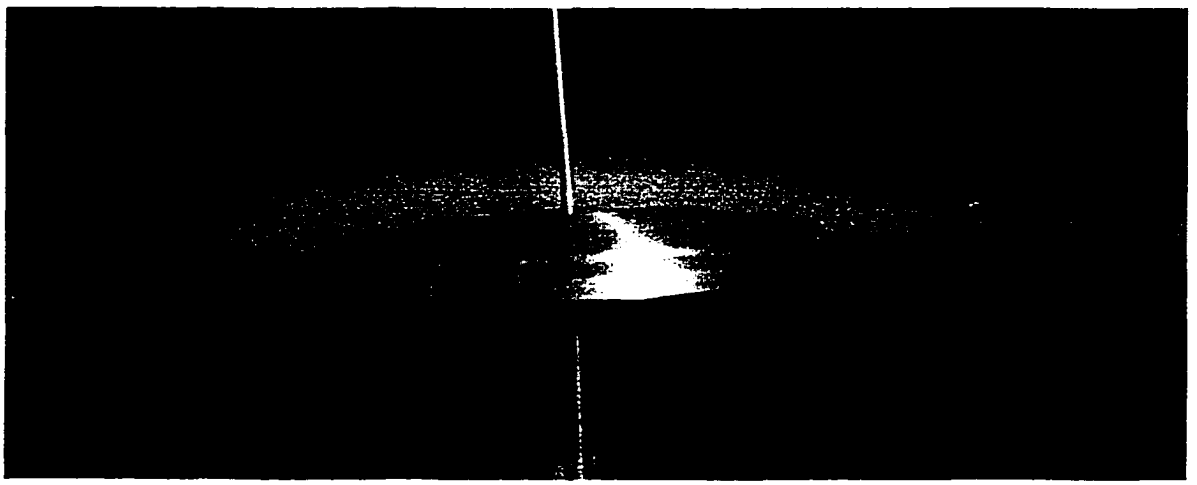

Figure A.17 Spinning disc photograph. Note the uplift ahead the disc and the downwash behind the disc.

Figure A.18 Spinning disc test. Note the detached underside of the disc.

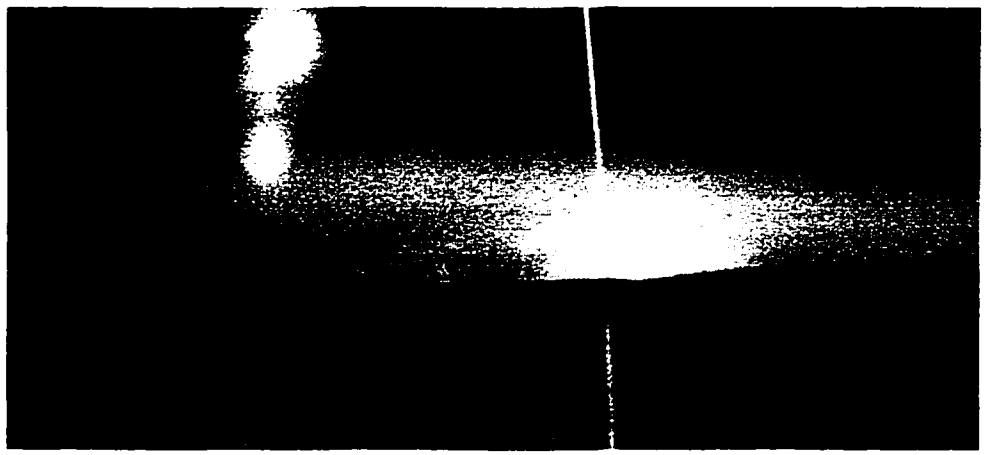

Figure A.19 Spinning disc test. Note the wingtip vortex generation.

BIBLIOGRAPHY

1. Chapman, R., P. Johnston, and D. Keenan, "Experiments With Frisbees," Ryerson Polytechnic Institute, Toronto, Ontario, Canada, 1972.

2. De Mestre, N., "The Mathematics Of Projectiles In Sport," Australian Mathematical Society, Lecture Series No. 6, Cambridge University Press, pp. 120-130, pp. 156-162, 1990.

3. Frohlich, C., "Aerodynamic Effects On Discus Flights," American Journal of Physics, v. 49, pp. 1125-1132, 1980.

4. Imber, R., and E. Rogers, "Investigation Of A Circular Planform Wing With Tangential Fluid Ejection," AIAA 96-0558, 34th Aerospace Sciences Meeting & Exhibit, Reno, Nevada, 1996.

5. Johnson, S. E. D., "Frisbee, A Practitioner's Manual And Definitive Treatise," Workman Publishing Co., New York, New York, 1975.

6. Katz, P., "The Free Flight Of A Rotating Disk," Israel Journal of Technology, v. 6, n. 1-2, pp. 150-155, 1968.

7. Koon, B., "Spinning Disks In Flight," Unpublished paper, State University of New York, Buffalo, New York, 1989.

8. Lissaman, P. B. S., "Stability And Dynamics Of A Spinning Oblate Spheriod," Unpublished paper, University of Southern California, Los Angeles, California, 1994.

9. Lissaman, P. B. S., "Where Lift Comes From," Unpublished paper, University of Southern California, Los Angeles, California, 1994.

10. Maozhang, C., and Z. Guojun, "Numerical Study Of Three-Dimensional Boundary Layers On Rotating Bodies," AIAA 96-0434, 34th Aerospace Sciences Meeting and Exhibit, Reno, Nevada, 1996.

11. McMahon, J., "Where The Frisbee First Flew," New Times Magazine, Los Angeles, California, 24 July 1997.

12. Nakamura, Y., and N. Fukamachi, "Visualization Of Flow Past A Frisbee," Fluid Dynamics Research, v. 7, pp. 31-35, 1991.

13. Rae, W., "Computer Simulation Of The Flight Of An American Football," Accepted for publication in AIAA Journal, 1996.

14. Shelton, J., "The Physics Of Frisbee Flight," Unpublished paper, Williams College, Williamston, Massachusetts.

15. Shunke, B. A., "The Flight Of A Frisbee," Unpublished paper, State University of New York, Buffalo, New York, 1989.

16. Soong, T. C., "The Dynamics Of A Discus Throw," Journal of Applied Mechanics, pp. 531-536, 1976.

17. Stilley, G. D., "Aerodynamic Analysis Of A Self Suspended Flare," Honeywell Inc., Hopkins, Minnesota, U. S. Naval Ammunition Depot, Crane, IN., RDTR No. 199, 23 February 1972.

18. Staff Editor, "Flying Farther Than A Frisbee," American Society of Mechanical Engineers, Mechanical Engineering Magazine, August 1995.

19. Ragsdale, J., "Darkstar Stealth Uav Crashes," 1996, http://pollux.com/defenseweb/1996/may96/darkstar.html

20. Rozell, N., "Fun With Physics, Starring The Flying Disc," Alaska Science Forum, Article #1299, 1996, http://www.gi.alaska.edu/ScienceForum/ASF12/1299.html

21. Unknown Author, "Frisbee Physics," 1997, http://www.ktca.org/newtons/9/frisbee.html

22. Unknown Author, "The Flying Disk," Lemelson-MIT prize program, 1997, http://web.mit.edu/invent/www/inventorsA-H/flyingdisk.html

23. Unknown Author, "Laser Propulsion Research Projects," 1998, http://www.aero-meche.rpi.edu/research/laserpropulsion.html

24. Scotland, I., "The History Of The Frisbee Disc," 1997, http://wol.ra.phy.cam.ac.uk/buf/odd/frisbee.htm

25. Andersen J. D., "Fundamentals Of Aerodynamics," ISBN 0-07-001679-8 McGraw-Hill, New York, New York, 1991.

26. Crowther, W., Unpublished Experiments, Cambridge University, England, 1998.

VITA

Graduate College
University of Nevada, Las Vegas

Timothy Lewis Mitchell

Local Address:
P.O. Box 73161
Las Vegas, Nevada 89170

Home Address:
2324 Florissant Drive
Las Vegas, Nevada 89128

Degrees:
Associate of Applied Science, 1988
Clark College

Bachelor of Science, Mechanical Engineering, 1994
University of Nevada, Las Vegas

Special Honors and Awards:
Golden Key National Honor Society member, 1993
NASA Scholarship, 1993
NASA Fellowship, 1994

Thesis Title: The Aerodynamic Response of Airborne Discs

Thesis Examination Committee:
Chairperson, Dr. Darrell Pepper, Ph.D.
Committee Member, Dr. William Culbreth, Ph.D.
Committee Member, Dr. William Graebel, Ph.D.
Graduate Faculty Representative, Dr. Michelle Schultz, Ph.D.